High-Order Contact Transformations of Molecular Hamiltonians: General approach, fast computational algorithm and convergence of rovibrational polyad models

Vladimir Tyuterev, Sergey Tashkun, Michael M. Rey, Andrei Nikitin

High-Order Contact Transformations of Molecular Hamiltonians: General approach, fast computational algorithm and convergence of ro-vibrational polyad models

Vladimir Tyuterev [ab*], Sergei Tashkun[c], Michael Rey[a] and Andrei Nikitin[c]

[a] *GSMA, University of Reims, BP 1039, 51687 Reims Cedex 2, France;*
[b] *Tomsk State University, Russia*
[c] *LTS, Institute of Atmospheric Optics, 634055, Tomsk, Russia*

**) Contact author email: vladimir.tyuterev@univ-reims.fr*
Tel: +33 (0)6 60 29 17 56 (Reims)

ABSTRACT

The paper describes methods and fast computational algorithm for building effective Hamiltonians in molecular physics using perturbative approach. Various techniques of separation of fast and slow variables are considered in the general mathematical framework of contact transformations. The particular focus is on a systematic derivation of effective models for vibration-rotation spectroscopy from ab initio based potential energy surfaces with an exhaustive review of the previous studies in this field. We consider applications to various types of polyads coupled by Fermi, Coriolis, Darling-Dennison and other types of resonance interactions with the examples for asymmetric top, symmetric top and spherical top molecules. A flexible choce of the modelling operator accounts for strong coupling of various types of nuclear motion in molecules among closely lying levels including vibrational resonance schemes (2:1:2) , (2:1:2:1), (4:2:6:3), (3:2:1:2:1:1) etc that occur for C_{2v}, C_{3v}, and T_d molecules and their isotopic species. The method is implemented in the MOL_CT program suite that offers a complementary tool to variational methods in terms of convergence and computational time. This permits an inclusion of a priori information to obtain physically meaningful values for the the resonance coupling terms in order to developing mixed “ab initio/effective” models with smaller number of adjustable parameters for analyses of molecular spectra.

1. INTRODUCTION

Effective Hamiltonians (EH) are widely used in many domains of molecular physics, chemistry and spectroscopy. Numerous examples are reported in textbooks and in a large panel of publications (see for example [1-25] and references therein). EHs are often introduced from phenomenological and symmetry considerations and serve as rather simple mathematical models containing adjustable parameters fitted to experimental data. On the other hand, they can be derived by appropriate mathematical transformations [26-40]. The major advantage of the EH is that this approach allows one to reduce an extent of calculations by focusing on a certain group of quantum states (polyads) "localized" within a limited energy interval. The latter is supposed to be of interest for an interpretation of a concrete experimental spectrum within a considered frequency range. Historically, most of analyses of high-resolution molecular spectra used empirically fitted effective Hamiltonians for vibrational polyads [11,17, 41-48]

An important contribution to the theory of effective Hamiltonians in molecular spectroscopy is due to series of works by Jean-Marie Flaud and co-workers, who successfully applied the corresponding vibration-rotation models for analyses of many high-resolution spectra of triatomic [41, 49-51] and polyatomic molecules [52-56] in the infra-red, including the first Atlas of ozone spectral transitions [57]. Camy-Peyret and Flaud [8] have contributed to development of effective dipole transition moments for vibration-rotation transitions. These works were at the origin of many studies for spectroscopic data reductions and for creation of line lists for several generations of spectroscopic databases like HITRAN, GEISA [58-59].

In many cases these effective models and analyses have allowed for identifying resonance interactions resulting in various perturbations in observed spectra, including line intensity transfer due to wave functions mixing (see for instance [11,15, 41-52,60-63] and references therein).

Another very important application of effective Hamiltonians including interactions of strongly coupled states, concerned the studies of the dynamics of nuclear motion in molecules. The impact of vibrational and ro-vibrational resonance interactions on qualitative changes in excited states using classical or quantum effective models has been evidenced in many works [64-88]. These changes induced by resonance couplings of quantum states appear as counterparts of bifurcations in classical phase space [72,77,81]. Well-known examples are normal-to-local mode transitions [64,65,68], as well as fingerprints of saddle-node bifurcations in vibrational spectra [84]. Effective Hamiltonians provide a local description of the dynamics by incorporating those resonances among the degrees of freedom active at a certain energy range. This approach retains the most essential features for a qualitative description and makes the understanding of related phenomena much easier than corresponding bifurcation analyses of periodic orbits and wavefunctions on the full potential energy surfaces (PES) [90-96 and refs therein]. EH models also proved to be very useful for predicting re-organization of vibration-rotation patterns and of "level clustering" at high rotational quantum numbers [66-68,71,15].

A derivation of many EH models can be achieved by the method of *Contact Transformations* (CT), which since the original work by Van Vleck [1] has been developed in works of many groups for various applications [2,3,6-13, 16, 29, 32-39, 98-141]. CTs can be considered as a quantum counterpart of canonical transformations [85,142-144] related to degenerate or quasi-degenerate perturbation theory. In practical terms, the CT method provides links between PES and effective constants involved in empirical EH models. CTs also apply to other molecular properties relating for example dipole moment surfaces (DMS) with effective transition moment band parameters [7,8, 145-155]. Though basic framework of CT is well-established and widely used in molecular physics, a further development will be beneficial in order to achieve a spectroscopic accuracy and to consider vibrational polyads in higher energy range. In this paper, a rather general and flexible formulation for high-order CT is described, which can combine different techniques in order to study

convergence properties of EH expansions and to extend calculations to arbitrary number of states involved.

(!!! up to here the reference numbering does not change !!!)

A large number of methods has been developed for quantum nuclear motion calculations in molecules. Among them there are a various alternative versions of the perturbation theory [155, 157], vibrational self-consistent field (VSCF) and vibrational configuration interaction (VCI) approaches [158-165], vibrational coupled-cluster (VCC) theory [167], descrete variable representation (DVR) [168-171] and collocation [172] methods. Several computerational codes of variational calculations using exact kinetic energy operator (KEO), like VTET [173] and 6A [174] (with redundant coordinates), were reported. Some other program tools like TROVE [175] , TENSOR [176] or MIRS [14] use well converged expansion of KEO for calculations of rotationally resolved spectra. In view of a large number of related publications, this citation list is by no means exhaustive, some more detailed complementary references are give in Sections ***.

The CT method allows for computing enegies and wavefunctions as well. Recent examples of CT applications have shown that it can be competitive with above mention approaches in terms of the accuracy, at least for a certain range of nuclear or electronic motion. Note, however, that the main purpose of the CT method is different. The aim of CT is to build accurate mathematical models of strongly interacting states for interpretation / analyses of experiments for molecular spectroscopy and dynamics. In other words , this … provide efficient tools for experimental data reduction.

In this paper *we review the general CT method and fast computational algorithm for building effective Hamiltonians in molecular physics* using perturbative approach (or mixed perturbative/variational one in case of overlapping polyads).

The introduction of the modelling operator and of related conditions for the CT Lie algebra can be easily adapted for a separation of various types of variables. The final aim is to develop an efficient tool for building accurate models of strongly interacting states for molecular spectroscopy and dynamics. The most important challenge is a precise derivation of resonance coupling parameters from a molecular PES which are responsible for irregular features in observed spectra such as line intensity borrowing [11,15, 41-52,60-63]. An example of a practical application of this approach was recent prediction of high-order coupling parameters for a vibrational polyads of the ozone and methane molecules [15, 47, 156] that allowed determining much more robust EH model for the high-resolution data reduction.

Convergence issues are considered, particularly for application related to the derivation of effective vibration-rotation models for vibrational polyads with examples for diatomic, asymmetric, symmetric and spherical top molecules.

2. CONTACT TRANSFORMATIONS

The method of Effective Hamiltonians aims at building up some simple models for the sets of strongly coupled nearby states has been widely used in various domains of physics. The main idea of the method is in transforming the complete Hamiltonian H to a simpler operator $\mathcal{H}^{eff}$ defined in a sub-space $\mathcal{E}$ spanned by known functions φ_i which are easy to handle. Most often, this is realized by making use of a similarity transformation followed by the projection $P_{\mathcal{E}}$ onto the corresponding sub-space $\mathcal{H}^{eff} = P_{\mathcal{E}}\tilde{H}P_{\mathcal{E}}$. In many applications for molecular physics and quantum chemistry, one can reduce the problem to a finite dimensional sub-space $\mathcal{E}$ spanned by eigen functions φ_i of an exactly solvable equation, that results in an obvious simplification.

Technically, it is convenient to apply a unitary transformation in an exponential form *T=exp(-iS)* with hermitian *S*-generators using the Baker-Hausdorff expansion in terms of multiple commutators

$$\tilde{H} = T^{+}HT = e^{iS}He^{-iS} = H + [iS, H] + ... + (1/n!)[i\underbrace{S,[iS,...[iS}_{n}, H]...]] + ... \quad (1)$$

After having chosen a zero-order approximation H_0 and a *small parameter* $\lambda \square 1$, one can use this expansion to build up an operator form of the perturbation theory with subsequent diagonalisation of blocks corresponding to degenerate or near-degenerate zero-order states.

In molecular physics and spectroscopy, a Hamiltonian H is often developed in increasing powers of a small parameter λ

$$H = H_0 + H_1 + ... H_n + ..., \quad \text{where} \quad H_n \sim O(\lambda^n H_0), \quad (2)$$

where the conventional notaion *O(...)* means "of the order of", and T is chosen in a form of successive unitary *Contact Transformations* (CT)

$$T = T_1 T_2 ... T_n ... = e^{-iS_1} e^{-iS_2} ... e^{-iS_n} ..., \quad \text{where} \quad S_n \sim O(\lambda^n) \quad (3)$$

It is supposed that the CT can be chosen in a way that they keep the rate of convergence of the Hamiltonian expansion. Generators S_n of CT are usually chosen to be *hermitian* ($S_n^{+} = S_n$), *totally symmetric on the molecular point group, and invariant under the time reversal* in order to keep the corresponding properties of the transformed Hamiltonian $\tilde{H}$. The latter one is also expanded in successive orders of λ

$$\tilde{H} = H_0 + \Delta\tilde{H}_1 + \Delta\tilde{H}_2 + ... + \Delta\tilde{H}_n + ..., \quad \text{where} \quad \Delta\tilde{H}_n \sim O(\lambda^n H_0) \quad (4)$$

The zero-order term remains unaltered and the corrections are obtained by gathering the terms of the same order in expansions (1)-(3):

$$\Delta\tilde{H}_1 = H_1 + [iS_1, H_0] \qquad \sim O(\lambda^1 H_0) \quad (5)$$

$$\Delta\tilde{H}_2 = H_2 + [iS_1, H_1] + (1/2)[iS_1,[iS_1, H_0]] + [iS_2, H_0] \qquad \sim O(\lambda^2 H_0) \quad (6)$$

…

CTs are usually used for a systematic simplification of the Hamiltonian. Suppose for example, that a first order perturbation contains two types of terms $H_1 = H_1^{(a)} + H_1^{(b)}$ where *(a)*-terms are important for the considered spectral range corresponding to a sub-space $\mathcal{E}$ and should be explicitly included in the effective Hamiltonian. Let *(b)*-type contributions be some non-essential terms which are difficult to handle or prevent from isolating a considered set of

states. They can be removed by a first-order transformation if one finds a small generator $S_1 = S_1^{(b)} \sim \lambda^1$ satisfying the equation $[iS_1^{(b)}, H_0] = -H_1^{(b)}$. If this is the case, one simplifies the first order term $\Delta\tilde{H}_1 = (H_1 + [iS_1^{(b)}, H_0]) = H_1^{(a)}$, but $S_1^{(b)}$ induces new second-order contributions according to eq.(6). A second order CT generator $S_2 \sim \lambda^2$ should then be used in a similar way to remove *(b)*-type terms from $\Delta\tilde{H}_2$ and so on.

Most often CTs are used to make $\tilde{H}$ diagonal or block-diagonal in the basis of zero-order wave functions. A transformation $H \Rightarrow \mathcal{H}^{eff}$ often results in an effective separation of a part of variables, their contribution being not neglected but accounted for parametrically.

After the pioneering work of Van Vleck [1], the CT method has been extensively developed in many works on molecular spectroscopy in particular for vibration-rotation Hamiltonian in rectilinear normal coordinates. Series of works by Nielsen and Amat [2,3], Legay [145], Rothman and Clough [16], Chedin and Cihla [32, 101], Aliev and Watson [7, 104, 106], Camy-Peyet and Flaud [8,148] were among first important contributions in this subject. Bunker and Moss [12] and Schwenke [13] have applies CT method to the separation of electronic and nuclear variables in molecules. Mathematical aspects of CT equations have been studied by Primas [29,98], Tyuterev, Tashkun, Perevalov and co-workers [15, 33, 36, 39, 127], whereas application to non-rigid molecules were considered by Jensen and Bunker [38], Papousek et al [157,158] and Starikov and Tyuterev [107, 111, 127]. Siebert, McCoy, Wang and co-workers [9, 117-125, 128-132] and Zuniga et al [130,133] have applied Van Vleck transformations both for rectilinear and curvilinear normal coordinates.

Recent applications of CT for vibrational polyads and further developments have been reported by Krasnoshchekov et al [135-141]. Joyeux and Sugny [85, 142-144] have worked out a classical counterpart of CT based on Birkhoff- Gustavson [159,160] canonical transformations. Relevant time-dependent formulations were discussed in [109, 114, 161-163].

This reference list is not exhaustive, various aspects of the CT method have been reviewed in [6,7,15,123, 127]. Non-perturbative numerical transformations to effective ro-vibrational Hamiltonians have been recently proposed by Rey [165] that can offer complementary tools for spectra analyses.

2.1 Recurrent scheme of CT

It is convenient to introduce a once transformed Hamiltonian $H^{(1)}$, twice transformed Hamiltonian $H^{(2)}$, …k-times transformed Hamiltonian $H^{(k)}$ and so on

$$H^{(0)} \equiv H \tag{7a}$$

$$H^{(1)} = exp(iS_1) H^{(0)} exp(-iS_1) \tag{7b}$$

…

$$H^{(k)} = exp(iS_k) H^{(k-1)} exp(-iS_k) \tag{7c}$$

…

$$\tilde{H} = H^{(\infty)} \equiv \lim_{k\to\infty} H^{(k)} \tag{7d}$$

Similarly to (2), (4) each k-times transformed Hamiltonian $H^{(k)}$ can be also expanded in successive orders of λ:

$$H^{(k)} = \sum_{n=0}^{\infty} H_n^{(k)} \text{, where } H_n^{(k)} \square O(\lambda^n H_0) \quad , \tag{8}$$

upper *(k)* index in $H_n^{(k)}$ being the number of CT and lower index *n* being the order of magnitude of the term. This ordering suggests that a transformation $exp(-iS_k)$ brings the Hamiltonian to a required form up to the order λ^k. This means that the terms in eq.(8) are no more altered as soon as the upper index becomes equal to or superior of the lower one:

$$H_k^{(k+i)} = H_k^{(k)} = \Delta\tilde{H}_k \quad \text{for} \quad i > 0 \tag{9}$$

A recurrent scheme of CT is given in Table 1. It can be seen as a sequence of "layer-by-layer" transformations which are symbolized by vertical arrows in Table 1, the *k*-number of CT being shown at the left hand panel. The "zero's-layer" with k=0 (first row in Table 1) corresponds to the expansion of the initial untransformed Hamiltonian in power series of λ^n. The next layer with k=1 (second row in Table 1) corresponds to the expansion of once transformed Hamiltonian $H^{(1)}$ and on. Columns at the right-hand side panel of Table 1 correspond to the terms of a given order of magnitude.

Table 1: Recurrent scheme of Contact Transformations

$CT \setminus order$			λ^0	λ^1	λ^2	λ^3	λ^4		λ^n
$k=0:$	H	$=$	$H_0 +$	$H_1 +$	$H_2 +$	$H_3 +$	$H_4 +$	$\ldots$	$H_n +$
$\downarrow$ $k=1:$	$H^{(1)}$	$=$	$H_0 +$	$H_1^{(1)} +$	$H_2^{(1)} +$	$H_3^{(1)} +$	$H_4^{(1)} +$	$\ldots$	$H_n^{(1)} +$
$\downarrow$ $k=2:$	$H^{(2)}$	$=$	$H_0 +$	$H_1^{(1)} +$	$H_2^{(2)} +$	$H_3^{(2)} +$	$H_4^{(2)} +$	$\ldots$	$H_n^{(2)} +$
$\downarrow$ $k=3:$	$H^{(3)}$	$=$	$H_0 +$	$H_1^{(1)} +$	$H_2^{(2)} +$	$H_3^{(3)} +$	$H_4^{(3)} +$	$\ldots$	$H_n^{(3)} +$
$\downarrow$ $k=4:$	$H^{(4)}$	$=$	$H_0 +$	$H_1^{(1)} +$	$H_2^{(2)} +$	$H_3^{(3)} +$	$H_4^{(4)} +$	$\ldots$	$H_n^{(4)} +$
$\downarrow$ $\ldots$	$\ldots$	$\ldots$	$\ldots$						$\ldots$
$k=n:$	$H^{(k)}$	$=$	$H_0 +$	$H_1^{(1)} +$	$H_2^{(2)} +$	$H_3^{(3)} +$	$H_4^{(4)} +$	$\ldots$	$H_k^{(k)} +$

$\Rightarrow \tilde{H}$

The lower "triangle" at the right-hand panel of Table 1 collects all terms which have been already simplified by CT :

$$H^{(k)} = \{H_0 + \Delta\tilde{H}_1 + \Delta\tilde{H}_2 + \ldots + \Delta\tilde{H}_k\} + H_{k+1}^{(k)} + \ldots H_{k+l}^{(k)} + \ldots = \tilde{H} + O(\lambda^{k+1}) \tag{10}$$

As it follows from Eq.(9), these terms in braces $\{\ldots\}$ are ready to use up to the order λ^k. The upper "triangle" contains contributions which are removed at the following layers with

increasing *k*. The encircled terms in Table 1 give successive corrections to the final transformed operator:

$$\tilde{H} = H_0 + \sum_m H_m^{(m)} = H_0 + \sum_m \Delta\tilde{H}_m \qquad (11)$$

The terms involved in the *k*-times transformed Hamiltonian $H^{(k)}$ can be computed from previously calculated $H^{(k-1)}$ operators using the recurrence relation [6,99]

$$H_n^{(k)} = H_n^{(k-1)} + \sum_{m=1}^{[[n/k]]} (1/m!)[iS_k,...[iS_k, H_{n-km}^{(k-1)}]...]_m \quad , \qquad (12)$$

which is obtained by applying the Backer-Hausdorff relations (1) and by identifying expansion terms of a given order λ^n in both sides of Eq.(7c). Here the notation $[[n/k]]$ stands for the integer part of *n/k*. If $k > n$ then $[[n/k]]=0$ and in this case all terms in the second part summation of Eq.(12) vanish $H_n^{(k)} = H_n^{(k-1)} = ... = H_n^{(n)}$, that justifies Eq.(9) as well as the lower triangle representation in Table 1.

Suppose that S_n-generators of CT are chosen in some arbitrary way satisfying standard hermicity, symmetry and order of magnitude requirements (3) only. Then Eqs. (9), (12) provide simple algorithmic relations that allow filling up successive layers of Table 1 and computing successive corrections in the finally transformed Hamiltonian (11) up to any needed order.

The only condition was that a formal convergence of expansions in terms of λ^n ordering should be conserved at every layer of Table 1. Note that in the general recurrent scheme of this Section we did not yet specified concretely the meaning of a simplification $H \Rightarrow \tilde{H}$ provided by CT. The above general scheme *is equally valid for any other operator representing a physical property like dipole moment operator and so on*. Using an appropriate definition of a Hamiltonian "simplification" which one expects to obtain with CT, it is possible to further optimize the above recurrent algorithm and considerably economise a computational effort as it will be discussed in the following sections.

2.2 Commutator equations, modelling operator and $\mathbb{L}$ algebra of CT

An important question is how to formalize mathematically an idea of a Hamiltonian simplification which could be provided by CT in a sufficiently general case? For this purpose it is instructive to consider the *Lie algebra of CT* generated by all *multiple commutators* involving operators $\{H_0, \ldots, H_n, \ldots, S_1, \ldots, S_m \ldots\}$. Let us denote this algebra $\mathbb{L}$. It obviously includes all $H_n^{(k)}$ terms belonging to successive layers of Table 1. Would it be possible to choose within $\mathbb{L}$ a certain simpler subset in such a way that all $H_n^{(n)}$ terms of the lower triangle of Table 1 and consequently $\tilde{H}$ belong to this subset ?

One possibility is to use as such simple subset a sub-algebra $\mathbb{L}^{(0)}$ containing all operators which commute with H_0. This is equivalent to the condition $[\tilde{H}, H_0] = 0$ imposed on the transformed Hamiltonian which was used in many applications of CT in molecular physics and spectroscopy . In cases of quasi-degenerate zero-order approximation (accidental resonances) the latter condition is not compatible with the requirement (3) because of small denominators appearing in S_n. Consequently, the usual CT scheme based on a λ^n ordering is not applicable under this condition.

In [36] it was proposed to extend the condition of CT to the following more general form: $[\tilde{H}, \mathcal{A}] = 0$ where $\mathcal{A}$ called *modelling operator* determines the final model of an effective Hamiltonian. To meet the requirements of CT, the modelling operator has to commute with the zero-order approximation $[H_0, \mathcal{A}] = 0$ so that the CT algebra $\mathbb{L}$ is decomposed in two subsets as follows [127]:

$$\mathbb{L} = \mathbb{L}^{(\mathcal{A})} \oplus \mathbb{L}^{(\perp)}, \text{ where } \quad \mathbb{L}^{(\mathcal{A})} \supset \mathbb{L}^{(0)} \qquad (13a)$$

Here $\mathbb{L}^{(\mathcal{A})}$ contains all operators commuting with $\mathcal{A}$, and $\mathbb{L}^{(\perp)}$ is its orthogonal complement. In practical terms, this means that any operator X involved in CT calculations can be written in a unique way as a sum of two contributions $X = X^{(\mathcal{A})} + X^{(\perp)}$, where $X^{(\mathcal{A})}$ belongs to the subset $\mathbb{L}^{(\mathcal{A})}$. With respect to the definition (13a) one can then define an operation $< \ldots > \equiv < \ldots >_{\mathcal{A}}$ of the extraction of the $\mathbb{L}^{(\mathcal{A})}$-contribution from any operator of CT :

$$< X >= X^{(\mathcal{A})}, \text{ where } \qquad X^{(\mathcal{A})} \in \mathbb{L}^{(\mathcal{A})} \qquad (13b)$$

Using these notations one can formalize a simplification provided by CT as follows. Consider an initial Hamiltonian (2), for which the expansion terms H_n belong to $\mathbb{L}$. The transformations aim at converting H to a unitary equivalent operator $\tilde{H}$, which would belong to a limited and hence more simple subset $\mathbb{L}^{(\mathcal{A})}$. Using the operation (13b) this can be expressed in the following equivalent way:

$$\tilde{H} = < \tilde{H} > \quad \text{or} \qquad \tilde{H} \in \mathbb{L}^{(\mathcal{A})} \qquad (14)$$

that implies the same condition for all corrections $\Delta\tilde{H}_n = < \Delta\tilde{H}_n >$.

In the recurrence scheme of the previous Section 2.1 the S_n generators of CT were not yet explicitly defined. One can do this by imposing the condition (14). At the first order CT one should consider k=n=1. Substituting this to Eqs. (9), (12) one obtains the following system of equations for the first-order CT iteration:

$$[H_0, iS_1] = H_1 - \Delta\tilde{H}_1 \qquad (15a)$$

$$\Delta\tilde{H}_1 = < \Delta\tilde{H}_1 > \qquad (15b)$$

This system of two equations contains two unknown quantities S_1 and $\Delta\tilde{H}_1$. The formal particular solutions are written as follows

$$\Delta\tilde{H}_1 = < H_1 > \qquad (16a)$$

$$iS_1 = \frac{1}{\mathfrak{D}}(H_1) \qquad (16b)$$

where H_1 is known (2), the operation $< \ldots >$ is defined by (13b) and the operation $\frac{1}{\mathfrak{D}}(...)$ makes an inversion of a commutator equation (see the mathematical Appendix I). With an appropriate convention of (13a) these operations $< \ldots >$, $\frac{1}{\mathfrak{D}}(...)$ are well defined on the CT algebra $\mathbb{L}$. They act on operators belonging to $\mathbb{L}$, and for this reason are often called “super-operators” in a

mathematical literature [156]. A way to explicitly calculate their action is discussed in the following sections and in Appendix I.

As soon as S_1 is obtained, one can compute the once transformed Hamiltonian $H^{(1)}$ in a straightforward way and to fill the *k=1* layer of Table 1 using the recurrent relation (12). By repeating the procedure of the Section 2.1 one can determine S_2 that produces the twice transformed Hamiltonian $H^{(2)}$ and so on. Suppose that S_1 , S_2 ,…S_{n-1} generators were determined and successive layers *k=2 , k=3, … k=n-1* of Table 1 were filled this way. This means that all terms up to $H_n^{(n-1)}$ were already calculated. At the next step *k=n* the recurrence scheme (9), (12) gives the system of two equations

$$[H_0, iS_n] = H_n^{(n-1)} - \Delta\tilde{H}_n \tag{17a}$$

$$\Delta\tilde{H}_n = <\Delta\tilde{H}_n> \tag{17b}$$

with a solution

$$\Delta\tilde{H}_n = <H_n^{(n-1)}> \tag{18a}$$

$$iS_n = \frac{1}{\mathfrak{D}}(H_n^{(n-1)}) \tag{18b}$$

Note that Eqs.(16),(18) give a particular solution of CT equations (Appendix I) fixed by a supplementary constraint

$$<S_1> = <S_2> = \ldots = <S_n> = 0 \tag{19}$$

A general solution in discussed in Sect 2.7.

Unitary transformations conserve eigenvalues E of the Hamiltonian, but in many cases the decomposition (13)-(14) can simplify a solution of the new stationary Schrödinger equation $\tilde{H}|\tilde{\psi}>= E|\tilde{\psi}>$ with respect to the initial one $H|\psi>= E|\psi>$. As soon as S_n generators of CT are calculated (18b), the true wave functions $|\psi>$ are related to an effective ones $|\tilde{\psi}>$ as follows

$$|\psi>= e^{-iS_1}e^{-iS_2}...e^{-iS_n}...|\tilde{\psi}> \tag{20}$$

A rather flexible choice of the modelling operator $\mathscr{A}$ and of the decomposition (13a) permit adapting CT to a particular physical problem. This provides a systematic way to build various forms of effective Hamiltonians for a wide class of applications using exactly the same recurrent procedure (12) and the same formal solutions (18).

In many cases $\tilde{H}$ can take block-diagonal forms in the zero-order basis depending on quasi-degeneracy of the energy spectrum and on the definitions of resonances (§§2.6,2.7,8,9). For this reason the operation $<\ldots>\equiv<\ldots>_{\mathscr{A}}$ can be called *block-diagonal part extraction* operation. If $\mathscr{A}$ depends on a part of coordinates only, the CTs result in a full or in a partial separation of molecular variables (§3.1). Using a particular definition of $\mathscr{A}$ one can apply this formulation of CT to time-depending problems (§3.2).

2.3 Generalisation of Wigner theorem

In the standard Rayleigh-Schrödinger perturbation theory one often applies the Wigner theorem: if a wave function is known up to n-th order approximation ${}^{(n)}\psi = \psi + O(\lambda^{n+1})$ then the

diagonal matrix element of the Hamiltonian using $^{(n)}\psi$ gives the energy valid to (2n+1)-order approximation: $E =< {}^{(n)}\psi \mid H \mid {}^{(n)}\psi > +O(\lambda^{2n+2})$. Using remarkable mathematical properties of the operations $< \ldots >$, $\frac{1}{\mathfrak{D}}(...)$ [6], the relations (9),(12) and formal solutions (18) one can extend this result to effective Hamiltonian transformations. For any decomposition (13a) satisfying the conditions of §2.2 the diagonal parts for many recurrent commutator contributions in (12) exactly vanish leading to:

$$\Delta\tilde{H}_n = H_n^{(n)} =< H_n^{(n-1)} >=< H_n^{(n-1)} >= ... =< H_n^{[[n/2]]} > \tag{21}$$

This means that n-times transformed Hamiltonian is directly expressed via results of [[n/2]] transformations only. This result helps economising a lot of computations, and the solutions (18) of CT equations take the form [6]

$$\Delta\tilde{H}_{2k} =< H_{2k}^{(k-1)} > \tag{22a}$$

$$\Delta\tilde{H}_{2k+1} =< H_{2k+1}^{(k-1)} > \tag{22b}$$

$$iS_k = \frac{1}{\mathfrak{D}}(H_k^{(k-1)}) \tag{22c}$$

The Wigner theorem in case of CT can thus be generalised as follows. Suppose that *k* generators of CT S_1 ,…, S_k were calculated according to Eq.(18b). Then the block-diagonal part of the *k*-times transformed Hamiltonian $H^{(k)}$ gives the effective Hamiltonian $\tilde{H}$ valid up to the order $(2k+1)$:

$$\tilde{H} =< e^{iS_k} ... e^{iS_2} e^{iS_1} H e^{-iS_1} e^{-iS_2} ... e^{-iS_k} > +O(\lambda^{2k+2}) \tag{23}$$

The recurrent scheme of CT accounting for the generalised Wigner theorem takes the form of Table 2:

Table 2. General scheme of successive Contact Transformations in the « layer-by-layer » algorithm

	CT		*order* :	λ^0	λ^1	λ^2	λ^3	λ^4	λ^5 $\cdots$	λ^m	$\cdots$	λ^{2m+1}		*effective Hamiltonian*
S ↓	$k=0$	H	=	$\boldsymbol{H_0}+$	$((H_1))+$	H_2+	H_3+	H_4+	$H_5+\cdots$	H_m+	$\cdots$	H_{2m+1}	$\Rightarrow$	$\tilde{H} =< H > +O(\lambda^2)$
S ↓	$k=1$	$H^{(1)}$	=	$\boldsymbol{H_0}+$	$\boldsymbol{H_1^{(1)}}+$	$((H_2^{(1)}))+$	$((H_3^{(1)}))+$	$H_4^{(1)}+$	$H_5^{(1)}+\cdots$	$H_m^{(1)}+$	$\cdots$	$H_{2m+1}^{(1)}$	$\Rightarrow$	$\tilde{H} =< H^{(1)} > +O(\lambda^4)$
S ↓	$k=2$	$H^{(2)}$	=	$\boldsymbol{H_0}+$	$\boldsymbol{H_1^{(1)}}+$	$\boldsymbol{H_2^{(2)}}+$	$((H_3^{(2)}))+$	$((H_4^{(2)}))+$	$((H_5^{(2)}))+\cdots$	$H_m^{(2)}+$	$\cdots$	$H_{2m+1}^{(2)}$	$\Rightarrow$	$\tilde{H} =< H^{(2)} > +O(\lambda^6)$
S ↓	...	...		$\cdots$								$\cdots$		$\cdots$
S ↓	$k=m$	$H^{(k)}$	=	$\boldsymbol{H_0}+$	$\boldsymbol{H_1^{(1)}}+$	$\boldsymbol{H_2^{(2)}}+$	$\boldsymbol{H_3^{(3)}}+$	$\boldsymbol{H_4^{(4)}}+$	$\boldsymbol{H_5^{(5)}}+\cdots$	$\boldsymbol{H_m^{(m)}}+$	$\cdots$	$((H_{2m+1}^{(m)}))$	$\Rightarrow$	$\tilde{H} =< H^{(m)} > +O(\lambda^{2m+2})$

The terms shown with boldface font are completely block-diagonalized by CT and are thus equal to corresponding terms of the effective Hamiltonian. It is not yet the case of the terms shown in double parentheses ((…)) , but their block-diagonal parts <((…))> also produce direct contributions to $\tilde{H}$ according to generalized Wigner theorem.

For any Lie algebra decomposition satisfying the conditions of §2.2 one can conclude that only one transformation $exp(iS_1)$ is required in order to calculate third-order $\tilde{H}$, another transformations $exp(iS_2)$ gives fifth-order $\tilde{H}$ and so on, as indicated at the right-hand panel of Table 2.

2.4 Eigen representation in $\mathbb{L}$

For practical computations of S_k and $\Delta\tilde{H}_n$ (22a)-(22c), it is convenient to choose a set of elementary operators $\{\mathbf{e}_r\}$ which form a basis in the $\mathbb{L}$ algebra of CT in such a way that all operators involved in transformations could be expanded in this basis

$$iS_k = \sum_r b_r^k \mathbf{e}_r \qquad\qquad H_n^{(k)} = \sum_r C_r^{n,k} \mathbf{e}_r \tag{24}$$

Here b_r^k and $C_r^{n,k}$ are expansion coefficients. A choice of a basis $\{\mathbf{e}_r\}$ defines a representation in the CT algebra $\mathbb{L}$. The latter can be called canonical representation [6] if

(i) operations $< \ldots >$, $\frac{1}{\mathfrak{D}}(...)$ defined in Appendix I can be easily calculated in this basis

(ii) expansions (24) are finite at a given order or well convergent

The most convenient choice would be an eigen basis $\{\mathbf{e}_r\}$ for operations $< \ldots >$, $\frac{1}{\mathfrak{D}}(...)$ satisfying

$$< \mathbf{e}_r >= \rho_r \, \mathbf{e}_r , \qquad\qquad \frac{1}{\mathfrak{D}}(\mathbf{e}_r) = \kappa_r \mathbf{e}_r \quad , \tag{25}$$

where ρ_r and κ_r are eigenvalues of these operations. Formally an eigenbasis $\{\mathbf{e}_r\}$ always exists. In case of degenerate or quasi-degenerate zero-order approximation of the stationary Schrödinger equation it is formed by "ket-bra" operators $P_{LM} = \sum_{ij} |L,i>_{0\ 0}< M,j|$ (Appendix I)

$$< P_{LM} >= \delta_{L,M} \, P_{LM} , \qquad\qquad \frac{1}{\mathfrak{D}}(P_{LM}) = \frac{1-\delta_{L,M}}{E_L^{(0)} - E_M^{(0)}} P_{LM} \quad , \tag{26}$$

For the latter equation in case of $L=M$ the convention 0/0 = 0 is adopted. With this choice of the basis $\{\mathbf{e}_r\}$ the technique of calculations is similar to that of a conventional perturbation theory involving intermediate summations in quantum numbers. But it is not always the best choice as far as computational effort is concerned. For example, in case of vibration Hamiltonian of semi-rigid molecules it is more convenient to choose the eigen basis formed by elementary operators $\mathbf{e}_r = a_i^+ \ldots a_j^+ a_l \ldots a_t$ where a_i^+ and a_i are creation and annihilation operators for harmonic oscillator normal modes (§ 5.3). The latter choice allows avoiding intermediate summations in quantum numbers. Consequently, expansions (24) are finite ones. Similar properties apply for elementary operators $\mathbf{e}_r = b_i^+ \ldots b_j^+ b_l \ldots b_t$ involved in CT of multi-fermion systems [6].

Suppose that for a considered problem there exist an eigen basis (25) in the CT algebra $\mathbb{L}$ satisfying the condition (ii). In this case a computation of S_k generators of CT reduces to a trivial operation of a multiplication by ρ_r numbers. Eqs (18,21,22) thus give

$$iS_n = \sum_r (\rho_r C_r^{n,n-1}) \, \mathbf{e}_r , \qquad\qquad \Delta\tilde{H}_n = \sum_r (\kappa_r C_r^{n,[[n/2]]}) \, \mathbf{e}_r \tag{27}$$

Coefficients $C_r^{n,[[n/2]]}$, $C_r^{n,n-1}$ are calculated through the recurrent relation

$$C_r^{n,k} = \sum_{m=1}^{[[n/k]]} \sum_{i_1 \ldots i_{m+1}} (\rho / m!) \, \tau^r_{i_1 \ldots i_{m+1}} C_{i_1}^{k,k-1} \ldots C_{i_m}^{k,k-1} C_{i_{m+1}}^{n-km,k-1} \quad , \tag{28}$$

following from Eq.(12). Here $\rho = \rho_{i_1}\rho_{i_2}...\rho_{i_{m+1}}$ and $\tau^r_{i_1...i_{m+1}}$ are structural constants of the CT algebra $\mathbb{L}$ defined as

$$[\mathbf{e}_i,...[\mathbf{e}_j,\mathbf{e}_t]] = \sum_r \tau^r_{i...jt}\mathbf{e}_r \tag{29}$$

Recurrent relations (28) contain numerical coefficients only and can be programmed in order to fill successive layers of Table 2. This provides a possible computer assisted calculation scheme [113, 115] for a derivation of effective Hamiltonian as an analytical function of elementary operators $\mathbf{e}_r$.

With respect to the decomposition (13a), the basis set (25) can be divided in two subsets

$$\{\mathbf{e}_r\} = \{\mathbf{e}_t^{(\mathcal{A})}\} \oplus \{\mathbf{e}_s^{(\perp)}\} \tag{30}$$

where $\mathbf{e}_t^{(\mathcal{A})} \in \mathbb{L}^{(\mathcal{A})}$ and $\mathbf{e}_s^{(\perp)} \in \mathbb{L}^{(\perp)}$. Simplifications due to CT can be summarized as follows

$$H = \sum_{r\in R} C_r\mathbf{e}_r \quad \Rightarrow CT \Rightarrow \quad \tilde{H} =< \tilde{H} >= \sum_t \tilde{C}_t\mathbf{e}_t^{(\mathcal{A})} \tag{31}$$

An initial non-transformed Hamiltonian H does not obligatory contain all operators of the algebra $\mathbb{L}$. That is why the first summation in Eq.(31) can be restricted by a certain subset of indices $R=\{r_1,r_2,...\}$. But H usually contains some "inconvenient" terms belonging to $\mathbb{L}^{(\perp)}$ that we do not want to find in a simplified effective model. In the transformed Hamiltonian $\tilde{H}$ these terms are systematically removed in such a way that the eigen values E of the Hamiltonian remain unaltered. In case of the condition (19) all S_n contain elementary operators $\{\mathbf{e}_s^{(\perp)}\}$ only. For the sake of simplicity we did not impose here conditions of hermicity or time reversal invariance on elementary operators $\mathbf{e}_r$ but the above procedure can be easily extended for linear combinations of $\mathbf{e}_r$ preserving these properties (§ 5.3).

Note that if a canonical representation satisfying conditions (i),(ii) exists, the decomposition (13) and the form of effective Hamiltonians can be defined by choosing a list of elementary operators $\{\mathbf{e}_t^{(\mathcal{A})}\}$ which are expected to be involved in $\tilde{H}$ expansion (31). In order to apply the formulation of §2.2 one should include in $\{\mathbf{e}_t^{(\mathcal{A})}\}$ a subset of all operators commuting with H_0.

2.5 Degenerate zero-order approximation

In case of a *non-degenerate spectrum* of H_0 the standard choice of the modelling operator $\mathcal{A} = H_0$ results in a transformed Hamiltonian which is *fully diagonal in the zero-order wave functions*: $_0< i \mid \tilde{H} \mid j >_0 = E_i\delta_{i,j}$. True energies E_i of stationary states of the system are represented by diagonal elements of this matrix. Another natural choice would be $\mathcal{A} = P_n = \mid n >_{0\,0}< n \mid$. With this latter choice only one stationary state corresponding to E_n is isolated by transformations (7)-(23) and CTs give power series expansions in λ^n, which are very similar to the conventional Rayleigh-Schrödinger perturbation theory.

In case of a *degenerate spectrum* of H_0 the choice $\mathcal{A} = H_0$ results in a transformed Hamiltonian which is *block-diagonal in the zero-order wave functions*:

$$\tilde{H} = <\tilde{H}> = P_0\tilde{H}P_0 + P_1\tilde{H}P_1 + ... + P_n\tilde{H}P_n + ..., \qquad [\tilde{H}, H_0] = 0 \tag{32}$$

where $P_n = \sum_i |n,i>_{0\,0}<n,i|$ are projectors on eigen subspaces $\Gamma_n^{(0)}$ of zero-order stationary states $|n,i>_0$ (see Appendix A1 for notations). All operators $\mathbf{e}_s^{(\perp)}$, which possess nonzero off-diagonal matrix elements ${}_0<m,j|\mathbf{e}_s^{(\perp)}|n,i>_0 \neq 0$ for $m \neq n$ are removed by CTs. Every term in the expansion (32) corresponding to a block in the matrix ${}_0<n,j|\tilde{H}|n,i>_0$ can be considered as an effective Hamiltonian

$$\mathcal{H}_n^{eff} = P_n\tilde{H}P_n \tag{33}$$

defined on a corresponding subspace $\Gamma_n^{(0)}$ spanned by zero-order wave functions.

Another choice $\mathcal{A} = P_n$ results in $\tilde{H}$ having only one isolated block (33) but $P_m\tilde{H}P_r \neq 0$ for $m,r \neq n$. The latter form of the transformed Hamiltonian is sometimes called *even* form [167].

2.6 Near degenerate case

In case of quasi-degenerate zero-order energies $E_{n_1}^{(0)} \approx E_{n_2}^{(0)} \approx ... \approx E_{n_s}^{(0)}$, one cannot apply the conditions $[\tilde{H}, H_0] = 0$ or $[\tilde{H}, P_n] = 0$ of the previous Section because successive CTs would not converge due to small energy denominators in Eqs. (26). The sub-algebra $\mathbb{L}^{(\mathcal{A})}$ of CT has to be extended in this case. One can define the modelling operator as a projector $\mathcal{P}_{\mathcal{E}}$ on a $\mathcal{E}$*-polyad of near degenerate states* corresponding to a set of closely lying zero-order energies

$$\mathcal{A} = \mathcal{P}_{\mathcal{E}} \equiv P_{n_1} + P_{n_2} + ... + P_{n_s} \tag{34}$$

CTs (7)-(22) isolate then an extended $\mathcal{E}$-block in the transformed Hamiltonian corresponding to this polyad $\mathcal{H}_{\mathcal{E}}^{eff} = \mathcal{P}_{\mathcal{E}}\tilde{H}\mathcal{P}_{\mathcal{E}}$. The transformation results in an effective model that explicitly contains coupling elements $<\psi|\mathcal{H}_{\mathcal{E}}^{eff}|\psi'>$ between states of the same symmetry type belonging to this polyad $\psi, \psi' \in \mathcal{E}$. These intra-polyad couplings describe effects which are often called *accidental resonance* perturbations. They cannot be accounted for by small transformations and their contributions are usually calculated using a numerical diagonalisation of the matrix of $\mathcal{H}_{\mathcal{E}}^{eff}$. The advantage is that the matrix of $\mathcal{H}_{\mathcal{E}}^{eff}$ built in a simple zero-order basis has usually much lower dimension then the matrix of *H* built in the same basis. In many cases this allows reducing infinite dimensional matrices of initial Hamiltonians to finite dimensional matrices of effective polyad Hamiltonians.

If there are several quasi-degenerate polyads $\mathcal{E}_M$ it is convenient to use CT in order to isolate all these polyads simultaneously:

$$\mathcal{A} = \sum_M \alpha_M \mathcal{P}_{\mathcal{E}_M} \quad \Rightarrow \quad \tilde{H} = <\tilde{H}> = \sum_M \mathcal{P}_{\mathcal{E}_M}\tilde{H}\mathcal{P}_{\mathcal{E}_M} \tag{35}$$

Here eigen values α_M of $\mathcal{A}$ can be arbitrarily chosen. A convenient choice would be mean values of energies for corresponding quasi-degenerate clusters. If all α_M are chosen distinct (to be different) the polyads $\mathcal{E}_M$ are treated separately, if two of them coincide $\alpha_M = \alpha_L$ the transformation accounts for an overlapping of polyads $\mathcal{E}_M$ and $\mathcal{E}_L$.
Alternative formulations of the perturbation theory in terms of projector operators were described in [26-28,30-31,34, 134,167-170].

2.7 Ambiguities, particular cases and relations with other formulations of degenerate perturbation theory

A derivation of effective Hamiltonians is a fundamentally ambiguous procedure. This is because of a possibility of an additional unitary transformation within a subspace $\mathcal{E}$, which can modify parameters and effective eigen functions but not eigen values of $\mathcal{H}_{\mathcal{E}}^{eff}$. In the context of degenerate and quasi-degenerate perturbation theory for vibration-rotation polyad models the related ambiguities have been studied in [174-179]. In our formulation of CT the ambiguity of $\mathcal{H}_{\mathcal{E}}^{eff}$ originates from three sources. *First*, for a given definition of the zero-order approximation and the Hamiltonian development (2) it is possible to choose a modelling operator $\mathcal{A}$ in different ways in order to build an effective Hamiltonian $\mathcal{H}_{\mathcal{E}}^{eff}$ on the same subspace $\mathcal{E}$. *Second*, the condition (19) selects a particular solution of CT equations. This condition simplifies calculations but is not obligatory. For a chosen decomposition of the CT algebra (13) a general solution (Appendix I) of CT equations (17a)-(17b) takes the form

$$\Delta\tilde{H}_n = < H_n^{(n-1)} > + [H_0, < iz_n >] \tag{36a}$$

$$iS_n = \frac{1}{\mathfrak{D}}(H_n^{(n-1)}) + < iz_n > \tag{36b}$$

where $< z_n > \in \mathbb{L}^{(\mathcal{A})}$ are arbitrary hermitian operators of the order λ^n . This is because CT equations impose a definite condition on the part of S_n which belongs to $\mathbb{L}^{(\perp)}$ only whereas a choice of their $\mathbb{L}^{(\mathcal{A})}$ contributions remains free.

It can be shown [6, 36] that with particular choices of conditions for block-diagonal parts of generators of Contact Transformations $< S_n > = < z_n >$ and of the modelling operator $\mathcal{A}$ one can easily obtain from $\tilde{H}^{(CT)} = \tilde{H}(z_1, ...z_n ...; \mathcal{A})$ the expansions of other formulations of degenerate and quasi-degenerate perturbation theory [26-28, 30, 167-169]. Finally, a reordering of the perturbation expansion terms H_n ($n > 1$) in the initial Hamiltonian (2) also produces changes in the transformed Hamiltonian at third-order and higher order terms [6]. All these three sources of ambiguities result in different but unitary equivalent hermitian effective Hamiltonians. The relations among various formalisms of effective Hamiltonians have been described by Klein [31], Jorgensen [34] , Tyuterev [33] and Watson [171].

This has permitted explaining apparent contradictions in empirically fitted effective ro-vibrational Hamiltonian belonging to the same vibrational polyads [172,173]. In order to avoid the ambiguity of EH in practical applications that leads to poorly determinable parameters, the so called procedure of EH reduction [174-177, 10] is commonly applied. Another possibility

would be working with invariant combinations [178-179] of EH parameters , which are independent on the constrains applied on the EH form.

3. Effective separation of variables

The most interesting applications of CT correspond to effective (full or partial) separations of molecular variables. Consider two physically different sets of independent coordinates $x=\{x_1,x_2,...\}$ and $y=\{y_1,y_2,...\}$. The space of wave functions is a direct product $\Gamma=\Gamma_x\otimes\Gamma_y$ where Γ_x is spanned by *ψ(x)* functions and Γ_y is spanned by *φ(y)* functions.

Let us denote $X=\{X_1,X_2,...\}$ and $Y=\{Y_1,Y_2,...\}$ operators acting in these spaces on *x* and *y* coordinates correspondingly following the general scheme discussed in ref. [6]. A full Hamiltonian *H(X,Y)* acts on both types of coordinates. A corresponding stationary Schrödinger equation defined in the full space Γ

$$H(X,Y)\psi_{m\mu}(x,y)=E_{m\mu}\psi_{m\mu}(x,y) \tag{37}$$

usually does not allow for an exact solution. Very often, physical considerations permit defining a set of $\{m\}$ quantum numbers which are mainly determined by *x* type motion and $\{\mu\}$ quantum numbers which are mainly determined by *y* type motion. Suppose that in a zero-order approximation X and Y variables are decoupled

$$H_0=H_0(X)+H_0(Y) \tag{38}$$

and the perturbation $V(X,Y)=H_1(X,Y)+...=\sum_i X_iY_i$ accounts for their coupling.

Let the zero-order equation for the *X* part of the problem be written as

$$H_0(X)\psi^{(0)}_{m_t}(x)=E^{(0)}_m\psi^{(0)}_{m_t}(x), \qquad H_0(X)=\sum_m E^{(0)}_m P^{(X)}_m \tag{39}$$

The $\mathbb{L}$ algebra of CT is a direct product $\mathbb{L}=\mathbb{L}_X\otimes\mathbb{L}_Y$ where $X_i\in\mathbb{L}_X$ and $Y_j\in\mathbb{L}_Y$.

For a partial effective separation of *X* variables using contact transformations one can try a modelling operator of CT which depends on these variables only $\mathcal{A}=\mathcal{A}(X)$. For example

$$\mathcal{A}=P^{(X)}_m \quad \text{or} \quad \mathcal{A}=H_0(X) \tag{40}$$

where $P^{(X)}_m=\sum_t|\psi^{(0)}_{m_t}><\psi^{(0)}_{m_t}|$ is a projector on an eigen subspace of $H_0(X)$. The CT condition $[\tilde{H},\mathcal{A}]=0$ results in a transformed Hamiltonian $\tilde{H}=<\tilde{H}>_x$ which has an isolated block in the Γ_x space corresponding to the projector $P^{(X)}_m$. With the first choice of Eq.(40) this gives $\tilde{H}=P^{(X)}_m\tilde{H}P^{(X)}_m+Q^{(X)}_m\tilde{H}Q^{(X)}_m$ where $Q^{(X)}_m=1-P^{(X)}_m$ is the orthogonal complement to $P^{(X)}_m$ on Γ_x. With the second choice of Eq.(40) the transformed Hamiltonian

$\tilde{H}(X^{(0)},Y)$ contains only those $X^{(0)}$ operators which commute with $H_0(X)$. These $X^{(0)}$ operators are then block-diagonal in the zero-order basis (39) . In both cases the *X* dependence of resulting effective Hamiltonians ${}^{[m]}\mathcal{H}^{eff} = P_m^{(X)}\tilde{H}P_m^{(X)}$ is considerably simplified.

In case of a non-degenerate $E_m^{(0)}$ energy this procedure can provide a full separation of *X* variables. This allows for replacing the initial equation (37) by more simple equation

$$\{{}^{[m]}\mathcal{H}^{eff}(Y)\}\,\Phi_\mu^{[m]}(y) = E_{m\mu}\Phi_\mu^{[m]}(y) \tag{41}$$

defined on Γ_y space only. Here the effective Hamiltonian

$${}^{[m]}\mathcal{H}^{eff}(Y) = <\psi_m^{(0)}(x)\,|\,\tilde{H}(X^{(0)},Y)\,|\,\psi_m^{(0)}(x)> \tag{42}$$

depends on *Y* operators only because the right hand side of (42) corresponds to the integration over *x* coordinates. If CTs converge, then eigen values (41) of ${}^{[m]}\mathcal{H}^{eff}(Y)$ give successive approximations to the true energies with increasing orders of CT. True wave functions are related with effective ones by Eq. (20). This procedure of effective separation of variables applies for those energy ranges where there are no accidental resonances between *x* and *y* motions, which would result in small denominators in Eqs.(26).

3.1 Fast and slow motions

A separation of "fast" (*X*) and "slow" (*Y*) variables is a most common and straightforward application of CT as discussed in [6]. Suppose that characteristic frequencies corresponding to *X* variables are much larger that those for Y variable. This means that $E_{m+1\mu} - E_{m\mu} \ll E_{m\mu+1} - E_{m\mu}$ because changes in *m* quantum numbers correspond to an excitation of *x* motion and changes in μ quantum numbers correspond to an excitation of *y* motion. One can thus assume that the zero-order approximation H_0 is defined by the fast motion. For clarity let us consider a simple case:

$$H(X,Y) = H_0(X) + V(X,Y) \tag{43}$$

It is convenient to formally extend this zero-order approximation on the entire space Γ of $\psi(x,y)$ functions

$$H_0 = \{H_0(X)\}\times 1_Y \tag{44}$$

Eq.(44) emphasize that the choice (43) results in a zero-order spectrum on the $\Gamma = \Gamma_x \otimes \Gamma_y$ space which is degenerate in μ quantum numbers corresponding to slow *Y* variables. Even if the spectrum (39) corresponding to the fast *x* motion is non-degenerate, the total degeneracy remains and is equal to the dimension of the Γ_y space. An effective separation of fast *X* variables is equivalent to a block-diagonalization of the Hamiltonian (43) in the eigen basis of the degenerate zero-order approximation (44). Let a perturbation be written as

$$V(X,Y) = \sum_i X_i Y_i \tag{45}$$

With the standard choice of the modelling operator $\mathcal{A} = H_0(X)$ according to eq.(40) one has

$$< XY > = < X > Y\,, \qquad \frac{1}{\mathfrak{D}}(XY) = \frac{1}{\mathfrak{D}}(X)\cdot Y \tag{46}$$

A straightforward application of CT according to eqs.(7),(12),(22) results in the transformed Hamiltonian expanded in successive orders

$$\tilde{H} = H_0 + \sum_i < X_i > Y_i + \tfrac{1}{4}\sum_{ij}\{< [\frac{1}{\mathfrak{D}}(X_i), X_j]_- > [Y_i, Y_j]_+ + < [\frac{1}{\mathfrak{D}}(X_i), X_j]_+ > [Y_i, Y_j]_-\} + ... \tag{47}$$

which is block-diagonal in the $\psi_{m_t}^{(0)}(x)$ basis. Developing commutators […,…]- and anti-commutators […,…]+ in eq.(47) one readily obtains

$$\tilde{H} = H_0 + \sum_i \mathbf{B}_i Y_i + \sum_{ij} \mathbf{B}_{ij} Y_i Y_j + \sum_{ijl} \mathbf{B}_{ijl} Y_i Y_j Y_l + ... \tag{48}$$

where

$\mathbf{B}_i = < X_i >$,

$\mathbf{B}_{ij} = - < X_i \frac{1}{\mathfrak{D}} X_j >$,

$$\mathbf{B}_{ijl} = \tfrac{1}{2}\{< X_i >< (\frac{1}{\mathfrak{D}} X_j)(\frac{1}{\mathfrak{D}} X_l) > -2 < (\frac{1}{\mathfrak{D}} X_i) X_j (\frac{1}{\mathfrak{D}} X_l) > + < (\frac{1}{\mathfrak{D}} X_i)(\frac{1}{\mathfrak{D}} X_j) >< X_l >\} \tag{49}$$

…

The simplification is due to the fact that all terms $\mathbf{B}_{ijl...} = \mathbf{B}_{ijl...}(X^{(0)})$ in (48),(49) are block-diagonal and thus contain those $X^{(0)}$ operators only which commute with $H_0(X)$.

In case of a non-degenerate spectrum (39) of the fast *x* motion the transformed Hamiltonian (48) is diagonal in $\psi_m^{(0)}(x)$ basis and CT produce a set of effective Hamiltonians for the $E_m^{(0)}$ level set

$$^{[m]}H^{\,eff}(Y) = < \psi_m^{(0)}(x) \,|\, \tilde{H} \,|\, \psi_m^{(0)}(x) > = E_m^{(0)} + \sum_i {}^{[m]}c_i Y_i + \sum_{ij} {}^{[m]}c_{ij} Y_i Y_j + \sum_{ijl} {}^{[m]}c_{ijl} Y_i Y_j Y_l + ... \tag{50}$$

acting on *y* coordinates only. *A full separation of X variables* is thus achieved. Parameters of these effective Hamiltonians calculated as $^{[m]}c_{ijl...} = < \psi_m^{(0)}(x) \,|\, \mathbf{B}_{ijl...} \,|\, \psi_m^{(0)}(x) >$, depend on *m* quantum numbers corresponding to the fast *x* motion .

In case of a two-fold degenerate or near-degenerate level corresponding to the *x* motion the terms $\mathbf{B}_{ijl...}$ involved in eq.(48) can be seen as 2×2 matrices in the $\psi_{m_t}^{(0)}(x)$ basis. For three-fold (near)-degenerate $E_m^{(0)}$ levels 3×3 matrices $\mathbf{B}_{ijl...}$ appear in the expansion (48) etc. Off-diagonal terms describe an *X*-*X* or *X*-*Y* coupling. In general, the CT method results in a partial separation of fast variables that allows decreasing the dimension of the eigen values problem.

A similar procedure for generalised form of Rayleigh-Schrödinger perturbation theory has been considered by Cassam-Chenai [170].

3.2 Some examples

- *Separation of vibration variables in the vibration-rotation Hamiltonian.*

Vibrations of a semirigid molecule described by nuclear displacement coordinates $x=\{q_1,q_2,...\}$ correspond to the fast motion compared to slower rotational motion described by Euler angles $y=\{\varphi,\theta,\chi\}$ which relate spaced-fixed and molecular-fixed axis systems. Vibration-rotation Hamiltonian $H(X,Y)$ = $H_{vib\text{-}rot}$ involves vibration operators $X_i=\{C_{jk...rt...}q_jq_k...p_rp_t...\}$ and rotational operators $Y_i=\{1,J_\alpha,J_\beta J_\gamma,...\}$. Here $C_{jk...rt...}$ are molecular parameters, p_r , p_l , …are vibration momenta corresponding to q_r , q_l , … and J_α , J_β …are angular momentum components acting on Euler angles [110]. Quantum numbers m involved in Eqs.(39)-(50) are quantum numbers m=v={v_1,v_2,…} of a zero-order vibration model. CT transform $H_{vib\text{-}rot}$ to effectives Hamiltonians for individual isolated vibration states or for sets (polyads) of coupled vibration states. In case of a non-degenerate vibration state the resulting effective Hamiltonian (50) is a pure rotational operator ${}^{[v]}\mathcal{H}^{eff}_{rot}(J_x,J_y,J_z)$. The eigen value problems is thus considerably simplified because a full separation of vibration variables is achieved in this case. For near degenerate vibrations, the off – diagonal matrix elements $<\psi_v^{(0)}|\mathbf{B}_{ijl...}|\psi_{v'}^{(0)}>$ provide expressions for resonance coupling parameters within a polyad of vibration states. This type of separation of vibration variables have been widely used in the literature on high-resolution molecular spectroscopy as reviewed by Amat, Nielsen et al. [2,3] , Makushkin and Tyuterev [6], Aliev and Watson [7], Camy-Peyret and Flaud [8], Sarka and Demaison [10]. (see also [15, 120, 126, 129, 134] and references therein).

The vibration polyad structure related to Darling-Dennison and Fermi resonances in triatomic molecules, as well as the mixing of zero-order wave functions induced by these resonance interactions are discussed in the following Sections. Application of CT formulation described in Sections 2-4 allows for building accurate non-empirical rotational and ro-vibrational H^{eff} from potential energy functions [15,39,134]. A spectroscopic accuracy similar to variational calculations can be achieved in case of semi-rigid molecules thanks to an account of high-order contributions.

- *Separation of electronic variables in the electronic-nuclear Hamiltonian.*

In this case $x=r=\{r_i\}$ are electronic and $y=R=\{R_n\}$ are nuclear coordinates of a molecule, $X=\{r_i,\partial/\partial r_j\}$ and $Y=\{R_n,\partial/\partial R_k\}$ being electronic and nuclear operators. The well-known difficulty [12] for the standard Rayleigh-Schrödinger perturbation theory is that zero-order Born-Oppenheimer (BO) electronic energies $E_e^{(0)}(R)$ depend on vibrational coordinates $\{R_n\}$. Matrix elements of the electronic-nuclear interaction terms over BO wave functions are nuclear operators Y and thus do not commute with energy denominators $(E_e^{(0)}(R)-E_{e'}^{(0)}(R))^{-1}$. CT correctly account for the ordering of terms in the perturbation expansion. A natural choice of the modelling operator is a projector on an isolated BO electronic state $\mathcal{A}=P_e^{(R)}$ which depends parametrically on internuclear distances R. Though simple properties (43),(46) do not apply in this case, the recurrent relations of CT (7)-(12) and the general solutions (18)-(22) remain valid with explicit expressions for the action of $<\dots>$, $\frac{1}{\mathfrak{D}}(...)$ operations on electronic-nuclear terms given in [6]. Their straightforward application allows reproducing expressions for effective

rotaton-vibration Hamiltonian ${}^{[e]}\mathcal{H}^{eff}(R_n, \partial/\partial R_k)$ for the ground electronic state $|e>$ derived by Bunker and Moss [12] and by Schwenke [13] up to the second order. First order corrections produce adiabatic contributions and second order terms account for non-adiabatic coupling of electronic states. These contributions prove to give significant contributions to ro-vibration energies [12-13, 180,181] much larger than experimental accuracy of high-resolution molecular spectroscopy. Using the recurrent scheme of table 2 one could derive higher order corrections in a systematic way, though the calculations rapidly become very involved with increasing orders.

- *CT for time-dependent problems*

The formulation of CT described above can be also applied to some time-dependent problems. An example is a simplification of evolution operator *U(t)* for the resonance interaction between quantum electromagnetic field and *n*-level atomic or molecular system [161]. Assuming atomic units ($\hbar = 1$) the initial Schrödinger equation reads $i\frac{\partial}{\partial t}U' = (H_0 + W(t))U'$ where H_0 is the Hamiltonian of the model system and the field whereas *W(t)* describes their interaction. In the interaction representation it takes the form $\{-i\frac{\partial}{\partial t} + V(t)\}U = 0$ where $U = exp(iH_0)U'$ and $V(t) = exp(iH_0 t)W(t)exp(-iH_0 t)$. One can apply the CT method to the operator $L = -i\frac{\partial}{\partial t} + V(t,Y)$ in quite a similar way, were *Y* stands for molecular variables. Replacing *H* by *L* in eqs.(1)-(23) we write $\tilde{L} = T^{+}LT = -i\frac{\partial}{\partial t} + \mathcal{V}$. By choosing the modeling operator as $\mathcal{A} = -i\frac{\partial}{\partial t}$ one applies the condition $[\tilde{L}, \mathcal{A}] = 0$ of Section 2.2 equivalent to $\partial\tilde{L}/\partial t = 0$ as suggested by Zakharov and Tyuterev [110,114,161]. Under certain assumptions [6, 109,114,161] this permits obtaining the CT expansion for the *time independent* effective interaction $\mathcal{V} = const(t)$.

Relations of Sections 2.1, 2.3 and the scheme of Table 2 are valid in this case. Unlike the operator $V(t,Y)$ the effective one $\mathcal{V} = \mathcal{V}(Y)$ depends on molecular variables only. In this example $X = \{t, \frac{\partial}{\partial t}\}$ and the CT $L \Rightarrow \tilde{L}$ aims at effective separation of time: $V(t,Y) \Rightarrow \mathcal{V}(Y)$. The transformed Schrödinger equation $\{-i\frac{\partial}{\partial t} + \mathcal{V}\}\tilde{U} = 0$ has then an obvious solution $\tilde{U}(t) = exp(-i\mathcal{V}\cdot(t - t_0))$. The evolution operator takes the form $U = T\cdot\tilde{U}$. Secular terms corresponding to resonance effects are all gathered in the $\tilde{U}$ operator whereas *T* can be represented by a convergent expansion without small denominators. This is equivalent to the summation of secular terms in Dyson [182] and Magnus [183] expansions and simplifies the study of multiphoton processes [161]. Alternative formulations for time-dependent equations have been considered by Jauslin et al. [162-164].

4. Optimized algorithm

In general, a calculation of a commutator is more computationally expensive operation than a summation and gathering of similar terms. A recurrent algorithm of CT can be further optimised by re-arranging and gathering terms at intermediate steps before commutator contributions are computed. In order to minimise an amount of computations the recurrence relation (12) can be re-written as

$$H_n^{(k)} = [\underbrace{i S_k, [iS_k, ...[iS_k}_{L-1}, F_1^{(k-1)} + F_2^{(k-1)}\,] + ... + F_L^{(k-1)}\,], \tag{51}$$

where $n > k$ and operators $F_1^{(k-1)}, F_2^{(k-1)}, ..., F_L^{(k-1)}$ are known from previous steps of CT and will be defined below. The generator iS_k of the k-th layer of CT is calculated according to Eqs.(22c).

The number of the commutators in Eq.(51) is *L-1*. The value of L and the expressions for the operators $F_m^{(k-1)}$ are calculated according to the values of two parameters $l = \lfloor n/k \rfloor$ and $\tau = n - kl$.

If $\tau \neq 0$ then $L = l+1$ and

$$F_m^{(k-1)} = \frac{1}{(l-m+1)!} H_{k(m-1)+\tau}^{(k-1)}, \tag{52}$$

If $\tau = 0$ then $L = l$ and

$$F_1^{(k-1)} = \frac{1}{l!}[(l-1)H_k^{(k-1)} + \langle H_k^{(k-1)} \rangle]\ , \qquad \text{and } F_m^{(k-1)} = \frac{1}{(l-m)!} H_{km}^{(k-1)}, \quad m > 1 \tag{53}$$

This algorithm allows faster calculations than those based on initial eqs.(11)-(12). The general "layer-by-layer scheme" of Table 2 is still valid and allows systematic CT up to a given order n_{max}. This part of the algorithm is applicable to all types of quantum-mechanical problems for bond stationary non-degenerate, degenerate or near-degenerate state calculations provided that a perturbation is sufficiently small and the usual conditions of the validity of the perturbation theory are fulfilled.

Trees of CT contributions

Suppose that one wishes to derive $\mathscr{H}^{eff}$ up to the order n_{max}. By substituting $n = n_{max}$ in eq.(21) and using the recurrent relations (22),(51) it is easy to see that not all terms in lower layers of Tables 1,2 are necessary for this calculation. In order to build a scheme involving the tree of required $H_m^{(l)}$ terms we have to start from the highest layer $k_{max} = [[n_{max}/2]]$ and decrease the layer number progressively: $k = k_{max}-1, k_{max}-2$ … down to k=0.

5. Molecular vibrations

In the next sections we apply the above described algorithm of high-order CT to molecular vibrational and rotational calculations. In recent decades, much effort has been devoted to calculation of quantum vibrational energy levels of polyatomic molecules from ab initio or empirical potential energy functions. A number of "non-perturbational" methods are available [184-215] (and references therein) that aim at an accurate numerical solving of the nuclear motion problem in molecules. This includes variational methods using either exact kinetic energy operator (KEO) operator or its approximations [184-204], discrete variable representation (DVR) method [205-210], the filter diagonalization techniques [211,212] , Multi Configuration Time Dependent Hartree (MCTDH) calculations [212, 214] and some other computational techniques. More extensive list of references can be found in [215]. The advantage of some of these methods is that they offer a large choices of coordinates and are applicable to non-rigid molecules. But computational expenses of variational methods using exact KEO scale vary rapidly with the number of vibrational modes and they suffer from the basis set convergence issues. This concerns also DVR methods.

There exist also various implementations of the perturbation theory for calculation of vibration levels [4,5, 134, 170, 216-221], which are computationally less expensive than variational and DVR methods. Carter, Bowman and co-workers [222-224] have developed MULTIMODE code using self-consistent field method and an expansion of the potential energy function in normal coordinates. In this section we review the normal mode approach in the CT method which had been developed in many earlier works [2,3,6-10, 32, 36, 117-142] in the context of the general formalism of Sections 2-6.

In further Section 8-13 we compare our calculations with variational and DVR results as a benchmarks in order to study the convergence of CT. In the considered test-examples of semi-rigid molecules, a systematic account of high-order terms permits converging CT to very accurate results in a large domain of energies, whereas calculations prove to be very fast. Unlike most of variational and DVR methods the present approach is purely algebraic one and the major part of calculations which involves operators is done analytically.

5.1. Normal modes

The general expression for the vibration-rotation Eckart frame molecular Hamiltonian in normal coordinates has been derived by Watson [225, 226] based on previous work of Wilson and Howard [227] and Darling and Dennison [228]. It is convenient to divide Hamiltonian and the energy by *hc* and all momenta by $\hbar$ in order to convert all quantities in units traditionally used in molecular spectroscopy. The vibration (J=0) part of this Hamiltonian of a non-linear molecule expressed in wavenumber units [*E/hc*] takes the form

$$H_{\rm vib} = \frac{1}{2}\sum_{k=1}^{3N-6} \omega_k p_k^2 + \frac{1}{2}\sum_{\alpha,\beta} \pi_\alpha \mu_{\alpha\beta} \pi_\beta - \frac{1}{8}\sum_{\alpha} \mu_{\alpha\alpha} + U(q) \qquad , \tag{54}$$

where q = { q_1, …$q_{\rm k}$, …} denotes the set of normal coordinates, $p_k = -i\,\partial/\partial q_k$ is the momentum conjugated to the $q_{\rm k}$ coordinate, $\pi_\alpha = \sum_{i,k} \zeta_{i,k}^{\alpha} \left(\omega_i/\omega_k\right)^{1/2} q_i p_k$ are the Eckart frame components of the vibrational angular momentum, $\zeta_{i,k}^{\alpha}$ are the Coriolis zeta constants, $\mu_{\alpha\beta} = \mu_{\alpha\beta}(q)$ are the elements of the μ tensor, ω_k are the harmonic vibration frequencies and *U(q)* is the molecular potential energy function. Here the operators $q_{\rm k}$, $p_{\rm k}$, π_α and $\zeta_{i,k}^{\alpha}$ constants are dimensionless, $H_{\rm vib}$, U, $\mu_{\alpha\beta}$ and ω_k are expressed in wavenumber units. First three terms in (54) originate from the kinetic energy.

Ab initio electronic structure calculations usually yield the values of the potential energy on a grid of cartesian or internal nuclear coordinates **R**={R_1,R_2 , …R_t ,… } resulting in the potential energy surface (PES) $U(R_t)$ in the configuration space. In order to use an *an initio* or empirical PES with the Hamiltonian (54), a transformation from internal R to normal q coordinates is necessary. Angular internal coordinates R_t are not in general rectilinear in the cartesian space. If a linear approximation R=**L**q described in most of textbooks [110] is used, then the transformation U(R) => U(q) is computationally simple. But the resulting q would be non rectilinear as well, and a simple analytical form of Watson Hamiltonian would not be valid. This makes CT calculations more cumbersome. Here we maintain the Heisenberg vibrational algebra for rectilinear normal coordinates q, though the CT method can also work with curvilinear ones.

A non-linear transformation from internal to rectilinear normal coordinates has been considered by Hoy, Mills and Strey [229]. In the further applications we apply a more straightforward technique of Rey et al [202], which is valid at an arbitrary order

$$R_t = \sum_i L_i^t q_i + \sum_{i,j} L_{ij}^t q_i q_j + \cdots \sum_{i,j,k,\cdots} L_{i,j,k,\cdots}^t q_i q_j q_k \cdots + \cdots + O(q^n) \qquad (55)$$

Note that an account of non-linear terms in Eq. (55) is crucially important in order to achieve a spectroscopic accuracy of calculations.

5.2. Hamiltonian expansion for semirigid molecules

For a semirigid molecule it is usually assumed that *U(q)* and $\mu_{\alpha\beta}(q)$ can be expanded in a series which converge sufficiently rapidly for vibration states under study:

$$U = U_0 + \frac{1}{2}\sum_i \omega_i q_i^2 + \sum_{ijk} k_{ijk} q_i q_j q_k + \sum_{ijkl} k_{ijkl} q_i q_j q_k q_l + \cdots\cdots \qquad (56a)$$

$$\mu_{\alpha\beta} = \mu_{\alpha\beta}^0 \delta_{\alpha\beta} + \sum_i \mu_{\alpha\beta}^i q_i + \sum_{ij} \mu_{\alpha\beta}^{ij} q_i q_j + \sum_{ijk} \mu_{\alpha\beta}^{ijk} q_i q_j q_k + \cdots\cdots \qquad (56b)$$

The first term in Eq.(56b) defines the equilibrium rotational constants $B_\alpha = \mu_{\alpha\alpha}^0 / 2$. To apply the CT procedure, it is necessary to assess the relative orders of magnitude of the various terms. According to Nielsen and Amat [2,3] the small parameter of the expansions (2), (56) is introduced as follows:

$$\lambda \sim \left(\frac{\overline{B}}{\overline{\omega}}\right)^{1/2} \quad \text{and} \quad \left(\frac{k_{i_1 i_2 \cdots i_n}}{\overline{\omega}}\right) \sim \lambda^{n-2} \quad , \quad \left(\frac{\mu_{\alpha\beta}^{i_1 i_2 \cdots i_n}}{\overline{\omega}}\right) \sim \lambda^{n+2} \quad , \qquad (57)$$

where $\bar{B}$ and $\bar{\omega}$ are average values of rotational constants and harmonic frequencies. It is usually assumed that the Nielsen's λ parameter has the same order of magnitude as the Born-Oppenheimer κ parameter $\lambda \sim \kappa \sim (m_e / \bar{m}_n)^{1/4} \sim 1/10 - 1/30$. The ordering of various terms has been discussed in more detail by Oka [4] and Aliev and Watson [7]. For a semirigid molecule the potential energy function has a relatively deep minimum and the zero order approximation is conveniently described by a sum of uncoupled harmonic oscillators corresponding to normal vibration modes

$$H_0^{vib} = \frac{1}{2}\sum_k \omega_k (p_k^2 + q_k^2) \qquad (58)$$

We shall use the standard ket notations for the zero order eigen vectors $|v^{(0)}\rangle = |v_1^{(0)}\rangle |v_2^{(0)}\rangle \ldots |v_m^{(0)}\rangle$ where v is the set of vibration quantum numbers $v = \{v_1, v_2, \ldots, v_k\}$. According to Amat-Nielsen ordering scheme the order of magnitude of operators is assessed via the orders of magnitude of their matrix elements in the zero order wave functions. For relatively small vibration quantum numbers this implies $q \sim p \sim \sqrt{v} \sim 1$. The Coriolis $\zeta_{i,k}^\alpha$ constants are of order 1, and therefore $\pi_\alpha \sim 1$. The n-th order term of the Hamiltonian expansion for $n > 0$ reads

$$H_n^{vib} = \sum k_{i_1 \cdots i_{n+2}} q_{i_1} \cdots q_{i_{n+2}} + \frac{1}{2}\sum \mu_{\alpha\beta}^{i_0 \cdots i_{n-2}} (\pi_\alpha q_{i_1} \cdots q_{i_{n-2}} \pi_\beta) - \frac{1}{8}\sum (\mu_{\alpha\alpha}^{i_0 \cdots i_{n-2}}) q_{i_1} \cdots q_{i_{n-2}} \qquad (59)$$

The second and the third terms in (59) appear for $n \geq 2$. An alternative description of this procedure is to say that elementary operators $\{p \ldots pq \ldots q,\ q \ldots qp \ldots p\}$ form a basis for H expansion in the $\mathbb{L}$ algebra introduced in Sections 2.2 -2.4 because π_α operators are expressed in terms of *qp* products. But this basis in not the most convenient one for high-order CT calculations.

5.3. Vibrational operator eigen basis and vibrational algebra

In order to simplify CT computations, it is convenient to rewrite the expansions (56, 59) in terms of the creation and annihilation operators (a^+, a) of vibration normal mode quanta

$$a_i^+ = \frac{1}{\sqrt{2}}(q_i - ip_i), \qquad a_i = \frac{1}{\sqrt{2}}(q_i + ip_i), \qquad [a_i, a_i^+] = 1 \tag{60}$$

The products of creation and annihilation operators form a "canonical representation" for CT of the vibration Hamiltonian in a sense discussed in Section 2.4. From a computational point of view one can consider two forms of this representation.

(i) Representation of "running" indices.
The Hamiltonian terms are given by

$$H_0^{vib} = \sum_k \omega_k (a_k^+ a_k + 1/2) = \sum_k \omega_k (N_k + 1/2) \tag{61}$$

$$H_1^{vib} = (1/\sqrt{2})^3 \left\{ \sum_{ijl} k_{ijl} (a_i^+ a_j^+ a_l^+ + 3 a_i^+ a_j^+ a_l) + 3 \sum_{ijj} k_{ijj} a_i^+ \right\} + \{...\}^+ \tag{62}$$

…

$$H_n^{vib} = \left\{ \sum\nolimits^* C^n_{i...jl...m} a_i^+ ... a_j^+ a_l ... a_m \right\} + \{...\}^+ \tag{63}$$

Here $N_k = a_k^+ a_k$ is the "number operator" for a vibration mode. It is diagonal in the zero order wave functions $< v^{(0)} | N_k | v^{(0)\prime} >= v_k \delta_{v,v'}$. The asterisk in the summation of Eq.(63) means that H_n^{vib} contains the products of (a^+, a) operators of the total powers *n+2, n, n-2, …*down to 0 for n even or to 1 for n odd. The superscript "+" stands for hermitian conjugation.

The coefficients $C^n_{i...jl...m}$ depend on anharmonic force constants $k_{rs...t}$. For n>1 they depend also on harmonic frequencies ω_k, the Coriolis $\zeta^\alpha_{i,k}$ constants and the $\mu^{ij...k}_{\alpha\beta}$ parameters. An algorithm of their calculation in an arbitrary order is rather straightforward. Elementary operators $a_i^+ ... a_j^+ a_l ... a_m$ form another basis of expansions in the the $\mathbb{L}$ algebra of CT (Sections 2.2 , 2.4). The advantage is that this is an eigen basis for two fundamental operations <…> and $\frac{1}{\mathfrak{D}}(...)$ involved in the general solutions of the CT equations. With the standard choice $\mathcal{A} = H_0$ we have [36]

$$< \{a_i^+ ... a_j^+ a_l ... a_m\} >= \Delta(\omega) \{a_i^+ ... a_j^+ a_l ... a_m\} \tag{64a}$$

$$\frac{1}{\mathfrak{D}} \{a_i^+ ... a_j^+ a_l ... a_m\} >= \frac{1 - \Delta(\omega)}{(\omega_i + ... + \omega_j) - (\omega_l + ... + \omega_m)} \{a_i^+ ... a_j^+ a_l ... a_m\} \tag{64b}$$

Here the symbol $\Delta(\omega)$ takes the value 1 or 0 depending on the coincidence of the combinations of harmonic frequencies:

$$\Delta(\omega) = \delta_{(\omega_i + ... + \omega_j), (\omega_l + ... + \omega_m)} \tag{65}$$

As in Section 2.4 the convention 0/0 = 0 is adopted for Eq. (64b). The calculation of S_k generators of CT (18b) is thus straightforward. For example, one immediately obtains the first generator (16b) of CT:

$$iS_1^{vib} = \frac{1}{\mathfrak{D}}(H_1^{vib}) = (1/\sqrt{2})^3 \left\{ \sum_{ijl} \frac{k_{ijl} a_i^+ a_j^+ a_l^+}{\omega_i + \omega_j + \omega_l} + 3 \sum_{ijl}{}^{\#} \frac{k_{ijl} a_i^+ a_j^+ a_l}{\omega_i + \omega_j - \omega_l} + 3 \sum_{ijj} \frac{k_{ijj} a_i^+}{\omega_i} \right\} - \{...\}^+ \tag{66}$$

The symbol $^{(\#)}$ in the summation means that the vanishing or resonance denominators are excluded (see Sections 5.4, 5.5 for more details).

(ii) Representation of "fixed mode" indices

For a computer implementation of CT, it is more convenient to fix indices of operators for each vibration mode. In this convention, the expansions (56a), (56b) take the form

$$U = \sum K_{m_1 m_2 m_3 \ldots} q_1^{m_1} q_2^{m_2} q_3^{m_3} \ldots , \qquad \mu_{\alpha\beta} = \sum \mu_{\alpha\beta;\, m_1 m_2 m_3 \ldots} q_1^{m_1} q_2^{m_2} q_3^{m_3} \ldots \tag{67}$$

An elementary vibration operator of the $\mathbb{L}$ algebra of CT in (a^+, a) representation is written as follows

$$V_{\mathbf{ub}}^{\theta,\Gamma} = \frac{1}{2}\{W_{\mathbf{ub}} + (-1)^{\theta}(W_{\mathbf{ub}})^{+}\}, \quad \text{where } W_{\mathbf{ub}} = (a_1^{+})^{u_1}(a_2^{+})^{u_2}(a_3^{+})^{u_3}\ldots(a_1)^{b_1}(a_2)^{b_2}(a_3)^{b_3}\ldots \tag{68}$$

Here the super-index θ distinguishes hermitian (θ = 0) and anti-hermitian (θ = 1) operators. Γ is a symmetry species (irreducible representation) of a symmetry group of the molecule. The components of formal vectors $\mathbf{u}=\{u_1, u_2, u_3\ldots\}$ and $\mathbf{b}=\{b_1, b_2, b_3\ldots\}$ are integer powers of creation and annihilation operators. For non-degenerte vibrations these vectors unambiguously determine Γ. For example, in the case of a bent triatomic molecule of the C_{2V} group one has: $\Gamma=A_1$ if $u_3+b_3=even$ and $\Gamma=B_1$ if $u_3+b_3=odd$. For triatomics of the C_S group all vibrational operators (68) belong to $\Gamma = A'$.

From Eqs (68) one has the following hermicity properties $(W_{\mathbf{ub}})^{+} = W_{\mathbf{bu}}$ and $\left(V_{\mathbf{ub}}^{\theta,\Gamma}\right)^{+} = (-1)^{\theta} V_{\mathbf{ub}}^{\theta,\Gamma}$ in case of scalar vibration operators. The action of the operations <…> and $\frac{1}{\mathfrak{D}}(\ldots)$ on the elementary vibrational operator (68) reads

$$< V_{\mathbf{ub}}^{\theta,\Gamma} >= \Delta_{\mathbf{ub}}\, V_{\mathbf{ub}}^{\theta,\Gamma} \qquad \text{and} \qquad \frac{1}{\mathfrak{D}}(V_{\mathbf{ub}}^{\theta,\Gamma}) = \frac{1-\Delta_{\mathbf{ub}}}{\boldsymbol{\omega}\cdot(\mathbf{u}-\mathbf{b})} V_{\mathbf{ub}}^{\theta+1,\Gamma} \tag{69}$$

Here $\boldsymbol{\omega} = (\omega_1, \omega_2, \omega_3, \ldots)$ is a formal vector composed of harmonic frequencies. The constant $\Delta_{\mathbf{ub}}$ plays the role of an extended Kronecker symbol taking the values 0 or 1 only. In a non-degenerate or pure degenerate case

$$\Delta_{\mathbf{ub}} = 1 \text{ if } \boldsymbol{\omega}\cdot\mathbf{u} = \boldsymbol{\omega}\cdot\mathbf{b}, \qquad \Delta_{\mathbf{ub}} = 0 \text{ otherwise} \tag{70}$$

Here $\boldsymbol{\omega}\cdot\mathbf{u}$, $\boldsymbol{\omega}\cdot\mathbf{b}$, $\boldsymbol{\omega}\cdot(\mathbf{u}-\mathbf{b})$ denote usual scalar products: $\boldsymbol{\omega}\cdot\mathbf{u} = \omega_1 u_1 + \omega_2 u_2 + \ldots..$For a pure vibrational CT with scalar vibration operators one has

$$H_n^{(k)} = \sum_{\mathbf{ub}} t_{\mathbf{ub}}^{n,k} V_{\mathbf{ub}}^{0,A_1} = \frac{1}{2}\sum_{\mathbf{ub}} t_{\mathbf{ub}}^{n,k}\{W_{\mathbf{ub}} + W_{\mathbf{bu}}\}, \qquad iS_k = \sum_{\mathbf{ub}} s_{\mathbf{ub}}^{k} V_{\mathbf{ub}}^{1,A_1} = \frac{1}{2}\sum_{\mathbf{ub}} s_{\mathbf{ub}}^{k}\{W_{\mathbf{ub}} - W_{\mathbf{bu}}\}, \tag{71a}$$

where the coefficients t and s are real. This follows from hermicity and time reversal properties of CT. The maximum power $\sum(u_i + b_i)$ of vibrational operators in Eq.(71) is $n+2$ for the Hamiltonian term $H_n^{(k)}$ and $k+2$ for S_k generators of CT. After having completed $k-1$ transformations according to the scheme of Sections 2.1, 2.3 one immediately obtains the parameters of the k-th transformation

$$s_{\mathbf{ub}}^{k} = t_{\mathbf{ub}}^{k,k-1}(1-\Delta_{\mathbf{ub}})/(\boldsymbol{\omega}\cdot(\mathbf{u}-\mathbf{b})) \tag{71b}$$

For vibration-rotation CT, other types of operators (68) can be involved in the expansions (7)-(12) and we need to compute vibrational commutators and anti-commutators of a general form

$$[V_{\mathbf{ub}}^{\theta,\Gamma}, V_{\mathbf{u'b'}}^{\theta',\Gamma'}]_{\pm} = \sum {}^{\pm}\tau_{\mathbf{ub,u'b';u''b''}}^{\theta\Gamma,\theta'\Gamma';\theta''\Gamma''} V_{\mathbf{u''b''}}^{\theta'',\Gamma''} \tag{72}$$

From the mathematical point of view ${}^{\pm}\tau_{\mathbf{ub,u'b';u''b''}}^{\theta\Gamma,\theta'\Gamma';\theta''\Gamma''}$ are the structural constants of the $\mathbb{L}$ algebra of CT.

This part of the algorithm is a general one for a semirigid polyatomic molecules. Expressions for commutators of the operators $V_{\mathbf{ub}}^{\theta,\Gamma}$ are given in the Appendix I.

5.3 Non-degenerate case

The simplest case corresponds to non-degenerate vibrations without resonance coupling. The conditions (65), (70) allow non-vanishing diagonal contributions ($\Delta(\omega)=1$) for those terms in the transformed Hamiltonian $\tilde{H}$ which have the same powers of creation and annihilation operators. These contributions can be expressed in terms of the "number operator" $N_k = a_k^+ a_k$ of normal modes

$$< \sum_{ij} C_{ij} a_i^+ a_j >= \sum_{ii} C_{ii} N_i \tag{73}$$

$$< \sum_{ij} C_{ijkm} a_i^+ a_j^+ a_k a_m >= \sum_{i\neq j} (C_{ijij} + C_{ijji}) N_i N_j + \sum_{i\neq j} C_{iiii} N_i (N_i - 1) \tag{74}$$

…

In the representation of "fixed mode" indices on has

$$\Delta\tilde{H}_n = H_n^{(n)} = \sum_{\mathbf{u}} t_{\mathbf{uu}}^{n,n} W_{\mathbf{uu}} = \sum t_{\mathbf{uu}}^{n,n} N_1^{[u_1]} N_2^{[u_2]} ... \tag{75}$$

Only even order corrections are non-vanishing. Here the notation $N^{[m]}$ stands for the factorial polynomial

$$x^{[m]} = x(x-1)...(x-m+1) \text{ for } m \geq 1, \qquad x^{[0]} = 1 \tag{76}$$

The transformed Hamiltonian $\tilde{H} = \sum \Delta\tilde{H}_n = \sum H_n^{(n)}$ is then diagonal in the zero-order harmonic oscillator wave functions $< v^{(0)} | \tilde{H} | v^{(0)\prime} >= E_v \delta_{v,v'}$ and the vibration energies are directly obtained by replacing N_i with vibration quantum numbers v_i

$$E_v = \sum_n E_v^n = \sum_{n,\mathbf{u}} t_{\mathbf{uu}}^{n,n} v_1^{[u_1]} v_2^{[u_2]} ... \tag{77}$$

For the n-th order correction (75) the maximum total power of N_i operators is n/2+1.

This is rather trivial case, which is not of the major interest for molecular physics applications. The results are similar to a conventional perturbation theory, which can be found in standard textbooks on quantum mechanics. A technical difference is that CTs avoid intermediate summations in quantum numbers.

5.4 Degenerate vibrations: irreducible tensor operators

Consider first a twofold degenerate vibration described by the components (q_α, q_β) with $\omega_\alpha = \omega_\beta = \omega$. Eqs. (64a, 69) allow for additional block-diagonal operators $< n_\varphi >= n_\varphi$ and $< n_\varphi^+ >= n_\varphi^+$ where $n_\varphi = a_\alpha^+ a_\beta$ because $\Delta(\omega) = \delta_{(\omega_\alpha),(\omega_\beta)} = 1$. Due to the factor $1 - \Delta(\omega) = 0$ in Eqs.(64b), (69) these operators do not appear in S_k generators of CT but contribute to the transformed Hamiltonian $\tilde{H} = f(N_\alpha, N_\beta; n_\varphi, n_\varphi^+)$. All the equations and the recurrent algorithm of CT remain unaltered. The corresponding effective Hamiltonians are diagonal in the principal quantum number v but not in l quantum number of the zero-order wave functions $|v,l>^{(0)}$.

For molecules of high symmetry, a formulation in terms of irreducible tensor operators (ITO) [11, 14, 116, 202-204, 230-232] is the most suitable one for the description of degenerate vibrations. For example, normal mode vibrations of XY_4 type molecules are fully described by four irreducible tensor coordinates: $\mathbf{q}_1^{A_1} = \{q_1\}, \mathbf{q}_2^{E} = \{q_{2a}, q_{2b}\}$, $\mathbf{q}_t^{F_2} = \{q_{tx}, q_{ty}, q_{tz}\}$ (t=3,4) corresponding to one non-degenerate mode (ω_1), one twofold degenerate mode (ω_2) and two triply degenerate modes (ω_3 and ω_4). The upper indices are the symmetry types of the T_d point group.

In general, let us denote $(\mathbf{a_s})^\Gamma$ tensor annihilation operator with the components $\{a_{s\sigma}, a_{s\sigma'}, ...\}$ and $(\mathbf{a_s^+})^\Gamma$ tensor creation operator with the components $\{a_{s\sigma}^+, a_{s\sigma'}^+, ...\}$. Their components are related to the coordinate and momentum operators by the standard definition (60), and Γ is the irreducible representation of the molecular point group. A tensor product of two irreducible tensor operators $\mathbf{A}^{\Gamma'}$ and $\mathbf{B}^{\Gamma''}$ can be expressed as

$$(\mathbf{A}^{\Gamma'} \times \mathbf{B}^{\Gamma''})_\sigma^\Gamma = \sum_{\sigma,\sigma'} (\Gamma'\sigma, \Gamma''\sigma'' | \Gamma\sigma) A_{\sigma'} B_{\sigma''} \quad , \tag{78a}$$

where $(\Gamma'\sigma, \Gamma''\sigma'' | \Gamma\sigma)$ are the Clebsch-Gordan point group coefficients. For a molecule with k vibration modes the definition of a general elementary vibration operator (68) is extended as

$$W_{\mathbf{um}}^{\eta\Gamma} = \{ \underbrace{((\mathbf{a}_1^+ \times ... \mathbf{a}_1^+)}_{u_1} \times ... \underbrace{(\mathbf{a}_k^+ \times ... \mathbf{a}_k^+))}_{u_k} \times \underbrace{((\mathbf{a}_1 \times ... \mathbf{a}_1)}_{m_1} \times ... \underbrace{(\mathbf{a}_k \times ... \mathbf{a}_k))}_{m_k} \}^{\eta\Gamma} \tag{78b}$$

An unambiguous definition of the operator basis of the CT algebra $\mathbb{L}$ requires a full description of the coupling scheme for all nontrivial intermediate products involved in (79). Here η designate collectively the set of all intermediate coupling indices. Various coupling schemes for T_d, C_{3v} and O_h molecules have been described in detail by Champion et al [11], Zhilinskii et al [116], Nikitin et al [14, 231], Boudon et al [230] and Rey et al [202-204, 232].

All basic equations of CT remain unaltered in the tensorial formalisms. The actions of operations <…> and $\frac{1}{\mathfrak{D}}(\ldots)$ on the elementary vibrational operators (79) are exactly the same as described in the previous sections

$$< W_{\mathbf{um}}^{\eta\Gamma} >= \Delta_{\mathbf{um}} W_{\mathbf{um}}^{\eta\Gamma} \quad , \qquad \text{and} \qquad \frac{1}{\mathfrak{D}}(W_{\mathbf{um}}^{\eta\Gamma}) = \frac{1 - \Delta_{\mathbf{um}}}{\boldsymbol{\omega} \cdot (\mathbf{u} - \mathbf{m})} W_{\mathbf{um}}^{\eta\Gamma} \tag{79}$$

independently of the coupling scheme η and independently of the ordering of $(\mathbf{a_s^+}), (\mathbf{a_s})$ operators in (79). They are also independent of the components of degenerate vibrations.

The procedure of calculation of S_k generators of CT and of $H_n^{(k)}$ terms is thus very similar to a non-degenerate case. A considerable difference concerns only the computation of commutators because this requires a re-coupling of intermediate products in (79) as discussed in [116].

The transformed vibrational Hamiltonian $\tilde{H}$ is much simpler and contains less number of terms than the initial one. In the absence of accidental resonances, it takes the form

$$\tilde{H}^{vib} = C + \sum_s C_s (\mathbf{a}_\mathbf{s}^+ \times \mathbf{a}_\mathbf{s})^{A_1} + \sum_{sm} C_{sm} ((\mathbf{a}_\mathbf{s}^+ \times \mathbf{a}_\mathbf{m}^+) \times (\mathbf{a}_\mathbf{s} \times \mathbf{a}_\mathbf{m}))^{A_1} + ... \qquad (80)$$

Vibration sub-levels of overtone and combination states are obtained by the diagonalisation of the corresponding finite dimensional blocks. This simple example contains some common features for more interesting cases involving the separation of vibration and rotation variables and high-resolution spectra calculations. One of such features is the *vibrational extrapolation scheme* [11], which also applies for accidental resonances considered in the next sections and proves to be very useful in molecular spectroscopy

5.5 Resonances

For near-degenerate vibration states $E_V \approx E_{V'}$ the resonances can occur if the energy separation is not large compared to corresponding coupling matrix elements. Various types of resonances in polyatomic molecules including essential and accidental resonances have been extensively studied in the spectroscopic literature (see [2-11, 15, 41-63, 117-139,232] and references therein). In the zero order approximation the near degeneracy is due to a near coincidence of some combinations of harmonic frequencies $\omega_{b_1} + ... + \omega_{b_k} \approx \omega_{d_1} + ... + \omega_{d_m}$. A corresponding coupling matrix element results from the vibrationally off-diagonal resonance term $h^{res} = a_b^+ ... a_d^+ a_k ... a_m$ appearing in the Hamiltonian expansion (62-(63). The conventional condition $[\tilde{H}, H_0] = 0$ applied on the transformed Hamiltonian $\tilde{H}$ would result to small denominators in S_k generators of CT. In order to avoid a divergence of CT expansions a more general condition $[\tilde{H}, \mathcal{A}] = 0$ can be applied as discussed in Sections 2.2 and 2.6. The modelling operator of CT is naturally introduced as follows:

$$\mathcal{A} = \sum_m \Omega_m a_m^+ a_m , \qquad \text{where} \quad \Omega_{b_1} + ... + \Omega_{b_k} = \Omega_{d_1} + ... + \Omega_{d_m} \qquad , \qquad (81a)$$

which in the case of degenerate vibrations takes the form:

$$\mathcal{A} = \sum_s \Omega_s \{(\mathbf{a}_\mathbf{s}^+)^\Gamma \times (\mathbf{a}_\mathbf{s})^\Gamma\}^{A_1} \qquad (81b)$$

Here constants Ω_i are arbitrary chosen to strictly satisfy the requirement (81a). The relations among ω_i following from the molecular symmetry have to apply for Ω_i as well. All CT equations of the previous sections remain valid with the obvious substitution $\Delta(\omega) \Rightarrow \Delta(\Omega)$. Note that $\mathcal{A}$ is *not* considered here as a zero-order approximation. The operator (81) serves for the transformation condition $[\tilde{H}, \mathcal{A}] = 0$ only. Consequently all CT denominators $[(\omega_i + ... + \omega_j) - (\omega_l + ... + \omega_m)]^{-1}$ keep containing true vibration frequencies ω_t. The resonance terms $h^{res} = a_b^+ ... a_d^+ a_k ... a_m$ corresponding to $\Delta(\Omega) = \delta_{(\Omega_i + ... + \Omega_j),(\Omega_l + ... + \Omega_m)} = 1$ are then considered as block-diagonal ones. In this way the small resonance denominators are automatically excluded from S_k generators (18), (22) due to the factor $1 - \Delta(\Omega) = 0$ in Eqs.(64),(69).

In the representation of fix-mode indices (Section 5.2), this can be summarized as follows. A resonance condition reads

$$(\mathbf{r}-\mathbf{r}')\omega = \sum_i (r_i - r_i')\,\omega_i \approx 0 \qquad \Rightarrow \qquad (\mathbf{r}-\mathbf{r}')\Omega = 0 \tag{82}$$

where the vectors $\mathbf{r}=\{r_1, r_2,\ldots\}$ and $\mathbf{r}'=\{r'_1, r'_2,\ldots\}$ have integer positive components r_i , r'_i. The action of CT operations on elementary resonance terms is very easy to compute

$$h^{res} \equiv h^{res}_{\mathbf{rr}'} = (a_1^+)^{r_1}\ldots(a_k^+)^{r_k}\, a_1^{r'_1}\ldots a_k^{r'_k}\,, \qquad < h^{res} >= h^{res}, \qquad \frac{1}{\mathfrak{D}}(h^{res}) = 0 \tag{83}$$

Several resonance conditions of the type (82) can occur simultaneously. The transformed Hamiltonian $\tilde{H}$ obtained via Eqs. (18), (22) contains hermitian combinations of the vibration number operators $N_k = a_k^+ a_k$, block-diagonal n_φ like terms for degenerate vibrations, and various resonances operators $h^{res(1)}$, $h^{res(2)}$,…

$$\tilde{H} = f(N_i, n_\varphi, h^{res(j)},\ldots,(h^{res(1)})^m (h^{res(2)})^k N_i N_j n_\varphi,\ldots) + f^+(\ldots) \tag{84}$$

An extension of the relations (81)-(84) to molecules of high symmetry groups using the irreducible tensor formalism is straightforward.

The simplest 1:1 resonance occurs due to the condition $\omega_i \approx \omega_j$. For example, this condition generally occurs in bent triatomic XY_2 molecules between symmetric and anti-symmetric stretching vibrations $\omega_1 \approx \omega_3$. This results in the first-order vibration-rotation Coriolis resonances between fundamental vibrational states $\boldsymbol{v}$ =(100) and $\boldsymbol{v}'$=(001). A pure vibrational coupling between these states $h = a_1^+ a_3$ is only allowed for non-symmetric isotopologues with different edge atoms (C_s point groups). For C_{2V} point groups the same condition $2\omega_1 \approx 2\omega_3$ results in the vibrational 2:2 resonance between (200) and (002) states of A_1 symmetry type which is called Darling-Dennison (DD) resonance [228]. The simplest second-order resonance DD term is $h^{DD} = a_1^+ a_3^+ a_1 a_3$. It is not possible to eliminate resonance interaction terms from the Hamiltonian by a small contact transformation (3). This gives rise to subsequent polyads of coupled vibration state. The classical polyad scheme due to 1:1 and 2:2 resonances is described with the polyad number $P = v_1 + v_3$. The series of polyads for v_2=0 contain the following vibration (v_1 v_2 v_3) states:

P=0: {(000)}
P=1: {(100)/(001)}
P=2: {(200)/(101)/(002)}
…
P= v_1 +v_3: {(v_1,0,0)/(v_1-1,0,1)/(0,0,v_3)} (85)
…

According to Eq.(35) the transformed Hamiltonian takes a block-diagonal form in the zero order wave functions (Fig 1). Each block corresponds to an effective Hamiltonian “projected” onto the corresponding polyad sub-space

$$\mathcal{H}_{\mathrm{P}}^{eff} = \mathcal{P}_{\mathrm{P}} \tilde{H} \mathcal{P}_{\mathrm{P}} \tag{86}$$

Here $\mathcal{P}_{\mathrm{P}} = \sum_{v \in \mathrm{P}} |v>^{(0)}\ {}^{(0)}<v|$ is the projector onto the set of zero order wave functions belonging to the polyad P. An application of CT for an accurate derivation of $\mathcal{H}^{eff}$ for the polyads (85) of the water and ozone molecules in comparison with DVR calculations is discussed in Sections 8 and10. Another well-known example is the Fermi resonance $\omega_1 \approx 2\omega_2$ between bending and stretching vibrations {(020)/(100)}, …{(0,v_2,0)/(1,v_2-2,0)/ (2,v_2 -4,0)/…}, …The major coupling is due to the term $h^F = a_1^+ a_2 a_2$. An application of CT for the simultaneous DD and Fermi resonances in SO_2 molecule is discussed in Section 9.

For a case of degenerate vibrations and/or accidental resonances this procedure provides a separation of regular interactions and of secular terms. Regular anharmonic interactions are systematically accounted for by small successive CT. The vibrational extrapolation scheme discussed in Section 5.6 is also valid in this case but is formulated in terms of successive polyads. It is also valid for effective models accounting for resonance interactions. For example, in the case of the polyad scheme (85) the quadratic terms in $\tilde{H}$ specific for the dyad {(100)/(001)} contribute also to the matrix elements of the triad {(200)/(101)/(002)}, tetrad, and all higher polyads. More complicated examples of global analyses of high-resolution spectra using effective models with vibrational extrapolations were considered in [11, 42, 45, 233,234]. The secular problem is solved at once at the very end by the diagonalisation of $\mathcal{H}_P^{eff}$ on the finite dimensional polyad sub-spaces.

An alternative way of defining the polyad scheme is to give a list of all operators belonging to the requested subset $\mathbb{L}^{(\mathcal{A})}$ of the CT algebra as discussed in Section 2.2. This will unambiguously define the operation $< \ldots > \equiv < \ldots >_{\mathcal{A}}$ and thus impose the condition (14) on the desired effective resonance model. Strictly diagonal terms must be necessarily included in this list.

For highly excited vibration states an ***overlapping of polyads*** can occur. The general formulation of CT is still applicable for overlapping polyads. The definition of the subset $\mathbb{L}^{(\mathcal{A})}$ of the CT algebra (14) has to be extended by the explicit inclusion of the inter-polyad resonance coupling terms. The general solutions of CT equations (18a,18b) and the techniques of calculations remain unaltered. The CT operations $< \mathrm{X} > \equiv < \mathrm{X} >_{\mathcal{A}}$ and $\frac{1}{\mathfrak{D}}(X) = \frac{1}{\mathfrak{D}}(X - < X >_{\mathcal{A}})$ are correctly defined in this case as well (Appendix I)

6. Rotational operators

6.1. Elementary operators (“operator basis set”) for the rotational algebra

The angular momentum components J_x, J_y, J_z in the molecular embedded Eckart frame satisfy the following commutation relations

$$[J_\alpha, J_\beta]_- = -ie_{\alpha\beta\gamma} J_\gamma \,, \qquad (97)$$

where $e_{\alpha\beta\gamma}$ is the antisymmetric unitary tensor. Here they are defined as non-dimensional operators by the substitution $J_\alpha \Rightarrow J_\alpha / \hbar$. The molecular fixed ladder components are defined as $J_\pm = J_x \mp i J_y$. For an analytical function *f(x)* the shift-relations [6]

$$J_\pm^n f(J_z) = f(J_z \mp n) J_\pm^n \qquad \text{and} \qquad f(J_z) J_\pm^n = J_\pm^n f(J_z \pm n) \tag{88}$$

play a key role to derive algebraic properties of H_{rot} terms. For the generality of the approach it is appropriate to classify rotational operators according to the irreps A, B_x, B_y, B_z of the D_2 point group $\{E, C_2^x, C_2^y, C_2^z\}$ composed of three orthogonal axes of second orders. The full symmetry properties of the molecule will be accounted for at the final step of the H^{eff} transformations.

An elementary homogeneous polynomials can be characterised using the following labelling: powers of rotational components $J_\pm$, J_z and of $\mathbf{J}^2$ (below *n,m,l*); symmetry species Γ; hermicity index ε distinguishing hermitian (ε = +1) and anti-hermitian (ε = -1) operators; time reversal [15] index τ with τ = +1 for invariant and τ = -1for anti-invariant terms.

R-operators basis set in the D_2 point group.

This type of operator basis set [39] has been often employed for a modelling of high-resolutions spectra of low symmetry molecules as well as on sub-groups of high-symmetry species [15]. The definition was adapted to above explained hermicity and symmetry labelling

$$R_{m,n,2l}^{\varepsilon,\Gamma} = \frac{\kappa}{2}(Z_{+mn} + \varepsilon(-)^\Gamma Z_{-mn})\mathbf{J}^{2l}, \tag{89}$$

where κ is a phase factor, $\mathbf{J}^2 = J_x^2 + J_y^2 + J_z^2$ and "one-rotational-diagonal" operators are defined as

$$Z_{+mn} = J_+^m (J_z + m/2)^n \qquad \text{and} \qquad Z_{-mn} = (J_z + m/2)^n J_-^m, \tag{90}$$

being hermitian conjugate one to the other: $(Z_{+mn})^+ = Z_{-mn}$ and $(Z_{-mn})^+ = Z_{+mn}$. As mentioned above for the sake of generality one can consider the symmetry classification on the D_2 point group independently of the molecular point group according to [15]. Elementary rotational operators (89) fall in two sub-sets corresponding to the symmetry species $\Gamma' = \{A, B_y\}$ and $\Gamma'' = \{B_x, B_z\}$ for which the signs in Eq.(94) are defined as follows:

$$(-)^\Gamma = 1, \text{ if } \Gamma \in \Gamma' \qquad \text{and} \qquad (-)^\Gamma = -1, \text{ if } \Gamma \in \Gamma'' \tag{91}$$

By definition the hermicity index ε verifies the relation $\left(R_{m,n,2l}^{\varepsilon,\Gamma}\right)^+ = \varepsilon\,(R_{m,n,2l}^{\varepsilon,\Gamma})$ and is unambiguously determined by the powers *m, n* of the $J_\pm$, J_z components:

$$\varepsilon = (-1)^{m+n} \tag{92}$$

There are two convenient choices of the phase factor κ in the definition of elementary rotation operators [15].

(α) the simplest choice for which all $R_{m,n,2l}^{\varepsilon,\Gamma}$ have real matrix elements in the standard |J,k > basis set:

$$\kappa = 1 \quad \Rightarrow \quad \tau = (-)^\Gamma \tag{93}$$

However in this case rotational operators of Γ'' symmetry type are anti-invariant under the time reversal and consequently corresponding Hamiltonian parameters would take imaginary values.

(β) the choice for which all $R_{m,n,2l}^{\varepsilon,\Gamma}$ are invariant under the time reversal operation

$$\tau = +1 \quad \Rightarrow \quad \kappa = \begin{cases} 1, & for\ \Gamma = \Gamma' \\ i, & for\ \Gamma = \Gamma'' \end{cases} \tag{94}$$

As the full Hamiltonian H is also invariant under the time reversal, all parameters involved in the Hamiltonian expansion remain real. Though matrix elements of $R^{\varepsilon,\Gamma''}_{m,n,2l}$ in the standard |J,k > basis set are imaginary with this choice, it is possible to convert the Hamiltonian matrix in a real form by an appropriate transformation of the basis set functions.

The exact expressions for commutators and anti-commutators of the operators $R^{\varepsilon,\Gamma}_{m,n,2l}$ given in [39] for Γ' symmetry species could be easily extended to a general case.

$\mathcal{R}$-basis

This operator basis can be viewed as an extention of notations traditionally used in spectroscopic literature for A- reduction [255] of effective rotational Hamiltonian.

$$\mathcal{R}^{\theta,\Gamma}_{m,n,2l} = d\{(J_+^m + J_-^m), J_z^n\}\mathbf{J}^{2l}, \qquad \text{if } \Gamma \in (A_1, B_1) \text{ for } C_{2v} \quad \text{or } \Gamma = A' \text{ for } C_s$$

The hermicity and symmetry species are unambiguously defined by powers *m,n*. For the case defined by Eq. (16a)

$$(-)^{\theta} = (-)^{m+n}, \qquad \Gamma = B_1^{m+n} \text{ for } C_{2v}, \qquad \text{and} \qquad \Gamma = A' \text{ for } C_s$$

The "normalisation constant" *d* is chosen to preserve a simplicity of relations with traditional A-reduction notations[22]: d=1/4 for hermitian terms (θ=0, *m+n=even*) and d=1/2 for anti-hermitian terms (θ=1, *m+n=odd*).

J-basis

This is a standard cartesian component basis introduced by Watson [255]. We denote it as following

$$J^{\theta,\Gamma}_{a,b,c} = d(J_x^a J_y^b J_z^c + J_z^c J_y^b J_x^a), \text{ where } (-)^{\theta} = (-)^{a+b+c} \text{ and } \Gamma = \begin{cases} A_2^a B_1^b B_2^c & for \quad C_{2v} \\ (A'')^{a+b} & for \quad C_s \end{cases}$$

The hermicity is unambiguously defined by powers *a,b c* : an elementary operator is hermitian (θ=0) if *a+b+c=even* and anti-hermitian (θ=1)) if *a+b+c=odd.* The "normalisation constant" *d* is chosen to preserve the invariance of the operators under the time-reversal: d=1/2 for hermitian terms (θ=0) and d=i/2 for anti-hermitian terms (θ=1). Calculations (i), (iii) described in Sect. 2 are available in all three rotational *R*, $\mathcal{R}$ and *J* representations.

6.2. Perturbative approach for (partial) separation of vibrational and rotational motion in Watson-Eckart Hamiltonian

The Watson-Eckart vibration-rotation Hamiltonian of a semi-rigid molecule in the normal-mode representation can be partitioned in the following form

$$\begin{aligned} H_{vr} &= H_{vib} + \Delta H_{vib-rot} \quad , \\ \Delta H_{vib-rot} &= \frac{hc}{2}\sum_{\alpha,\beta}\{\mu_{\alpha\beta} J_\alpha J_\beta - J_\alpha[\mu_{\alpha\beta}, \pi_\beta]\} \end{aligned} \qquad (95)$$

It is usually considered that (except for floppy molecules having low bending or torsional modes) the vibrational motion is significantly faster that the rotational one. In this case the perturbation theory applies, as reviewed and well documented in [2-7].

Because the initial and transformed Hamiltonians have to be totally symmetric, all terms $H_n^{(k)}$ involved in CT are expressed as linear combination of totally symmetric rovibrational contributions. For this reason they contain products of vibrational V and rotational R factors of the same symmetry species $\Gamma_V = \Gamma_R = \Gamma$

$$H_n^{(k)} = \sum h_{\mathbf{ubr}}, \qquad h_{\mathbf{ubr}} = t_{\mathbf{ubr}} V^{\varepsilon,\Gamma}_{\mathbf{ub}} R^{\varepsilon,\Gamma}_{\mathbf{r}}, \qquad (96)$$

where t is a numerical parameter corresponding to the rovibrational contribution. In order to apply the latter condition, one has to establish an isomorphism between the D_2 group (see §3.3 above) and the molecular point group G or one of its sub-groups. If it is not the case one can work with a sub-group of D_2. For a very large panel of molecules one can use an isomorphism for subgroups $C_s \in G$ and $C_s \in D_2$. With an appropriate choice of axes we have $\Gamma' = A'$ and $\Gamma'' = A''$ in Eqs.(89-94) where A' and A'' are symmetry species of the C_s sub-group. Another approach would be working in the ITO representation accounting for the full molecular symmetry.

The hermicity of rotational and vibrational factors must be the same $\varepsilon_V = \varepsilon_R = \varepsilon$. As in Section 3.2, the vector indices in Eq.(26) $\mathbf{u}=\{u_1, u_2, u_3\ldots\}$ and $\mathbf{b}=\{b_1, b_2, b_3\ldots\}$ represent powers of creation and annihilation operators for normal vibration modes and $\mathbf{r}=(n,m,2l)$ represents powers of rotational components as in Section 3.3. In a framework of the conventional perturbation theory for a separation of molecular variables (vibrational zero-order approximation), the rotational factors behave like constant parameters with respect to operations of CT

$$\langle VR\rangle = \langle V\rangle R \qquad \text{and} \qquad \frac{1}{\mathfrak{D}}(VR) = \frac{1}{\mathfrak{D}}(V)R \tag{97}$$

This means that Eq. (64,97) and commutator relations are in principle sufficient to carry out computation up to a needed order. Note that the *exact formal polynomial algebra* for rovibrational operator involved in the ro-vibrational Hamiltonian transformations up to arbitrary power M has been implemented [39] accounting for all contributions in commutators and anti-commutators. These calculations are rather involved and are included as a FORTRAN routine of MOL_CT program or in the form of tables for Lie algebra structure constants readable by an external code.

In this context the approach outlined above (Section 3) for the effective separation of fast and slow motions applies, and the CT method is often used for approximate separation of vibrational motion in the $H_{vib\text{-}rot}$ Hamiltonian. This separation is complete in the case of relatively isolated non-degenerate vibrations leading to effective rotational Hamiltonian for this vibrational state. Otherwise (for degenerate vibrations or in cases of accidental resonances) the separation is only partial one leading to effective Hamiltonian composed of rotational blocks. However, the resulting effective Hamiltonian allows for building much simpler theoretical models. The advantage of such models is that corresponding matrices are finite-dimensional focused at a particular energy range. This makes easy to use effective models for the experimental data reduction by fitting parameters to observed transitions. The CT method allows for accurate computing initial physically meaningful values for these parameters from ab initio PESs.

7. Computer implementation : MOL_CT code

The method is implemented as a suite of MOL_CT computer programs at two different levels. The "*external level"* involves the recurrent scheme of CT based on "layer-by-layer calculations" (Sections 2.1-2.4) with the account of the generalised Wigner theorem (Sections 2.3) and the optimized algorithm of Section 4. Given the final order n of CT specified by the user, the program build the "tree of contributions" required for this order and produces a list of all necessary commutators. At this level the method is a general one applicable to the derivation of effective Hamiltonians for any quantum mechanical problem with a degenerate or quasi-degenerate zero order approximation and to a separation of variables by small successive transformations according to Section 3.

The "*internal level"* of MOL_CT specifies particular features of a concrete problem to solve. In order to build an H^{eff} at this level one needs to pass by the following steps:

(A) generate H_n in appropriate coordinates and axes and define the ordering scheme

(B) define an appropriate decomposition of the CT algebra $\mathbb{L} = \mathbb{L}^{(\mathcal{A})} \oplus \mathbb{L}^{(\perp)}$ depending on resonance conditions and the desired model

(C) specify the action of CT operations <…> , $\frac{1}{\mathfrak{D}}(...)$ on elementary expansion operators

(D) describe the commutator algebra in $\mathbb{L}$

(E) program the terms reduction

In the current implementation the "*internal level"* of MOL_CT is designed for molecular vibration-rotation calculations of semirigid molecules. A scheme for the implementation corresponding to the steps (A)-(E) is shown in Figure 6.1

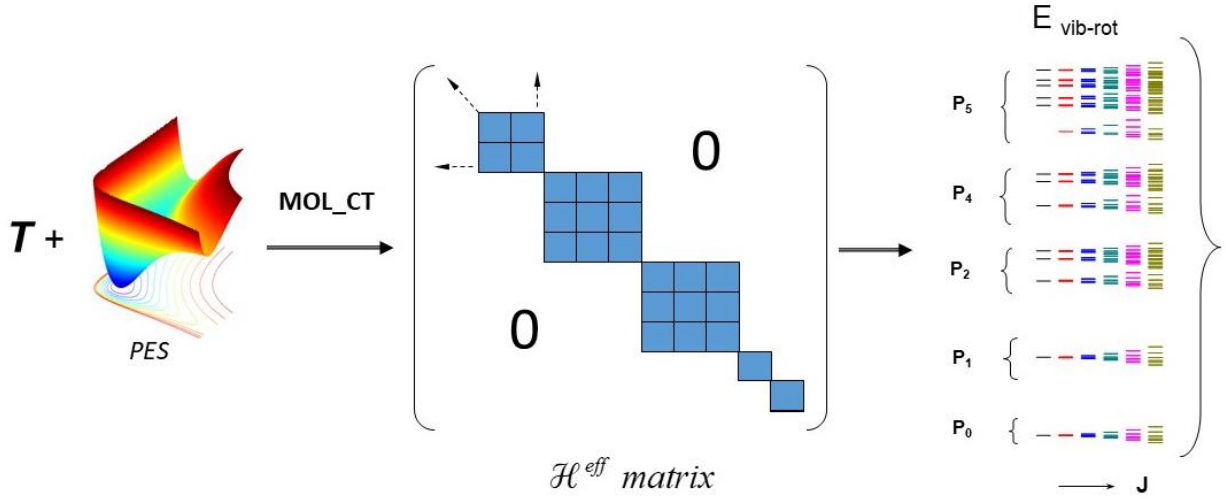

Fig 6.1 => **Figure 1.** Genergic scheme of the application of MOL_CT program suite to vibration-rotation polyad analysis. *T* stands for the kinetic energy operator, the *PES* for the potential energy surface , P_n for vibrational polyads and $\mathcal{P}_p$ for the corresponding projectors in the definition of effective Hamiltonian $\mathcal{H}^{eff} = \sum_P \mathcal{P}_p \tilde{H} \mathcal{P}_p$. The matrix of $\mathcal{H}^{eff}$ is taken over vibrational basis state functions, each matrix element being a rotational operator. The diagonalization of the matrix produces rovibrational level parrerns with increasing *J* schematically shown at the right-hand side.

Compared to previously available CT calculations, we take into account all these terms up to a given order in a numerically exact way. This has become possible since structural constants of rovibrational Lie algebra are programmed in MOL_CT without any omissions or approximations. In particular, we do not use a traditional approximation of "main (anti-)commutator contributions" [3,7] that limits the final accuracy. Even though many of high order terms would be small, an accumulation of a large amount of contributions (1.5 million for the 8-th order in triatomics) requires a full account of them in order to reach a spectroscopic accuracy in line positions. Otherwise a convergence of CT is rapidly deteriorated. A fast CT algorithm implemented in MOL_CT allows generating a full set of non-empirical rovibrational effective Hamiltonians H_P^{eff} for a triatomic molecule up to 8-th order takes few minutes with a standard desktop computer.

8. One-dimensional convergence test using exactly solvable potential

A simple test of the validity of the general recurrent scheme, of the vibrational commutator algebra and of the convergence of CT is possible with 1D exactly solvable potentials. The well known model Kratzer potential $U(r) = -2D(r_e / r - r_e^2/(2r^2))$ has a qualitatively correct asymptotes ($U \to \infty$ for $r \to 0$ and $U \to 0$ for $r \to \infty$) and allows for an exact solution of the stationary Schrödinger equation. Exact vibration energies expressed in wave number units [cm^{-1}] are [235, 6]

$$E_\upsilon^{Kr} / hc = -(1/2)\omega_e \beta^{-6}\{(\upsilon + 1/2) + \sqrt{1/4 + \beta^{-4}}\}^{-2} \qquad (98)$$

Here r_e is the equilibrium internuclear distance, ω_e is the harmonic frequency, D is the dissociation limit corresponding to the depth of the potential well and $\beta = \sqrt{\omega_e / 2D}$. To fulfil the CT test, we proceed with the same steps as described in the previous sections:

(i) The potential is expanded in Taylor series $U = (\omega_e / 2)q^2 + \sum_{m \geq 3} K_m q^m$ in the dimensionless normal coordinate $q = \beta^{-1}(r - r_e)/r_e$. This gives simple expressions for the anharmonic coefficients $K_m = (-1)^m (m-1)\beta^{m-2}\omega_e / 2$.

(ii) The vibration Hamiltonian $H=T+U$ is expanded in powers of the small parameter β and H_n terms are converted to the a+,a representation.

(iii) According to the prescriptions of CT the initial Hamiltonian H is transformed to $\tilde{H}$ which is diagonal in the zero order harmonic oscillator wave functions

$$H = \tfrac{1}{2}\sum_{n,i,j} t_{i,j}^{n,0}((a^+)^i a^j + (a^+)^j a^i) \quad \Rightarrow \quad \tilde{H} = \sum_{n,m} t_{m,m}^{n,n} N^{[m]} \Rightarrow \quad E_\upsilon = \sum_{n,m} t_{m,m}^{n,n} \upsilon(\upsilon\text{-}1)...(\upsilon\text{-}\mathrm{m}+1) \quad (99)$$

Such a test has been applied to check analytical formulae for Dunham spectroscopic constants at lower orders [6, 113]. The results given in Fig 2 show a good convergence of energy calculations up to υ =50. Fig 7.1 shows an exponential convergence of CT for such a simple model system.

Rather high orders are required to achieve a spectroscopic accuracy, but for the 24-th order the CT calculations take only tiny fraction of second of CPU time on a standard PC. Similar convergence trends are obtained with Morse and Pöschl–Teller potentials. This test helps validating general recurrent relations of CT and the vibrational commutator algebra at high orders

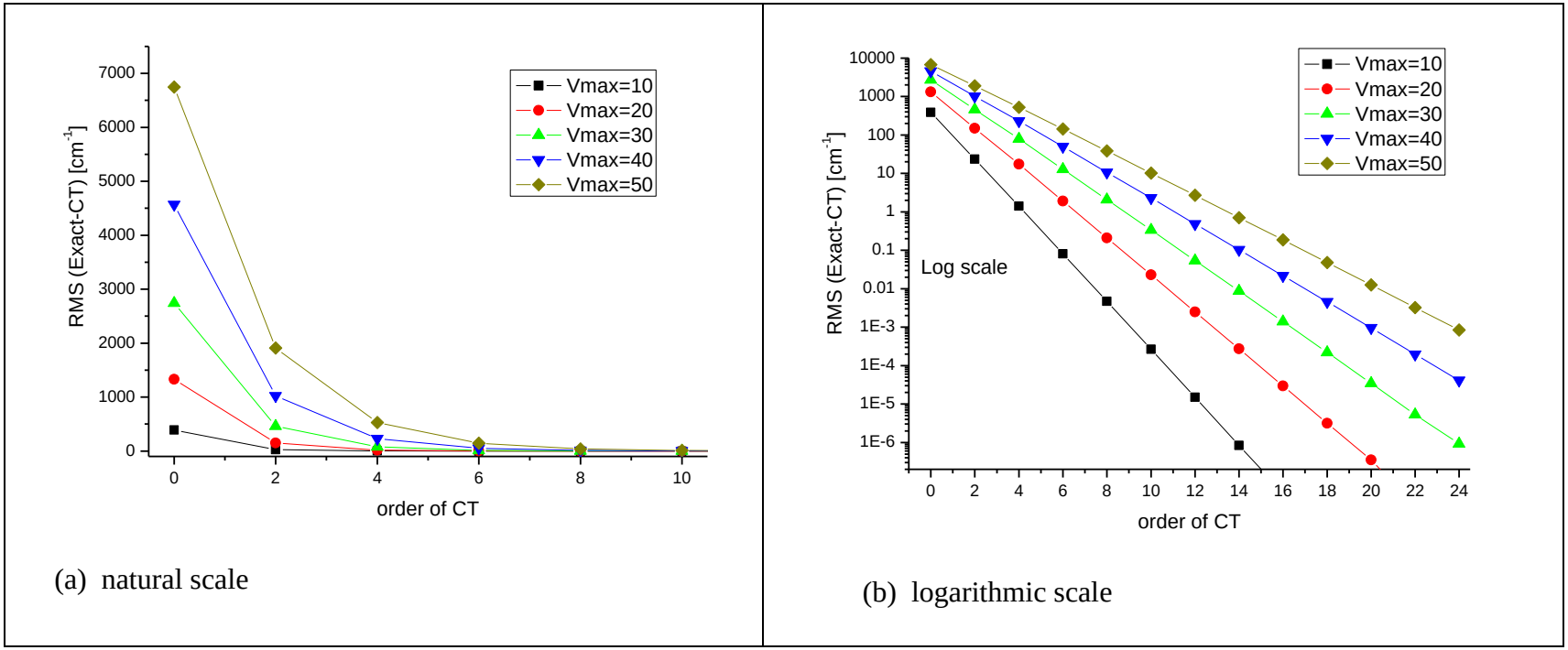

Fig 8.1. => **Figure 2.** CT convergence test using the exactly solvable Kratzer 1D potential. The parameter values ω=1000 cm^{-1} and β=0.07 are used. The RMS deviations (Eq(98)-CT) versus increasing orders are calculated up to V_{max} indicated in the frame.

9. DD resonance: example of vibrational stretching polyads for H_2O

As a simple example for CT application we consider first the 1:1 vibrational resonance with closed harmonic frequencies ($\omega_1 \approx \omega_3$). For a C_{2v} molecule a purely vibrational coupling of wavefunctions is symmetry allowed for the overtone states like (200)/(002) and is known as Darling-Dennison (DD) resonance. This type of resonance coupling is very common in molecular spectroscopy. In this case, in additional to the diagonal terms (75), the H^{eff} includes the resonance terms like $h_{DD}^{res} = a_1^+ a_1^+ a_3 a_3 + a_3^+ a_3^+ a_1 a_1$ at the order two (o2 in abbreviated notations), $h_{DD}^{res} = a_1^+ a_1^+ a_1^+ a_1 a_3 a_3 + a_1^+ a_3^+ a_3^+ a_1 a_1 a_1$ and $h_{DD}^{res} = a_1^+ a_1^+ a_3^+ a_3 a_3 a_3 + a_3^+ a_3^+ a_3^+ a_1 a_1 a_3$ at the order four (o4) and so on. Let us apply CT calculations to water stretching vibrations as a benchmark, which is usually considered as a quite challenging test, because this molecule is a nonrigid one possessing a low linearity barrier. It is well-known [238] that a standard power series expansion in the bending coordinate q_2 is not well convergent that represent a severe problem for a perturbation treatment, particular for an effective rotational Hamiltonian [239]. The calculation of rovibrational spectra of water is commonly considered as a touchstone for many theoretical models. Because of well-known non-rigidity effects, polynomial expansions for effective Hamiltonians have a very slow rate of convergence [239] even for medium values of quantum numbers. The strong bending-rotational coupling makes it extremely difficult to reach a high-resolution accuracy both in theoretical predictions and in empirical fits [240] to observed data. Numerically exact varitional [236] or DVR approaches [205-208, 241] are more appropriate to compute ro-vibrational spectra in this case being capable to produce accurate line lists for various databases [58, 241] .

Here we consider a possibility to decouple stretching modes from the bending mode using the above described CT technique. This can help understanding applicability limits of the method in such unfavourable case for a perturbative treatment. In high-resolution spectroscopy analyses it is well known [41] that for rovibrational calculation one has to account also for Fermi ro-vibrational resonance (due to $\omega_1 \approx 2\omega_2$), but for pure vibrational problem the latter one is much less important as will be seen in further results.

For this test, we used Partridge-Schwenke (PS) PES [236], which accounts for DBOC corrections, with nuclear masses in comparison with precise DVR calculations by Li and Guo [208]. The convergence of the eigenvalues of H^{eff}(CT) with orders o2, o4, o6, o8, o10 for vibrational levels of stretching DD polyads up to four vibrational quanta is given in Table 3.

Table 9.1 => Table 3. Convergence of CT for stretching vibration levels of H_2O: comparison with DVR calculations

Glob assign		Normal assign		E/hc (DVR)	E/hc (DVR – CT)				
Γ	N	Li[208]	CT	[208]	o2	o4	o6	o8	o10
A	4	(100)	(100)	3657.04	1.66	-0.29	0.03	0.04	-0.04
B	1	(001)	(001)	3755.95	2.02	-0.22	0.07	-0.02	0.01
A	9	(200)	(200)	7201.55	7.61	-1.03	0.06	0.06	-0.10
B	4	(101)	(101)	7249.85	7.54	-0.77	-0.06	0.03	-0.05
A	10	(002)	(002)	7445.11	4.73	-0.52	0.10	-0.06	0.02
A	20	(300)	(300)	10599.70	21.16	-2.10	-0.27	0.19	-0.08
B	9	(201)	(201)	10613.40	21.18	-2.04	-0.54	0.13	-0.08
A	21	(102)	(102)	10868.91	10.06	-1.92	0.24	0.02	-0.07
B	10	(003)	(003)	11032.45	11.44	-0.71	-0.12	-0.07	0.07
A	34	(400)	(202)	13828.16	44.80	-4.27	-2.03	0.28	0.05
B	18	(301)	(301)	13830.85	45.12	-4.03	-1.90	0.50	0.31

A	37	(202)	(400)	14221.13	23.05	-4.87	0.95	0.26	-0.32
B	21	(103)	(103)	14318.77	22.21	-2.45	-0.62	0.18	0.06
A	38	(004)	(004)	14537.40	21.15	-0.87	-0.66	-0.06	0.16
	rms				22.02	2.39	0.84	0.19	0.14

Notes : all E/hc values are in cm^{-1}, Γ - symmetry type (A –symmetric and B anti-symmetric with respect to permutation of edge nucleas) , N –global ranking number in DVR calculations using PS PES[236], (v1v2v3) - normal mod assignment

It is seen that CT calculations for stretching vibrations converge well to numerically exact DVR values computed with the same PES [236] . A comparison with experimental values is shown in Table 8.2. The third column gives the local mode assignment, whereas last three columns give squares $M_n(\%)$ of the expansion coefficients in the normal mode basis set. Both variational calculations by Child and Lawton [242], Li and Gou [208], Kellman effective model [70] and semi-classical analysis of bifurcations of periodic orbits by Mauguiere et al [93] have shown that a transformation from normal to local mode vibrations in water molecule occurs at the bottom of the stretching polyads. The local mode ("L") and normal mode ("N") behaviour of wavefunctions is indicated in Table 8.2 in with "L" and "N" symbols. An algebraic equivalence local mode anharmonic-oscillator model and Darling-Dennison coupling was demonstrated by Lehmann [243], but for a simplified quartic model.

A typical characteristic of the local mode behaviour is a near degeneracy of the doublets of corresponding levels with symmetric (A) and asymmetric (B) wavefunctions at the bottom of the stretching polyads. This effect, which is characterised by rapidly decreasing splitting between quasi-degenerate doublets $\Delta E = (E[n,0]+) - (E[n,0]-)$ for high values of local mode quantum number n, is commonly considered as a difficulty for the normal mode approach, which was not appropriate to describe this progressive ΔE quasi-degeneracy of local modes. It is quite surprising that the CT method describes well this effect (at least up to five quanta states) using the conventional normal mode representation in ab initio PES without any adjustable parameters, though sufficiently high orders are required to converge the results to experimental values as shown in Fig. 3.

Table 9.2. => Table 4. Stretching vibrational energies of H2O calculated with successive orders of CT: Comparison with DVR and with observations

P	n_P	Local mode assignement	Obs. cm^{-1}	Obs.-CT cm^{-1}	CT o10	N/L type ref [70]	Normal mode contributions (PS PES + CT)					
							M_1 (%)	$(v_1v_2v_3)$	M_2(%)	$(v_1v_2v_3)$	M_3(%)	$(v_1v_2v_3)$
1	1	$[1,0]_+$	3657.05	-0.03	3657.08	N	100	(100)				
1	2	$[1,0]_-$	3755.93	-0.01	3755.94	N	100	(001)				
2	1	$[2,0]_+$	7201.54	-0.11	7201.65	L	88	(200)	12	(002)		
2	2	$[2,0]_-$	7249.82	-0.08	7249.90	L	100	(101)				
2	3	$[1,1]_+$	7445.07	-0.02	7445.09	N	88	(002)	12	(200)		
3	1	$[3,0]_+$	10599.69	-0.09	10599.78	L	55	(300)	45	(102)		
3	2	$[3,0]_-$	10613.36	-0.12	10613.48	L	88	(201)	12	(003)		
3	3	$[2,1]_+$	10868.88	-0.10	10868.98	N	55	(102)	45	(300)		
3	4	$[2,1]_-$	11032.41	0.03	11032.38	N	88	(003)	12	(201)		
4	1	$[4,0]_+$	13828.28	0.17	13828.11	L	68	$(202)^{\#}$	26	(400)	6	(004)
4	2	$[4,0]_-$	13830.94	0.40	13830.54	L	67	(301)	33	(103)		
4	3	$[3,1]_+$	14221.16	-0.29	14221.45	L	71	$(400)^{\#}$	18	(202)	11	(004)
4	4	$[3,1]_-$	14318.81	0.10	14318.71	N	67	(103)	33	(301)		
4	5	$[2,2]_+$	14536.87	-0.37	14537.24	N	82	(004)	15	(202)	3	(400)
	rms			0.18								

Obs: experimental values of vibrational levels (compiled from [41, 58, 208,244-245]; CT: Contact transformation at order 10, all values are in cm-1. M_n(%) – squares of the expansion coefficients of the H^{eff}(CT) in the normal mode basis ($v_1v_2v_3$). N/L type column indicated the local or normal mode behaviour of the corresponding wavefunction according to [70].

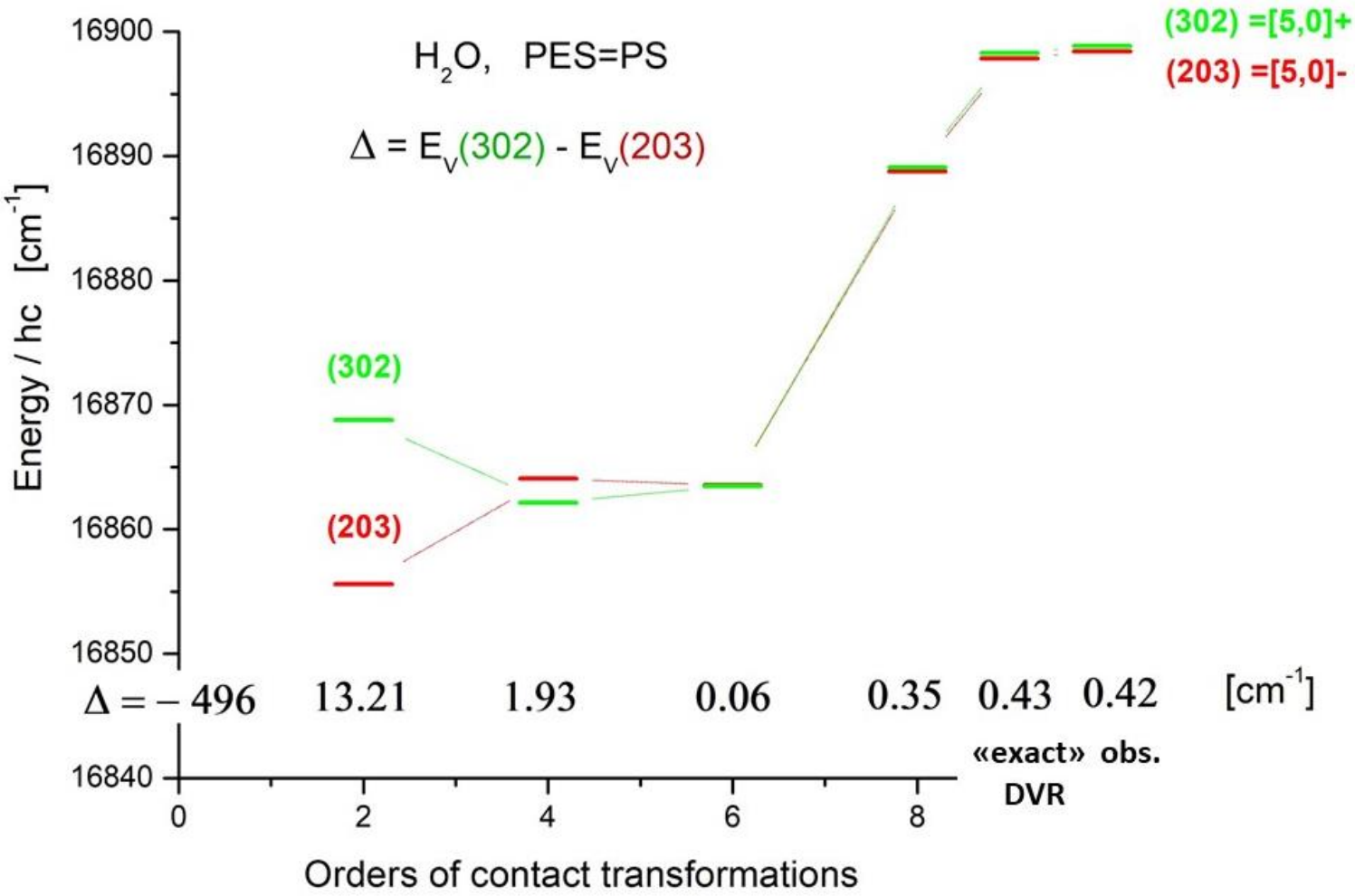

Fig 9.1. => **Figure 3.** Example of the convergence of CT for near degenerate "locale mode" vibrational states of H_2O. With the increasing orders the CT cnormal mode calculations tend to "exact" DVR calculations for the splitting $\Delta E = (E[5,0]+) - (E[5,0]-) = 0.43$ cm^{-1} between the local mode states is given according to [208], which is closed to the observed value 0.42 cm^{-1}.

At the top of the stretching polyads the (v_1=0,v_2=0,v_3) vibrational series keep the normal mode character as is clearly seen from the dominant contributions of the normal modes basis set terms to H^{eff}(CT) in Table 8.3. For (v_1=1, v_2=0,v_3) series, the normal modes basis states are heavily mixed due to the DD coupling. However, the CT results are still in a good agreement with DVR calculation using the same PES [236] as well as with calculations using more recent ab initio PES of ref [246].

TABLE 9.4 => Table 5: Normal mode series at the top of stretching polyads of H_2O

Global ass		Str. polyads		E/hc [cm^{-1}]			Normal mode contributions					
Γ	N	P	n_P	DVR	DVR-CT	CT(o8)	M_1(%)	($v_1v_2v_3$)	M_2(%)	($v_1v_2v_3$)	M_3(%)	($v_1v_2v_3$)
B	39	5	6	17948.30	-0.03	17948.33	81	(005)	16	(203)	3	(401)
A	96	6	7	21274.39	0.03	21274.36	77	(006)	17	(204)	5	(402)
B	97	7	8	24510.33	-0.06	24510.39	75	(007)	18	(205)	5	(403)
Γ	N	P	n_P	DVR	DVR-CT	CT(o10)	M_1(%)	($v_1v_2v_3$)	M_2(%)	($v_1v_2v_3$)	M_3(%)	($v_1v_2v_3$)
A	62	5	5	17747.97	-0.06	17748.03	45	(104)	33	(302)	22	(500)
B	62	6	6	21041.72	0.78	21040.94	50	(105)	35	(303)	15	(501)
A	136	7	7	24291.59	0.45	24291.14	37	(106)	31	(304)	20	(502)

Γ - symmetry type, N –global ranking number in DVR calculations using PS PES [236] , P – stretching polyad number in the DD model , nP – ranking number of the vibrational level with the polyad P.

10. Fermi + DD resonance (2:1:2) for SO_2: example of CT convergence to variational calculations

Let us consider now an example a triple 2:1:2 resonance scheme ($\omega_1 \approx 2\omega_2 \approx \omega_3$) corresponding to the simultaneous account of DD and Fermi coupling with application to SO_2 vibrational levels. This means that the modelling operator of CT is chosen as $\mathcal{A} = 2a_1^+a_1 + a_2^+a_2 + 2a_3^+a_3$, corresponding to the (2:1:2) ratio for $(\Omega_1 : \Omega_2 : \Omega_3)$ in equation (81). Various ab initio and empirical PESs [247,248,249] are available for this molecule. For the CT benchmark calculations with use PES by Martin-Zuniga et al [247-248]. The initial ab initio surface had been computed by Martin et al [247] at the CCSD(T) level with the AVQZ+1 basis. Zuniga et al. [248] converted the PES to a 3D Morse-cosine expansion and optimized a few lower order parameters in order to correct the potential energy function with respect to the (as) normal mode. The final PES has a consistent behavior at sufficiently large nuclear displacements. Because of two simultaneous resonances , in addition to the resonance h_{DD}^{res} term of the previous example, there appear the Fermi coupling terms like $h_F^{res} = a_1^+a_1^+a_2 + a_2^+a_1a_1$ and similar type of higher order terms that makes the blocks of the H^{eff} matrix larger. ~~The scheme of CT in this case is shown in Fig 10.1.~~

~~Fig 10.1. Scheme of block-diagonalisation of the nuclear motion Hamiltonian accounting for DD and Fermi resonances for SO_2~~
~~(rev 2 : figure has been published ! where ?)~~

The successive orders of the CT effective Hamiltonian in this case converge very rapidly to numerically exact results of variational method as shown in Table 9.2 and Figure 9.2. The calculations are very fast taking less than 1 sec on a standard 1 processor laptop computer.

Table 10.1 => Table 6. Comparison of vibration energies for SO_2 : variational and CT calculations in the (2:1:2) resonance scheme

Γ	Variational	CT - variational						CT			Normal mode contributions			
	Zuniga[248]	o0	o2	o4	o6	o8	o10	o10	P	nP	M_1 (%)	$(v_1v_2v_3)$	M_2 (%)	$(v_1v_2v_3)$
A	517.80	4.13	0.04	0.00	0.00	0.00	0.00	517.80	1	1	100.0	(010)		
A	1034.97	8.90	0.17	0.00	0.00	0.00	0.00	1034.97	2	1	99.8	(020)	0.2	(100)
A	1150.58	15.24	0.01	0.00	0.00	0.00	0.00	1150.58	2	2	99.8	(100)	0.2	(020)
B	1357.28	19.15	-0.01	0.01	0.01	0.01	0.01	1357.29	2	3	100.0	(001)	0.0	(020)
A	1551.40	14.40	0.48	0.02	0.00	0.00	0.00	1551.40	3	1	99.4	(030)	0.6	(110)

A	1665.31	22.44	0.07	0.00	0.00	0.00	0.00	1665.31	3	2	99.4	(110)	0.6	(030)
B	1871.12	27.25	-0.04	0.00	0.00	0.00	0.00	1871.12	3	3	100.0	(011)	0.0	(030)
A	2067.00	20.73	1.06	0.04	0.00	0.00	0.00	2067.00	4	1	98.7	(040)	1.3	(120)
A	2179.42	30.27	0.23	0.00	0.01	0.01	0.01	2179.43	4	2	98.3	(120)	1.3	(040)
A	2293.95	37.69	-0.02	0.00	0.00	0.00	0.00	2293.95	4	3	99.6	(200)	0.4	(120)
B	2384.37	35.93	-0.03	0.01	0.00	0.00	0.00	2384.37	4	4	99.8	(021)	0.2	(101)
B	2494.59	47.66	0.06	0.00	0.00	0.00	0.00	2494.59	4	5	99.8	(101)	0.2	(021)
A	2704.20	48.67	0.00	0.00	0.00	0.00	0.00	2704.20	4	6	100.0	(002)	0.0	(200)
A	2581.65	28.02	1.99	0.08	0.01	0.01	0.00	2581.65	5	1	97.7	(050)	2.3	(130)
A	2692.84	38.78	0.56	-0.01	0.00	0.00	0.00	2692.84	5	2	96.5	(130)	2.3	(050)
A	2805.61	47.96	0.06	-0.01	0.00	0.00	0.00	2805.61	5	3	98.7	(210)	1.2	(130)
B	2896.95	45.28	0.08	0.02	0.00	0.00	0.00	2896.95	5	4	99.4	(031)	0.6	(111)
B	3005.33	58.86	0.10	0.00	0.00	0.00	0.00	3005.33	5	5	99.4	(111)	0.6	(031)
A	3214.07	60.73	-0.09	0.00	0.00	0.00	0.00	3214.07	5	6	100.0	(012)	0.0	(210)
A	3095.26	36.34	3.35	0.16	0.02	0.00	0.00	3095.26	6	1	96.4	(060)	3.6	(140)
A	3205.44	48.11	1.17	0.01	0.01	0.01	0.01	3205.45	6	2	93.8	(140)	3.6	(060)
A	3316.68	58.82	0.24	-0.02	0.00	0.00	0.00	3316.68	6	3	96.8	(220)	2.6	(140)
B	3408.75	55.42	0.38	0.05	0.01	0.00	0.00	3408.75	6	4	98.7	(041)	1.3	(121)
A	3430.10	67.36	-0.10	0.00	0.00	0.00	0.00	3430.10	6	5	99.3	(300)	0.6	(220)
B	3515.52	70.60	0.16	0.00	0.01	0.00	0.00	3515.52	6	6	98.3	(121)	1.3	(041)
B	3624.39	83.68	0.03	-0.01	0.00	0.00	0.00	3624.39	6	7	99.5	(201)	0.4	(121)
A	3723.42	73.31	-0.23	0.02	0.00	0.00	0.00	3723.42	6	8	99.8	(022)	0.2	(102)
A	3828.48	90.21	0.25	0.01	0.00	0.00	0.00	3828.48	6	9	99.7	(102)	0.2	(022)
B	4040.74	88.56	0.03	0.01	0.00	0.00	0.00	4040.74	6	10	99.9	(003)	0.1	(201)
A	3607.70	45.83	5.26	0.28	0.04	0.00	0.00	3607.70	7	1	94.7	(070)	5.2	(150)
A	3717.14	58.35	2.11	0.03	0.01	0.00	0.00	3717.14	7	2	90.3	(150)	5.2	(070)
A	3827.08	70.36	0.60	-0.04	0.00	0.00	0.00	3827.08	7	3	93.6	(230)	4.5	(150)
B	3919.67	66.43	0.96	0.10	0.00	0.00	0.00	3919.67	7	4	97.7	(051)	2.3	(131)
A	3938.70	80.69	-0.01	-0.03	0.00	0.00	0.00	3938.70	7	5	98.0	(310)	1.8	(230)
B	4025.07	82.98	0.33	0.01	0.00	0.00	0.00	4025.07	7	6	96.5	(131)	2.3	(051)
B	4132.06	97.95	0.11	-0.02	-0.01	-0.01	-0.01	4132.05	7	7	98.6	(211)	1.2	(131)
A	4232.15	86.52	-0.32	0.04	0.00	0.00	0.00	4232.15	7	8	99.4	(032)	0.6	(112)
B	4546.66	104.58	-0.14	0.02	0.00	0.00	0.00	4546.66	7	10	99.9	(013)	0.1	(211)
A	4118.85	56.62	7.81	0.49	0.09	0.02	0.01	4118.86	8	1	92.7	(080)	7.2	(160)
A	4227.82	69.60	3.51	0.07	0.03	0.01	0.00	4227.82	8	2	85.8	(160)	7.2	(080)
A	4336.71	103.91	1.22	-0.06	0.00	0.00	0.00	4336.71	8	3	89.1	(240)	6.9	(160)
B	4429.59	78.44	1.92	0.18	0.01	0.00	0.00	4429.59	8	4	96.4	(061)	3.6	(141)
A	4446.73	94.59	0.20	-0.05	0.01	0.00	0.00	4446.73	8	5	95.2	(320)	3.8	(240)
B	4533.87	96.12	0.69	0.02	0.01	0.00	0.00	4533.87	8	6	93.8	(141)	3.6	(061)
A	4559.04	104.24	-0.26	-0.02	-0.01	-0.01	-0.01	4559.03	8	7	98.9	(400)	0.8	(320)
B	4639.20	112.74	0.50	-0.03	0.00	0.00	0.00	4639.20	8	8	96.7	(221)	2.6	(141)
A	4740.17	100.43	2.64	0.06	-0.01	-0.01	-0.01	4740.16	8	9	98.7	(042)	1.3	(122)
B	4746.67	127.22	-0.13	-0.02	-0.01	-0.01	-0.01	4746.66	8	10	99.0	(301)	0.6	(221)
A	4841.51	99.79	0.23	0.03	0.00	0.00	0.00	4841.51	8	11	98.2	(122)	1.3	(042)
A	4945.00	118.26	0.36	0.01	0.00	0.00	0.00	4945.00	8	12	99.1	(202)	0.4	(122)

B	5052.11	121.06	-0.42	0.04	0.00	0.00	0.00	5052.11	8	13	99.7	(023)	0.2	(103)
B	5152.24	142.88	0.57	0.04	0.00	0.00	0.00	5152.24	8	14	99.4	(103)	0.4	(301)
A	5366.94	138.80	0.04	0.02	0.00	0.00	0.00	5366.94	8	15	99.7	(004)	0.2	(202)
A	4628.62	68.78	10.81	0.78	0.14	0.03	0.00	4628.62	9	1	90.2	(090)	9.5	(170)
A	4737.36	81.99	2.50	0.17	0.06	0.02	0.02	4737.38	9	2	80.4	(170)	9.9	(250)
A	4845.46	117.09	2.20	-0.08	0.01	0.00	0.00	4845.46	9	3	83.2	(250)	9.9	(170)
B	4938.40	91.57	3.34	0.32	0.02	0.00	0.00	4938.40	9	4	94.7	(071)	5.2	(151)
A	4954.13	130.38	0.58	-0.10	0.00	0.00	0.00	4954.13	9	5	90.7	(330)	6.6	(250)
B	5041.82	110.10	1.34	0.05	0.01	0.00	0.00	5041.82	9	6	90.3	(151)	5.3	(071)
A	5064.57	120.64	-0.14	-0.04	0.00	0.00	0.00	5064.57	9	7	97.2	(410)	2.4	(330)
B	5145.73	128.14	6.31	-0.05	0.00	0.00	0.00	5145.73	9	8	93.5	(231)	4.5	(151)
A	5247.38	115.15	3.90	0.09	-0.05	-0.04	-0.04	5247.34	9	9	97.7	(052)	2.3	(132)
B	5251.26	144.56	2.43	-0.04	0.00	0.00	0.00	5251.26	9	10	97.8	(311)	1.8	(231)
A	5347.19	116.05	0.24	0.05	0.00	0.01	0.01	5347.20	9	11	96.4	(132)	2.3	(052)
A	5448.68	136.51	2.62	0.00	-0.01	0.00	0.00	5448.68	9	12	98.2	(212)	1.2	(132)
A	5136.86	82.47	9.33	1.20	0.23	0.05	0.00	5136.86	10	1	87.4	(0D0)	12.1	(180)
A	5245.64	95.65	1.64	0.34	0.12	0.05	0.04	5245.68	10	2	74.1	(180)	13.3	(260)
A	5353.24	131.25	3.60	-0.09	0.01	-0.01	-0.01	5353.23	10	3	76.0	(260)	13.4	(180)
B	5445.98	105.92	3.15	0.53	0.05	0.01	0.00	5445.98	10	4	92.6	(081)	7.3	(161)
A	5460.78	145.66	1.23	-0.15	0.01	0.00	0.00	5460.78	10	5	84.4	(340)	10.0	(260)
A	6465.88	184.43	2.46	0.09	0.01	0.00	0.00	6465.88	10	20	99.0	(104)	0.8	(302)
A	6183.21	167.82	-0.34	-0.07	0.01	0.00	0.00	6183.21	11	9	96.4	(510)	3.0	(430)

Γ - symmetry type, N –global ranking number in DVR calculations using PES[248] , P – stretching polyad number in the DD model , nP – ranking number of the vibrational level with the polyad P.

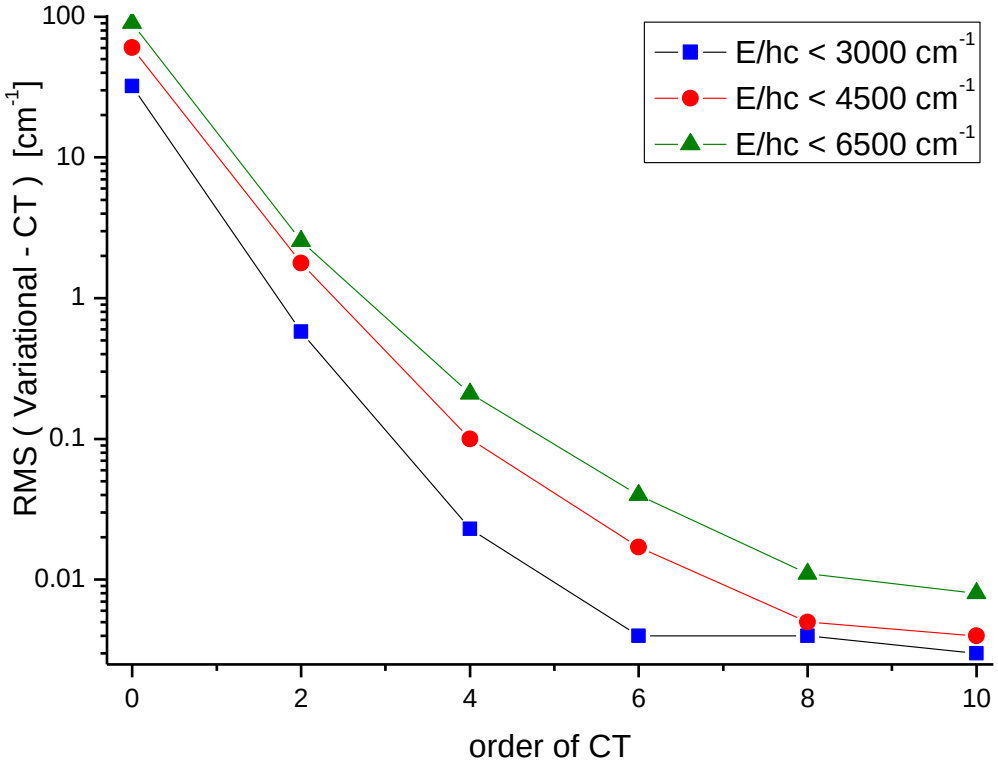

Fig 10.2. => Figure 4. Convergence of CT vibration energies of SO_2 to exact variational results

It is instructive that the Fermi interaction between (v_1=0, v_2, v_3=0), (v_1=1, v_2-2, v_3=0), (v_1=2, v_2-4, v_3=0), … normal mode basis set functions quite rapidly increases towards large values of the quantum numbers (Figure 9.3) . The dominant contributions of the harmonic oscillator (0, v_2,0) functions to the bending progression of SO_2 vibrational states gradually shut down to 75% at v_2 = 12 and to 50% at v_2=19. At higher energies basis set functions are heavily mixed that corroborate the classical analyses of periodic orbits [93].

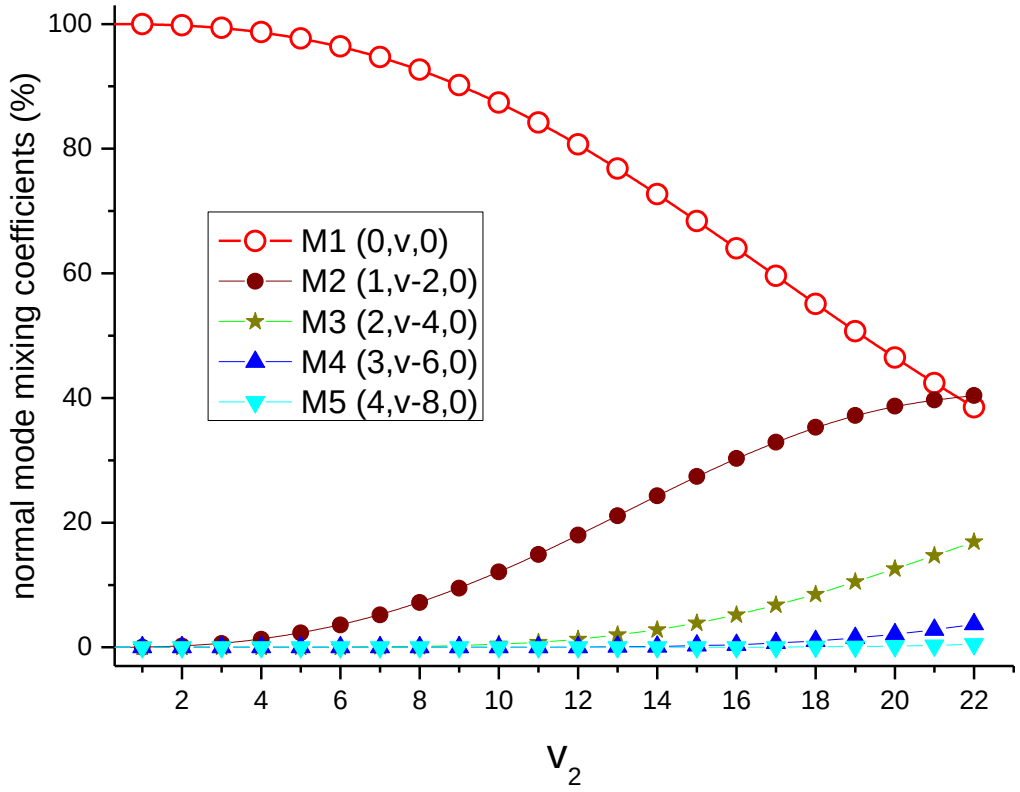

Fig 10.3 => Figure 5. Increasing Fermi resonance coupling versus bending quantum numbers for SO_2

11. CT-CONVERGENCE FOR ROTATIONS: Asymmetric top triatomics

One of major applications of CT in high-resolution molecular spectroscopy is a systematic derivation of effective rotational and vibration-rotational Hamiltonian for polyads of closely lying states.
A use of ab initio or empirically optimised PESs permit to obtain physically meaningful values for EH parameters, which can be further adjusted via a fit to experimental line positions in observed spectra.

11.1. Rotation levels for an isolated vibrational state

If a vibrational state is well isolated from other vibrational states with a sufficiently large energy gap, then the CT method can be used for a full separation of vibrational variables from the nuclear motions Hamiltonian as outlined in Section 3.2. This is typically the case of the vibrational ground state (GS).

For semi-rigid molecules, the CT usually rapidly converge and calculations are very fast. An example of the centrifugal distortion parameters of the ozone molecule computed from empirically optimised PES [268] of the ozone molecule is given in Table 7. The computed values match well the parameters determined by a simultaneous fit to experimental microwave (MW) and infrared (IR) spectra reported by Pickett et al. [270] and Colmonet et al. [271]. The only large discrepancy correspond to the H_{JK} parameter, for which there appear a big difference in experimentally determined values. Table 8 shows that CT calculations of rotational GS energy levels coverge quite rapidly. At eight order of CT that takes less than one second the CT calculations converge very close to numerically exact variational results [268].

Table 11.0 => **Table 7**
Comparison of rotational and centrifugal distortion parameters for the GS of $^{16}O_3$ molecule derived from the fit of (MW + IR) spectra with calculations using CT from the PES of [268]

	CT calc.	Fit MW+IR obs. spectra			exp2/exp1	(exp-CT)/exp	Power of J_α
Par.	Order 6	exp 1	exp 2	common			
	PES [268]	Pickett [270]	Colmont [271]	factor			
A	3.55368	3.55367	3.55367		1.000	5.2E-06	2
B	0.44529	0.44528	0.44528		1.000	3.5E-05	2
C	0.39466	0.39475	0.39475		1.000	2.2E-04	2
D_J	4.543	4.541	4.541	E-07	1.000	3.2E-04	4
D_{JK}	-1.862	-1.847	-1.847	E-06	1.000	7.7E-03	4
D_K	2.121	2.117	2.116	E-04	1.000	2.1E-03	4
d_J	6.993	6.979	6.979	E-08	1.000	2.1E-03	4
d_K	3.235	3.231	3.233	E-06	1.000	5.7E-04	4
H_J	3.48	3.46	3.29	E-13	0.951	0.058	6
H_{JK}	-3.14	-7.09	-4.96	E-12	0.700	0.367	6
H_{KJ}	-1.86	-1.85	-1.86	E-09	1.005	0.000	6

H_K	3.91	3.93	3.94	E-08	1.003	0.008	6
h_J	1.81	1.76	1.77	E-13	1.006	0.023	6
h_{KJ}	-7.40	-7.59	-7.78	E-12	1.025	0.049	6
h_K	2.40	2.15	2.43	E-09	1.130	0.012	6

Par.: Watson's A-reduced parameters [255] rotational EH for the (000) vibrational state of $^{16}O_3$.

Table 10.1 => Table 8. Example of the CT-convergence rotational GS levels computed from the ozone PES [268] for the orders o0,o2,o4, …o8. All values are given in cm^{-1}

E_rot/hc	J	Ka	Kc	exp-RR	exp-CT(o2)	exp-CT(o4)	exp-CT(o6)	exp-CT(o8)
50.643	10	1	9	-0.401	-0.008	0.002	0.002	0.002
74.431	10	3	7	-0.371	-0.010	0.004	0.003	0.003
245.911	10	8	2	-0.872	-0.064	0.007	0.002	0.002
298.672	10	9	1	-1.279	-0.086	0.009	0.002	0.002
357.503	10	10	0	-1.873	-0.110	0.011	0.002	0.002
...								
478.439	33	2	32	-4.610	-0.099	-0.006	-0.005	-0.005
499.790	33	3	31	-4.623	-0.066	0.030	0.032	0.031
1077.565	33	14	20	-11.049	-0.302	0.050	0.034	0.034
1166.010	33	15	19	-13.284	-0.315	0.052	0.034	0.034
1465.594	33	18	16	-23.288	-0.175	0.052	0.034	0.035
1576.648	33	19	15	-27.946	-0.025	0.045	0.036	0.036
1693.180	33	20	14	-33.381	0.205	0.031	0.040	0.039
					...			

Experimentally determined ("exp") rotational levels are taken from S&MPO [251] database. RR stands for the rigid rotor approximation. The RMS (CT-obs) deviation is of 0.06 cm^{-1} for all experimentally known rotation levels of ozone up to J=50.

For non-rigid molecules like H_2O, the applications of CT is less straightforward. The large amplitude bending vibration has to be treated with a particular care, using for example Hougen-Bunker-Johns approach [238] (considered further in Section 13). However, even in such unfavourable case for the standard semi-rigid Watson-Eckart normal mode approach [225], the CT calculations provide good convergence for effective rotational and centrifugal distortion parameters. An example of comparison of experimental values for the A-reduced Watson's centrifugal distortion EH and calculated ones from PS PES [236] using successive CT orders is illustrated in Table 10.2 . Higher order centrifugal distortion constants can be found in ref [39].

Table 11.2 . => Table 9. Reduced Effective Hamiltonian for vibrational GS of H_2O molecule computed by CT from the potential energy surface in comparison with experimental values.

	Computed from the PS PES				empirical values		
CT Orders:	ord=0	ord=2	ord=4	ord=6	ref. [252]	ref. [253]	Common factor
Bv	14.579	14.548	14.555	14.513	14.519	14.522	
Av	27.391	27.672	27.739	27.864	27.877	27.881	
Cv	9.515	9.314	9.317	9.274	9.279	9.277	
DJ		.117	.124	.122	.123	.125	e-2

DJK	-.501	-.572	-.545	-.563	-.577 e-2
DK	.257	.309	.315	.318	.325 e-1
dJ	.466	.500	.491	.494	.508 e-3
dK	.038	-.087	.095	-.124	-.130 e-2 (#)

…

PS PES: Partridge-Schwenke [236]; Resonance CT condition [$\omega_1 \approx \omega_3$]; A-reduction in I^r representation [236]. Two sets of empirical values [252,253] were obtained for the fit of experimental energy levels.
Symbol (#) stands for empirically poorly determinable parameter.

Convergence of CT for rotational and centrifugal distortion constants using the $\omega_1 \approx \omega_3$ resonance condition to experimental values within their error margins is shown in Figure 10.1

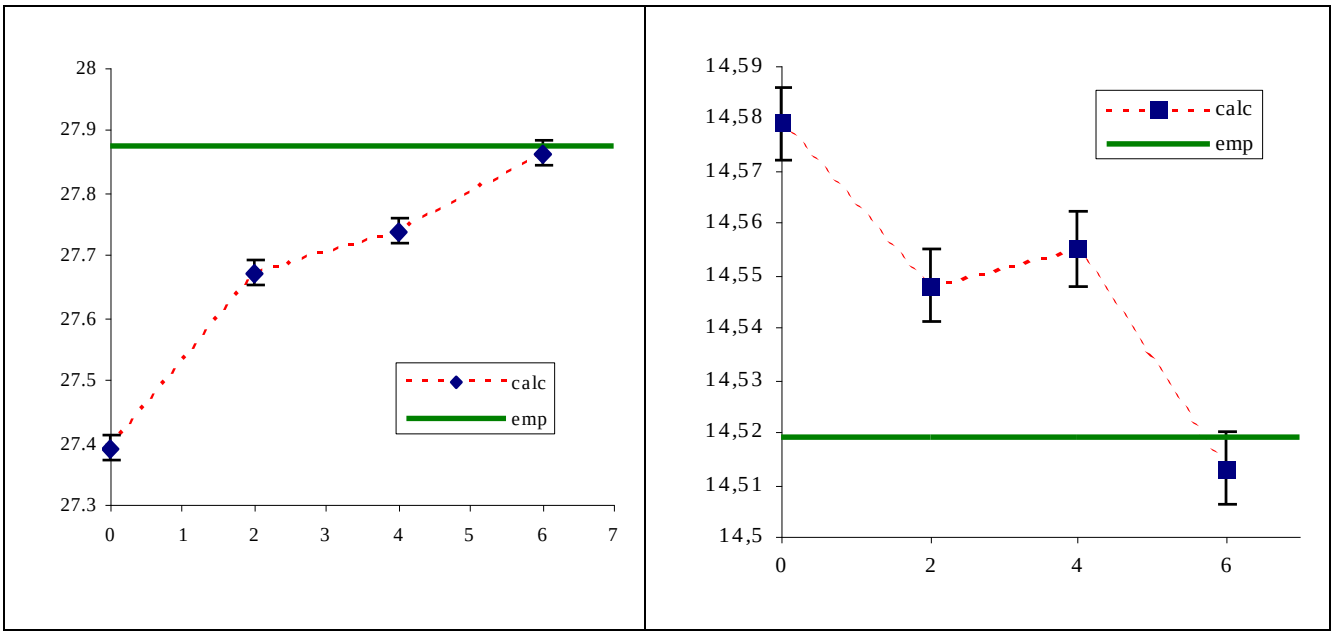

Fig 11.1. => **Figure 6.** Example of CT convergence (orders 0,2,4,6) for rotational and centrifugal disstortion constants of the GS of H_2O using PS PES [236] and the resonance condition $\omega_1 \approx \omega_3$. Squares and diamonds correspond to calculated values of A and B rotational constants, green horizon lines the experimental values [252,253] and vertical bars indicate the experimental uncertainty.

11.1. Ro-vibration levels for in case of strong accidental resonance : Example of {(100),(001)} dyad of ozone

More interesting cases represent nearby vibrational states with strong rovibrational resonance coupling. A well-known example is the dyad {(100),(001)} of vibrational fundamentals of the ozone $^{16}O_3$ molecule strongly perturbed by Coriolis resonance [254, 255, 256, 48]. The rovibrational H^{eff}(CT), in addition to the diagonal terms, includes successive resonance terms $h^{coriolis} = (a_1^+ a_3 + a_3^+ a_1) R^{\varepsilon,\Gamma}_{m,n,2l}$ where $R^{\varepsilon,\Gamma}_{m,n,2l}$ are symmetrised rotational operators (89). It is well known, that single-vibration state EHs do not to work in this case because the mixing coefficients for ro-vibrational wavefunctions reach 50% at relatively low rotational quantum number. The resonance

perturbations due to the Coriolis coupling are extremely strong. They exceed by three orders of magnitude an experimental accuracy of line positions in high-resolution spectra. Figure 10.1 shows that CT calculations for ro-vibrational levels rapidly converge to the same accuracy than variational method [250] using exact kinetic energy operator.

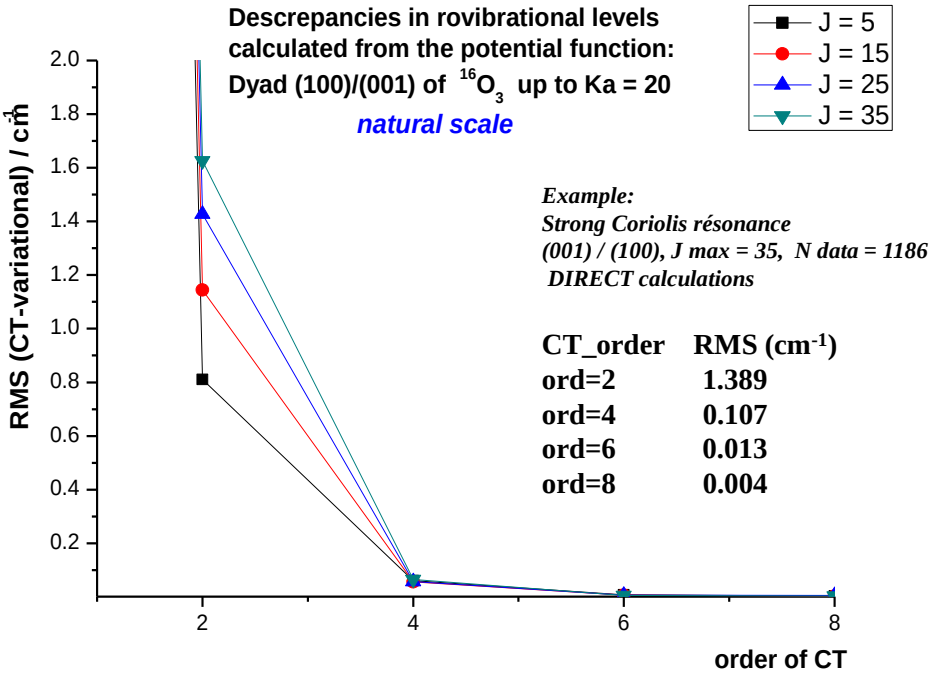

Figure 11.1.=> **Figure 7.** Example of CT convergence for the dyad of ozone ro-vibrational states coupled by strong Coriolis resonances: direct calculations from the potential energy function of ref [250].

In a purely empirical fit, the resonance coupling parameters of EH are poorly determined because of a correlation issues in the EH fitted parameters. The advantage of EH is that such parameters can be accurately predicted from ab initio or empirically optimised PESs. This is particularly important if an analysis of experimental spectrum in some frequency ranges has to account for so called "dark" bands [48, 256], which are not directly observed but could significantly perturb observed lines. In this case, the CT method permit constructing a physically meaningful H^{eff}(CT) model providing lacking information parameters for these dark states and for the corresponding interactions, as described for example in ref [257].

12. SYMMETRIC TOP MOLECULES

For symmetric top molecules there appear doubly degenerate vibrational states, consequently the corresponding terms appear in H^{eff}(CT) as outlined in Section 5.4. We consider below examples of CT application for the four-atomic (phosphine) and five-atomic (deuterated methane) molecules.

12.1 Four-atomic example (PH_3) with the CT polyad scheme 2:1:2:1

Phosphine (PH_3) is a semi-rigid symmetric top molecule, which has various industrial applications and had been discovered in the atmospheres of Jupiter and Saturn [258].The main

isotopologue possess four vibrational modes : two of them stretching non-degenerate ones ($\nu_1(A_1)$ =2321.14 cm^{-1}), $\nu_3(A_1)$ =2326.82 cm^{-1}) and two doubly degenerate bending modes ($\nu_2(E)$ = 992.14 cm^{-1}, $\nu_4(E)$ = 1118.31 cm^{-1}). Four normal mode frequencies of PH_3 exhibit an approximate relation among stretching and bending frequencies $\omega_1 \approx 2\omega_2 \approx \omega_3 \approx 2\omega_4$ resulting in vibrational levels being grouped into polyads with levels of similar energy, including GS (P=0), Dyad(P=1), Pentad(P=2), Octad (P=3) , etc [259-261]. Several ab initio and empirically refined PES have been published [262-265]. Investigation of vibration-rotation bands beyond the Octade range (3400 cm^{-1}) appears to be much more complicated and requires theoretical predictions, as discussed in [58, 202] . Based on an *ab initio* potential energy surface [263], the full Hamiltonian of phosphine nuclear motion was reduced to an effective Hamiltonian using high-order Contact Transformations method adapted to polyads of symmetric top AB_3-type molecules with a subsequent empirical optimization of parameters.

Figure 11.1. shows the convergence of the CT calculations to the results of the variational method [263] using exact KEO up to the polyad P=6, which had not yet been analyzed experimentally. The remaining (CT-Variational) deviations are smaller than the uncertainty of published ab initio calculations.

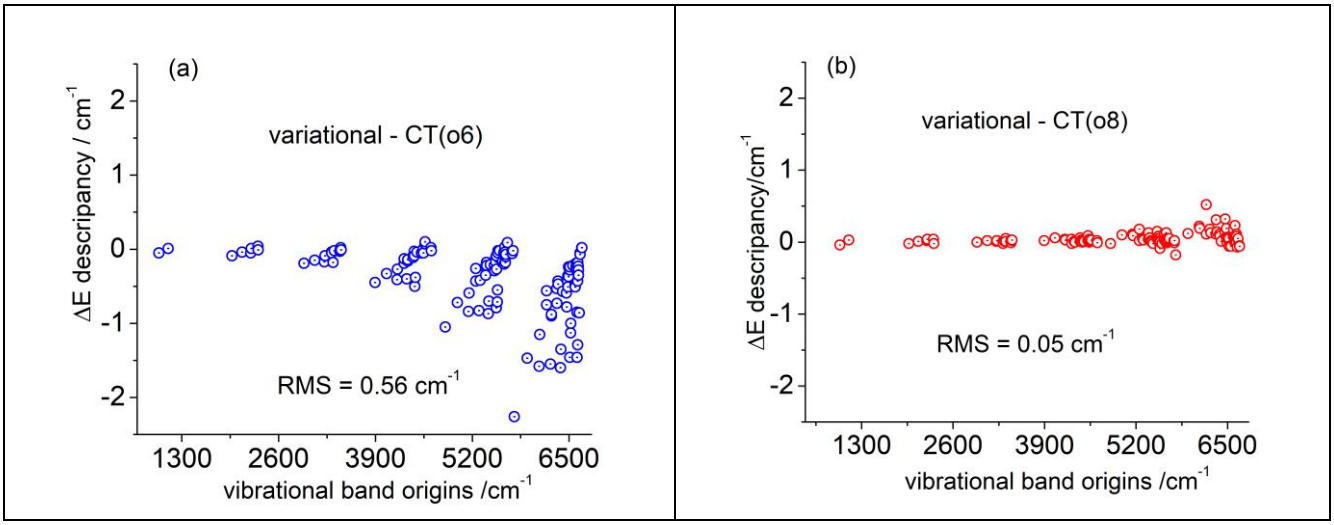

Fig 12.1. => **Figure 8.** Example of convergence of CT calculations of PH3 band centers in comparison with numerically exact variational method using exact kinetic energy operator (KEO) and the ab initio PES of Nikitin et al [264]

12.2 Five-atomic example with the (3:2:1:2:1:1) CT polyad scheme. Triply deuterated methane CHD_3

Variational calculations of ro-vibrational states and transition of deuterated methane molecules CH_3D (C_{3v} point group) and CH_2D_2 (C_{2v} point group) from ab initio PES and DMS were reported by Rey et al [265,266]. Wang and Carrington [267] published vibrational calculations of vibrational levels for all deuterated species of methane. To this end, they have empirically fitted their PES starting with ab initio parameters of Schwenke and Partridge [268]. Here we give an example of an application of the CT method for the triply deuterated methane isotopologue CHD_3 (C_{3v} point group) using ab initio PES initially scaled using funfamental vibrations of $^{12}CH_4$ [269]. To assure a

sufficiently complete account for various vibration-rotation couplings, the polyad scheme is more sophisticated than in the case of CH_4 (see below). The resonance scheme (3:2:1:2:1:1) corresponds to the ratios $(\Omega_1 : \Omega_2 : \Omega_3 : \Omega_4 : \Omega_5 : \Omega_6)$ in the modelling CT operator A in equation (81b).

Table 12.2. => **Table 10.** Comparison of vibrational levels of CHD_3 computed by CT method from methane PES 269] with experimental values and variational calculations of Wang and Carrington (WC) [267]

Γ	N	Obs.	O-CT(o6)	CT (o8)	O-CT(o8)	O-WC	assignment	P.c. Wf
A1	2	1004.548	0.08	1004.44	0.11	0.55	v3(A1)	0.99
E	1	1035.920	0.13	1035.83	0.09	0.42	v6(E)	0.99
E	2	1292.500	-0.12	1292.49	0.01	0.08	v5(E)	0.99
A1	3	1991.084	0.27	1990.92	0.16	0.80	2v3(A1)	0.91
E	3	2041.441	0.11	2041.28	0.16	0.77	v3+v6(E)	0.99
A1	4	2058.900	0.25	2058.85	0.05	0.69	2v6(A1)	0.90
E	4	2066.300	0.16	2066.24	0.06	0.67	2v6(E)	0.97
A1	5	2142.583	-0.10	2142.53	0.05	-0.20	v2(A1)	0.84
E	5	2250.828	-0.12	2250.87	-0.04	0.17	v4(E)	0.88
E	6	2301.165	-0.16	2301.02	0.14	0.43	v3+v5(E)	0.93
A1	7	2564.676	-0.89	2564.68	0.00	0.07	2v5(A1)	0.96
E	8	2586.043	-0.56	2586.03	0.01	0.14	2v5(E)	0.99
A1	8	2966.055	0.55	2966.17	-0.11	0.96	3v3(A1)	0.82
A1	9	2992.786	0.09	2992.76	0.03	-0.09	v1(A1)	0.90
A1	12	3154.341	-0.26	3154.30	0.04	-0.01	v2+v3(A1)	0.82
E	12	3178.224	-0.35	3178.12	0.10	-0.02	v2+v6(E)	0.81
E	13	3239.943	-0.08	3239.90	0.04	0.60	v3+v4(E)	0.81
E	14	3279.044	-0.08	3279.01	0.03	0.44	v4+v6(E)	0.89
E	19	3430.959	-0.32	3430.90	0.06	-0.16	v2+v5(E)	0.83
A1	16	3523.509	-0.74	3523.52	-0.01	0.15	v4+v5(A1)	0.81
E	20	3533.031	-0.44	3533.09	-0.05	0.24	v4+v5(E)	0.86
A1	17	3578.927	-1.16	3578.79	0.14	0.24	v3+2v5(A1)	0.84
E	24	3838.040	-2.69	3837.94	0.10	0.03	3v5(E)	0.94
A1	21	3988.646	0.00	3988.63	0.02	-0.05	v1+v3(A1)	0.90
E	25	3997.988	0.18	3998.25	-0.26	0.90	3v3+v6(E)	0.78
E	26	4027.331	-0.61	4028.03	-0.70	-0.40	v1+v6(E)	0.90
A1	25	4139.233	-0.26	4139.56	-0.33	-0.02	v2+2v3(A1)	0.61
E	33	4212.332	0.81	4211.80	0.53	1.36	2v3+v4(E)	0.70
E	34	4261.662	0.05	4261.65	0.01	-0.02	v1+v5(E)	0.83
E	37	4294.337	0.41	4294.02	0.32	0.89	v4+2v6(E)	0.71
E	40	4356.524	-0.09	4356.36	0.16	-0.31	v2+v4(E)	0.67
A1	33	4457.781	-0.16	4457.70	0.08	0.10	2v4(A1)	0.70
A1	34	4462.987	-0.56	4463.32	-0.33	-0.28	v2+v5+v6(A1)	0.71
E	48	4486.308	-0.27	4486.36	-0.05	0.26	2v4(E)	0.73
E	49	4529.062	-0.57	4529.00	0.06	0.41	v3+v4+v5(E)	0.63
A1	41	4698.882	-1.38	4698.89	-0.01	-0.20	v2+2v5(A1)	0.81
E	62	4855.300	-3.19	4854.91	0.39	0.03	v3+3v5(E)	0.77
A1	46	4968.171	-0.02	4968.20	-0.02	-0.65	v1+2v3(A1)	0.84
A1	54	5135.054	-0.15	5135.33	-0.28	-0.49	v1+v2(A1)	0.75

E	82	5237.638	-0.17	5237.99	-0.35	0.18	v1+v4(E)	0.56
E	84	5273.275	-0.25	5273.33	-0.06	-0.27	v1+v3+v5(E)	0.67
A1	73	5515.600	-0.55	5515.92	-0.32	-0.30	v1+2v5(A1)	0.82
E	111	5535.920	-0.23	5536.09	-0.17	-0.26	v1+2v5(E)	0.87
A1	86	5759.770	-0.92	5759.88	-0.11	0.31	2v4+v5(A1)	0.70
A1	91	5865.000	1.25	5863.99	1.01	1.07	2v1(A1)	0.77
A1	180	6848.112	1.04	6847.35	0.76	0.56	2v1+v3(A1)	0.75
Mean (obs-calc)			**-0.26**		**0.03**	**0.21**		
RMS (obs-calc)			**0.80**		**0.27**	**0.49**		

All values are in cm^{-1}. Obs: experimentally determined vibrational energy level as collected in Ref [267] using measurements of [270] (and references therein). O-CT(o6) and O-CT(o8) discrepancies between observed levels and CT calculations using CH_4 methane PES (Nikitin et al [268]) . WC = variational calculations of Wang and Carrington [267] using their empirically fitted PES including CHD_3 data. "P.C.wf" – principal contribution of the normal mode basis function.

It is seen that direct CT calculations without adjustable parameters produces un RMS deviation of 0.27 cm^{-1} and mean deviation of 0.03 cm^{-1} from all experimentally known vibrational levels up to 6850 cm^{-1}. This is significantly more accurate compared to published variational calculations [267] that gave RMS deviation of 0.49 cm^{-1} and 0.21 cm^{-1} for the mean deviation. Note that in both case the same three mis-assigned experimental levels (detected by Wang and Carrington [267]) were excluded. A similar kind of agreement in comparison with experimental levels [264, 270] is also obtained in CT calculations for another deuterated CH_3D methane isotopologue.

13. SPHERICAL TOP MOLECULES

There is a variety of spherical top molecules important for atmospheric and astrophysical applications belonging to T_d or O_h point groups. Due to their high symmetry, they possess doubly and triply degenerate vibrational modes. Here we consider two examples with quite different structures of vibrational polyads.

13.1. Five-atomic example with the (4:2:6:3) CT polyad scheme. Vibrational levels of CF_4

A growing interest to the study of the tetrafluoromethane (CF_4) molecule is explained by its very big estimated global warming potentials and a particularly long lifetime in the atmosphere that make it a potential greenhouse gas [271]. It is a spherical top molecule belonging to tetrahedral (T_d) point group at the equilibrium geometry with four fundamental vibrational modes: non-degenerate $\nu_1(A_1)$ =209.02 cm^{-1}, doubly degenerate $\nu_2(E)$ = 435.41 cm^{-1} and two triply degenerate modes $\nu_3(F_2)$ =1539.45 cm^{-1} and $\nu_4(F_2)$ =631.08 cm^{-1}. Experimental measurements of CF_4 spectra and empirical EH parameters have been reviewed in [272,273]. Van Vleck perturbation theory for CF_4 vibrations with empirically fitted PES has been reported by Wang et al [129]. Ab initio PES and DMS surfaces with refined equilibrium C-F distance and quadratic force constants as well as variational calculations of spectra were recently published by Rey et al [274]. Concerning the symmetry properties, CF_4 is similar to methane (CH_4) but has quite different relations between the values of bending and stretching frequencies. In order to account for the resonance coupling terms we use the resonance scheme (4:2:6:3) corresponding to the ratios $(\Omega_1 : \Omega_2 : \Omega_3 : \Omega_4)$ in the modelling CT

operator A defined in eq(81). A comparison of direct CT calculations at order o6 (without adjustable parameters) with experimental vibrational levels and precise variational calculations using the same PES [274] is given in Table 12.1.

Table 13.1. =>**Table 11.** Comparison of vibrational levels of CF_4 computed by CT method from the PES [274] with experimental values and variational calculations.

CT_o6	Γ	**obs**	**CT-Obs**	**var**	**CT-var**	**assignment**
435.4104	E	435.3990	-0.0114	435.4102	-0.0002	v2(E)
631.0851	F	631.0593	-0.0258	631.0857	0.0006	v4(F2)
868.0122	A1	867.9058	-0.1064	868.0117	-0.0005	2v2(A1)
909.0252	A1	909.0720	0.0468	909.0252	0.0000	v1(A1)
1066.2013	F	1066.1220	-0.0793	1066.2013	0.0000	v2 +v4(F2)
1066.7577	F	1066.6977	-0.0600	1066.7583	0.0006	v2 +v4(F1)
1260.5917	F	1260.4300	-0.1617	1260.5927	0.0010	2v4(F2)
1261.8583	A1	1261.8090	-0.0493	1261.8606	0.0023	2v4(A1)
1262.1876	E	1262.1120	-0.0756	1262.1892	0.0016	2v4(E)
1283.7693	F	1283.7201	-0.0492	1283.7704	0.0011	v3(F2)
1539.4572	F	1539.3000	-0.1572	1539.4575	0.0003	v1 +v4(F2)
2445.4555	F	2445.5964	0.1409	2445.4557	0.0002	2v1 +v4(F2)
2562.1725	F	2561.9120	-0.2605	2562.1749	0.0024	2v3(F2)
2570.2189	E	2570.0130	-0.2059	2570.2229	0.0040	2v3(E)

All values are given in cm^{-1}. Γ is the irreducible representation of the T_d point group.
Obs – experimental levels collected in [2712, 273, 275] . "Var" – variational calculations by Rey et al [274].

Figure 13.1. shows a perfect agreement between CT and variational calculations using the same PES [274] up to five vibrational quanta. The rovibrational H^{eff}(CT) has been recently used [275] for assignment and analyses of five CF_4 bands in the range 1600-1800 cm^{-1}.

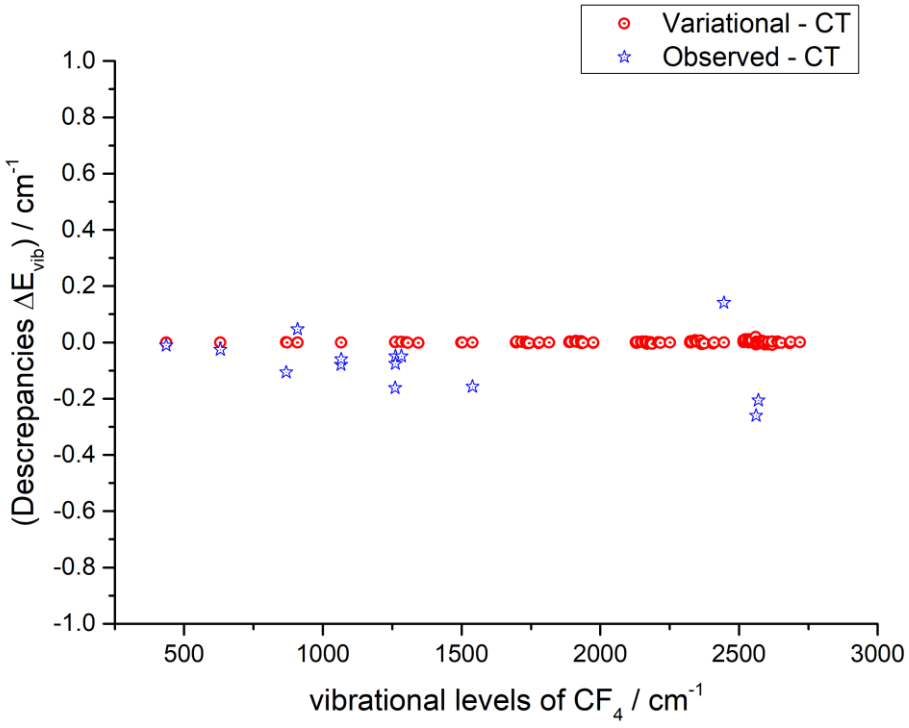

Fig.13.1. => **Figure 9.** Comparison of vibrational levels of CF_4 molecule directly computed by CT method from the PES with experimental values (blue stars) and with variatioan calculations (red circles) using the same PES [274]. RMS deviation (CT-variational) = 0.003 cm^{-1}

13.3 CT resonance scheme (2:1:2:1) for a tetrahedral molecule. Ro-vibrational level of methane polyads.

Methane (CH_4) is considered as one of the most important molecules for atmospheric, astrophysical and environmental applications [276, 277, 278]. Ab initio PESs of methane have been reported in by Lee et al [279], Marquardt and Quack [280,281], Schwenke [268, 282], Nikitin et al [269, 283], Yurchenko et al [284,285], Majumder et al [285], Owens et al [287] (and references therein). Several authors have investigated the convergence of variational calculations: Wang and Carrington [288,289] using contracted basis Lanczos method, and Bowman et al [222] with MULTIMODE approach. Resent comparisons with experimental spectra [290-294] have shown that currently the most accurate first-principle variational calculations of methane spectra based on DMS and PES of [61, 269, 283] were performed by Rey et al [203,295] including spectra up to T=3000 K [291,296,297]. Despite spectacular success of variational methods, ab initio calculations cannot yet achieve experimental accuracy for high-energy states of methane [298,299].

Over the years, effective models for the methane polyads have been used in many studies for assignments and analyses of high-resolution spectra [11,43, 233,300-310] and for quasi-classical investigations of ro-vibration patterns [11, 15, 68, 311, 312]. Methane has been used as a benchmark molecule for testing and validation of theoretical methods, including Van-Vleck transformations by Wang and Sibert [314] and generalised perturbation theory by Cassam-Chenai et al [134, 155, 170, 218] .The polyad structure of the methane molecule is essentially governed by the quasi-coincidence of the stretching fundamental frequencies with the first overtones of the bending frequencies $\nu_1(A_1) \approx \nu_3(F_2) \approx 2\nu_2(E) \approx 2\nu_4(F_2)$. In view of the approximate relation of the harmonic frequencies the commonly used (2:1:2:1) resonance scheme with corresponding relations $(\Omega_1 : \Omega_2 : \Omega_3 : \Omega_4)$ in the

modelling CT operator (81). Due to anharmonic interactions among vibrational modes, the vibration levels of methane are split in sub-levels whose number rapidly increases with energy. Every vibration sub-level possesses rotational states that form complicated patterns strongly coupled by Coriolis and anharmonic resonances.

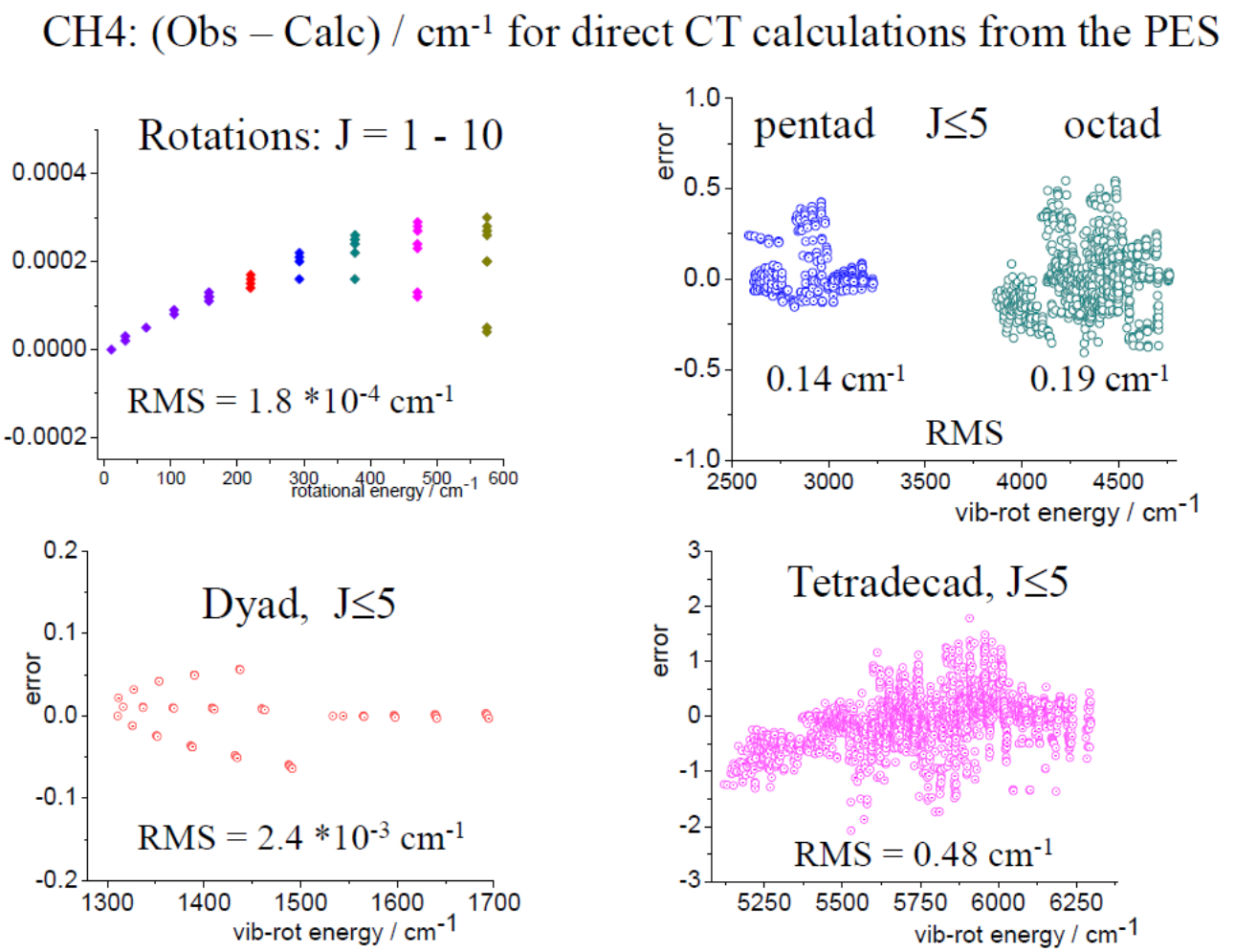

Fig 13.1 => **Figure 10.** Comparison of vibrational-rotation levels of the methane molecule directly computed by CT method [15] from the PES of Nikitin et al [269] with experimental values for five $^{12}CH_4$ polyads.

A mixed "ab initio => CT / effective" approach for building a robust polyad ro-vibrational model using *a priori* information from molecular PES has been suggested in our work [15]. At the initial step, a full set of ro-vibrational terms, including higher-order ones, in effective polyad Hamiltonian are accurately derived from PES using the MOL_CT program suit. Then the $H^{eff}(CT)$ was converted to the irreducible tensor representation using the auxiliary routines of the TENSOR program suite [176] as described in [15]. For polyatomic molecules the accuracy of ab initio PESs is usually not sufficient to directly reach the experimental precision of high-resolution spectra even though this could provide an excellent qualitative agreement. An example of deviations for ro-vibrational level of CH_4 between direct CT calculations and experimental data is shown in Figure 12.1. This step provides a physically consistent initial set of parameters values for H^{eff}. At the second

step, some of diagonal parameters are "relaxed" through the empirical optimisation, but only those of them which are well determined in the least squares fit. Recent progress in experimental data reduction of methane high-resolution spectra was achieved due to the use of CT method [15] that enable to derive physically meaningful initial values for H^{eff} with a successive fine tuning during the fit to experimental line positions [233, 309, 315, 316] including $^{12}CH_4$ and $^{13}CH_4$. The CT method was also used to compute high-temperature partition function of methane [317] by extrapolating ro-vibrational polyads towards the dissociation threshold. Calculations of methane energy levels from the $H^{eff}(CT)$ were carried out with the last version of the MIRS code [14].

14. CT for the dipole moment: effective transition moment operators for intensities of ro-vibrational bands

Another important subject concerns the line intensity calculations. Infrared line intensities I_{nm} for the transition $n \to m$ corresponding to the wavenumber ν_{nm} are defined by

$$I_{nm}(\nu) = \frac{8\pi^3 10^{-36}}{3hcQ(T)} I_0 g(C_n) \nu_{nm} \exp\left(-\frac{hcE_n}{kT}\right)\left(1-\exp\left(-\frac{hc\nu_{nm}}{kT}\right)\right)\mathcal{R}_{nm}$$

in standard spectroscopic units $cm^{-1}/(molecule \times cm^{-2})$. Here $c_2 = hc/k$ with k the Boltzmann constant, $g(C_n)$ and E_n are the nuclear spin statistical weight and the energy of the lower state. $Q(T)$ is the partition function [318], and I_0 is the isotopic abundance of the considered molecular species. The line strength of a dipole-allowed ro-vibrational transition $n \to m$ is defined as $\mathcal{R}_{nm} = \sum_{MM'} |\langle n | \boldsymbol{\mu} | m \rangle|^2 = 3\sum_{MM'} |\langle n | \mu_Z | m \rangle|^2$ in the absence of an external field, where the summation is over all magnetic sublevels of the initial and the final states. Here the dipole moment components (μ_X, μ_Y, μ_Z) of $\boldsymbol{\mu}$ are given in the laboratory-fixed frame (LEF) and $|n>$, $|m>$ are eigenfunctions of the full nuclear motion Hamiltonian.

For the consistency of the CT method, the transformations must be applied also for the dipole moment operator μ_Z

$$\tilde{\mu}_Z = \ldots e^{iS_2} e^{iS_1} \mu_Z e^{-iS_1} e^{-iS_2} \ldots \qquad (100)$$

In order to work in the same representation as the effective Hamiltonian, one has to use the eigen-functions of H^{eff} for line strength calculations

$$< \Psi_i \left| \mu_Z \right| \Psi_f > = {}^{eff} < \Psi_i \left| \tilde{\mu}_Z \right| \Psi_f >^{eff} . \qquad (101)$$

Ab initio DMSs depending on intra-molecular coordinates correspond to the three dipole moment components ${}^{\alpha}\mu(r_1, \ldots r_N)$ in the molecular fixed frame (MFF). They are related to the LFF components by the 3D space rotation $\mu_Z = \sum \varphi_{\alpha Z} {}^{\alpha}\mu$ via the matrix of direction cosines $\varphi_{\alpha Z}$. In the normal mode representation, the MFF dipole moment components can be expanded in the power series for small amplitude vibrations

$${}^{\alpha}\mu = \sum {}^{\alpha}\mu_{i_1 \cdots i_n} q_{i_1} \cdots q_{i_n} = \sum {}^{\alpha} m_{\mathbf{ub}} V_{\mathbf{ub}}^{1,\Gamma} = \sum {}^{\alpha} m_{\mathbf{ub}} \{W_{\mathbf{ub}} + (W_{\mathbf{ub}})^+\}/2 \qquad (102)$$

where ${}^{\alpha}\mu_{i_1 \cdots i_n}$ are computed via the derivatives of the MFF dipole moment functions with respect to the normal coordinate near the equilibrium geometrical configuration. The ${}^{\alpha} m_{\mathbf{ub}}$ coefficients are

simple liner combinations of ${}^{\alpha}\mu_{i_1\cdots i_n}$ computed by the straightforward transformation of normal coordinates to the $a_i^+...a_j^+a_l...a_m$ representation (67)-(68) in the same manner as for the Hamiltonian in Section 5.3.

Similarly to the Hamiltonian (1, 4) the transformed dipole moment (100) is usually expanded [7,8,145-155] in expanded in successive orders of small parameter λ . In what follows, we shall omit the arbitrarily chosen space-fixed Z index to make notations more concise:

$$\tilde{\mu}_Z \equiv \tilde{M} = M_0 + \Delta\tilde{M}_1 + \Delta\tilde{M}_2 + ... + \Delta\tilde{M}_n + ..., \quad \text{where} \qquad \Delta\tilde{M}_n \sim \lambda^n M_0 \tag{103}$$

In case of non-polar molecular with $M_0 = 0$ the $\Delta\tilde{M}_1$ is still considered as the first-order term and so on. Note that using contact transformations Watson [145] has predicted "forbidden" rotational spectrum of methane, which does not have a permanent dipole moment in the equilibrium geometry, but weak transitions are induced by ro-vibrational interactions due to the following terms in (103). The successive layer-by-layer CT are formally applied to the dipole moment in the same manner to give

$$\Delta\tilde{M}_1 = M_1 + [iS_1, M_0] \qquad \sim \lambda^1 \tag{104a}$$

$$\Delta\tilde{M}_2 = M_2 + [iS_1, M_1] + (1/2)[iS_1,[iS_1, M_0]] + [iS_2, M_0] \qquad \sim \lambda^2 \quad , \tag{104b}$$

…

and so on according to the recursive algorithm described in the previous sections.

Approximate analytical expressions for several types of $r^n J^m$ terms in $\tilde{M}$ have been derived by Legay [145], Aliev and Watson [7], Camy-Peyret and Flaud [8] , Makushkin and Tyuterev [100], Sulakshina et al [153] , Loete [152] and other research groups [11, 149, 151, 319-323], but main contributions only have been included in such formulae because of rapidly increasing complexity of calculations. Lamouroux et al [154,324] and Delahaye et al [325,326] have used S_n-generators and effective wavefunctions generated by the MOL_CT program [39,15] described in the previous sections for the dipole moment transformations. Technically, the calculations of commutator are more complicated than in the case of the Hamiltonian because of an extended rotational algebra. The CT –generators are the polynomials in $a_i^+...a_j^+a_l...a_m$ vibrational operators and in rotational operators that can be written in simplified notation as

$$S_n = S_n(a_i^+...a_j^+a_l...a_m;\, J_x, J_y, J_z, \mathrm{J}^2) \;=\; \sum s_{\mathbf{ub;r}} (V_{\mathbf{ub}}^{\Gamma} \square R_{\mathbf{r}}^{\Gamma})^{A_1} \tag{105}$$

to avoid a full nomenclature of cumbersome symmetry indices. Here $V_{\mathbf{ub}}^{\Gamma}$ are vibrational terms (68) and $R_{\mathbf{r}}^{\Gamma}$ are symmetrized powers of rotational operators, where **r** stands for the set of indices described in Section 6 and Γ is the irreducible symmetry representation.

The algebra involving powers of the corresponding rotational operator $\{J_x^n, J_y^k, J_z^m, (\mathrm{J}^2)^l\}$ is known in mathematics as Poincaré enveloping algebra of simple Lie algebra $\{J_x, J_y, J_z\}$. The Casimir operator $\mathbf{J}^2$ of the algebra commute with all other elements. The structural constants of the enveloping rotational algebra are exactly known [39] and are given in the Appendix III in the symmetrized form. In case of the dipole CT the cosine directors $\varphi_{\alpha Z} \equiv \varphi_\alpha$ are involved, which do not commute with rotational operators

$$[\varphi_\alpha, J_\beta] = [J_\alpha, \varphi_\beta] = -i\varphi_\gamma \quad \text{where } (\alpha,\beta,\gamma) = (x,y,z) \tag{106}$$

The rotational enveloping algebra $\{\varphi_x, \varphi_y, \varphi_z; J_x^n, J_y^k, J_z^m, (\mathrm{J}^2)^l\}$ of CT for the dipole moment is thus significantly larger. A supplementary complication is due to the fact that $\mathbf{J}^2$ does not play anymore the role of the Casimir operator because it does not commute with the direction cosines

$[\varphi_\alpha, \boldsymbol{J}^2] \neq 0$. Because of their algebraic properties the direction cosines are involved as a "linear factor" in the transformed dipole moment

$$\tilde{\mu}_Z = \frac{1}{2}\sum_\alpha \left({}^\alpha\tilde{\mu}\varphi_\alpha + \varphi_\alpha {}^\alpha\tilde{\mu} \right) = \sum {}^\alpha\tilde{m}_{\mathbf{ub;r}} V_{\mathbf{ub}}\{\varphi_\alpha, R_\mathbf{r}\} \qquad (107)$$

where the rotational factors involve total angular moment components in the Eckart MFF frame

$$\{\varphi_\alpha, R_\mathbf{r}\} = \frac{1}{2}(\varphi_\alpha R_\mathbf{r} + R_\mathbf{r}\varphi_\alpha) \qquad (107b)$$

The vibrational operators

$$V_{\mathbf{ub}} = \{(a_1^+)^{u_1}(a_2^+)^{u_2}(a_3^+)^{u_3}...(a_1)^{b_1}(a_2)^{b_2}(a_3)^{b_3}...\} \pm \{...\}^+ \qquad (108)$$

keep exactly the same properties both for the commutators (Appendix) and for the matrix elements, whereas related calculations for the rotational operators $\{\varphi_\alpha, R_\mathbf{r}\}$ (which are written here in a simplified concise form) are more complicated. In the works of Lamouroux et al [154, 323], the structure constants of the rotational CT algebra $\{\varphi_x,\varphi_y,\varphi_z; J_x^n, J_y^k, J_z^m, (J^2)^l\}$ for the dipole moment were computed in a specific symmetrized form up to 8-th total power of rotational operators.

14.1. Case of non-degenerate vibrations: asymmetric top molecules

Let us consider a vibrational band associated to the transitions $\upsilon' = (\upsilon'_1\, \upsilon'_2\, \upsilon'_3\, ...) \leftarrow \upsilon = (\upsilon_1\, \upsilon_2\, \upsilon_3\, ,..)$. The eigen-functions of ro-vibrational effective Hamiltonian can be obtained by a diagonalization of the finite-dimensional matrices at the polyad sub-space

$$|\ \Psi\ >^{eff} = |\ \upsilon_1\, \upsilon_2\, \upsilon_3 ...\ J\, K_a\, K_c >^{eff} \qquad (109)$$

Here $C^V_{JK\gamma}$ are expansion coefficients of rotational eigen functions in the Wang basis [110]. For the intensity data reduction during analyses of experimental spectra, an effective dipole transition moment (EDTM) for particular vibration-rotation bands

$${}^{V'V}M = {}^{eff}\!<\Psi_{V'}\,|\,\tilde{\mu}_Z\,|\,\Psi_V>^{eff} = \sum_r {}^{V'V}d_r\{\varphi_\alpha, R_r\} \qquad (110)$$

are often used. In case of asymmetric top molecules, this approach has been introduced by Camy-Peyret, Flaud and co-workers [8,57,148] who have given explicit forms of eight rotational operators $\{\varphi_\alpha, R_\mathbf{r}\}$ up to the third power [148] as well as their matrix elements in the symmetrised Wang basis set $|J\ K\ \gamma>$. Some higher-order rotational terms have been included by Toth [327]. Vibrational matrix elements in Eq. (108) allow for simple exact calculations because effective vibrational wavefunctions are expanded in the initial harmonic oscillator basis via the diagonalization procedure of H^{eff}. The effective dipole transition moment parameters ${}^{V'V}d_r$ for the ro-vibrational band were often fitted to reproduce observed line intensities and to produce line lists for spectroscopic databases.

On the other hand, the values of ${}^{V'V}d_r$ parameters and thus of vibration-rotation line intensities can be accurately computed by the CT method from ab initio PESs and DMSs. Figure 14.1 show an example of a comparison for ro-vibrational line intensities for the three fundamental bands of H_2O with experimental data included in HITRAN-2008 database by the above described CT method without adjustable parameters.

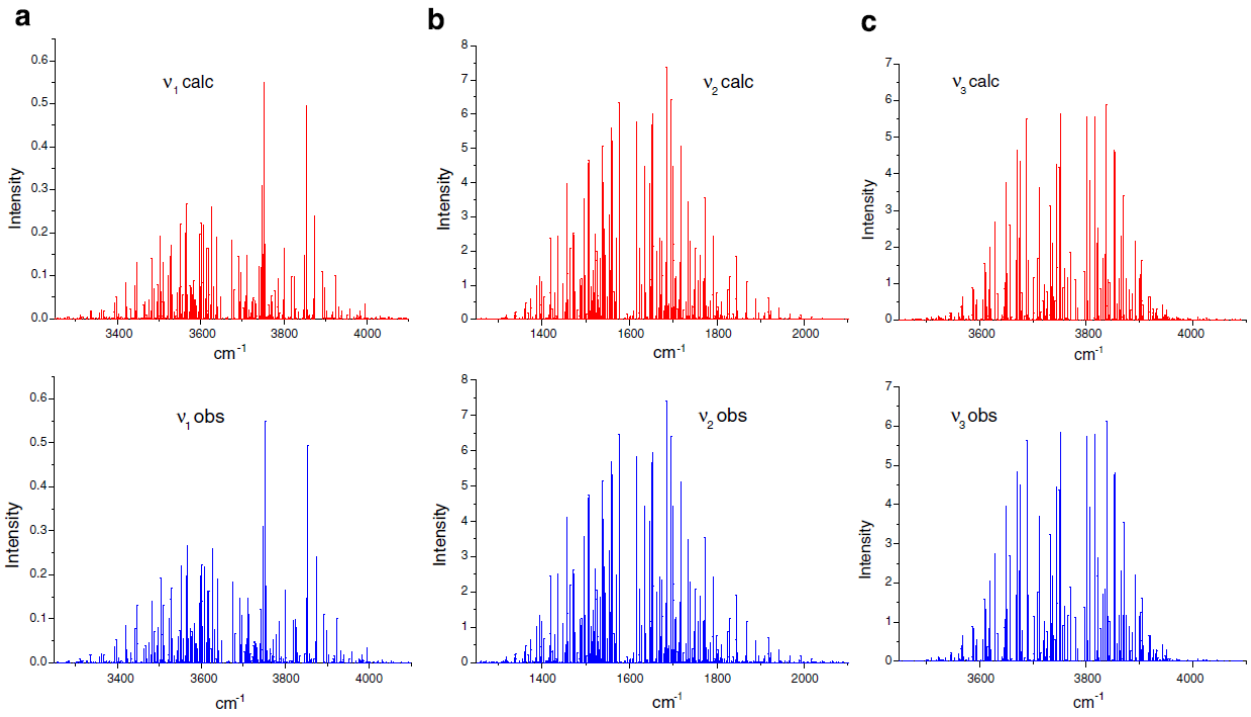

Fig 14.1. => **Figure 11.** Example of rovibrational intensity stick diagrams [cm^{-2}/atm] for fundamental bands of H_2 ^{16}O up to J < 20. CT-calculations. Lower panel: observations included in HITRAN-2008 database. N=1088 lines, **J≤20,** $(I_{obs}-I_{CT})/I_{CT}$ ~ 3% according to Lamouroux et al [154]

14.2. Case of degenerate vibrations : symmetric and spherical top molecules

In case of high-symmetry molecules, the formalism of irreducible tensor operator (ITO) represents an efficient tool permitting compact and precise description of degenerate energy levels, and rovibrational transitions. Various coupling schemes for T_d , C_{3v} and O_h molecules within the ITO formalism have been described in detail by Champion et al [11], Zhilinskii et al [116], Nikitin et al [14, 231], Boudon et al [230,309] and Rey et al [222-224, 252]. In somewhat simplified notations the ITO effective rovibrational Hamiltonian

$$H^{eff} = \sum t_{\mathbf{u,b}}^{\Omega(K,n\Gamma),\tau,\eta} \left(\mathbf{R}^{\Omega(K,n\Gamma)} \times {}^{\tau}\mathbf{V}_{\mathbf{u,b}}^{\eta\Gamma}\right)^{A_1} , \qquad (111)$$

and the transformed dipole moment operator in the MFF frame

$${}^{\alpha}\tilde{\mu} = \sum \tilde{\mu}_{\mathbf{u,b}}^{\Theta} \left(\mathbf{R}^{\Omega(K,n\Gamma_r)} \times {}^{\tau}\mathbf{V}_{\mathbf{u,b}}^{\eta\Gamma_V}\right)_{\alpha}^{\Gamma} \qquad (112)$$

can be written as an expansions containing the products of the rotational **R** and vibrational **V** tensors. Here rotational tensors $\mathbf{R}^{\Omega(K,n\Gamma_r)}$ are characterised by the total power Ω of rotational angular moment components, the tensor rank K in the full rotation group, and irreducible representation Γ_r of the point group. Vibrational tensors ${}^{\tau}\mathbf{V}_{\mathbf{u,b}}^{\eta\Gamma_V}$ are constructed by recursive couplings of elementary creation (a+) and annihilation (a) operators for each normal mode, where η designates collectively the set of all intermediate coupling indices leading to the vibrational

symmetry species Γ_V. This produces Hermitian or anti-hermitian combinations of vibrational tensors (79), where $\mathbf{u}=\{u_1, u_2, u_3\ldots\}$ and $\mathbf{b}=\{b_1, b_2, b_3\ldots\}$ are the vector strings of the corresponding powers of creation an annihilation operators of the normal modes as in eq (68), and $\tau = \pm 1$ is the parity under the time reversal. In Eq.(100), the EH parameters are denotes as $t_{\mathbf{u},\mathbf{b}}^{\Omega(K,n\Gamma),\tau,\eta}$, where $\Gamma = \Gamma_r = \Gamma_v$. In Eq. (101), the symbol Θ designs the string of all upper case indices involved in the tensor product. The transformation from the component-by-component representation in C_{2v} or C_s subgroups to the ITO formulation can be done with the TENSOR program suite [202, 203]. Freely accessible computational program suites MIRS [14,328] and STDS [302] permit computating rovibrational energies and line intensities for ro-vibrational polyads of C_{3v} and T_d molecules using empirically fitted or theoretically derived values of effective Hamiltonian parameters $t_{\mathbf{u},\mathbf{b}}^{\Omega(K,n\Gamma),\tau,\eta}$ and dipole moment parameters $\tilde{\mu}_{\mathbf{u},\mathbf{b}}^{\Theta}$.

Contact transformations for the dipole moment in the ITO formalisms for methane type molecules have been described by Loete [152], Perevalov et al [321], Sadovskii and Zhilinskii [329] and Delahaye et al [325,326]. In particular, Delahaye et al [325,326] have shown that using PES and ab initio DMS of refs [269, 61], the CT method together with MIRS computational code [14,328] has permitted excellent agreement for line intensities of CH_4. The RMS deviation of line intensities between CT and rigorous variational calculations [203] were only of 0.60 % for the Dyad bands and of 0.35% for the Pentad bands up to J=20 without adjusted parameters.

14.2.2. Accurate determination of the resonance coupling parameters and the issue of "sensitive" line intensities : example of the Octad CH_4

Ab initio variational calculations can produce reliable overall description of rovibrational patterns in molecular spectra, many recent works reported a significant progress in this domain [***] (and references therein). However, available ab initio PESs cannot provide the experimental accuracy of line positions ~ 0.001 - 0.0001 cm^{-1} in high-resolution spectra except for tiny molecules with two or three electrons. In cases of accidental resonances between nearby rovibrational states, the wavefunctions could be very sensitive to small errors in energy level calculations. Such small errors in energies could have a large impact on the basis sets mixing coefficients and thus produce large errors in line strengths.

Enhenced accidental mixings in the wavefunctions result in irregular intensity transferts among absorption lines which is known in the literature the "intensity borrowing" effect [15, 61]. This effect is particularly pronounced for relatively weak bands which can "steal" the intensity from stronger bands via a resonance intensity transfer. The accuracy of intensity calculations for such "sensitive" lines is an issue both for purely empirical models and for ab initio variational methods [61]. Such lines are also called "unstable" ones [15], because they correspond to erratic intensity values [61] depending on the model or on the approximation used. Note that by replacing calculated line positions by experimental frequencies, which is a common practice in a construction of line lists, one does not solve the issue of resonance perturbations in line intensities because this improves calculated energies but not wavefunctions involved in the line strengthes (101).

As discussed in [15], the CT method offers a possibility to develop a mixed approach combining advantages of ab initio methods and effective models. As an illustrative example, we consider here an extension of this approach to the first four polyads P of methane molecules. This includes the vibrational ground state (P=0) and the transitions to the Dyad (P=1), Pentade (P=2) and Octad (P=3). The latter one involves eight vibrational ($v_1v_2v_3v_4$) states {(0300)/(0110)/(1100)/(0201)/(0011)/(1001)/(0102)/(0003)} with 24 vibrational sublevels of A_1,A_2,

E, F_1, F_2 symmetry types. In ealier works [Albert , Daumont] the experimental data reduction for the line positions and intensities measured in rotationally resolved spectra has been carried out using purely empirical effective Hamiltonian (111) and effective transition dipole moment (112). A very large set of $t_{\mathbf{u,b}}^{\Omega(K,n\Gamma),\tau,\eta}$ paratmeter in EH fitted to observed line positions was required to achieve an experimental accuracy. For example, in Ref. [Albert] the set of 1494 EH parameters was simultaneously fitted to achieve de RMS (obs-calc) deviation of ~ 0.0013 , 0.006 and 0.0035 cm^{-1} for the Dyad, Pentade and Octad transitions correspondingly. The most part of the empirically fitted terms corresponded to the resonance coupling parameters between upper vibrational states. It is well-known [***] that such parameters cannot be unambiguously determined from experimental line positions because of the correlation issues during the least-square fit. For example, their relative signes could be wrong that is hardly possible to fix with the "closed eyes" fit for thousands of interaction terms. A poorly defined coupling term could then induce an error in rovibrational wavefunctions with an impact on "sensitive" line intensities.

Following the approach outlined in [15], the two-steps method based on CT can be applied in order to stabilise a modelling of experimental spectra. At the first step, the full ro-vibrational EH was directly computed from the PES of ref [**] up to the order o8 for vibrations and order o6 for rotations. This gives the RMS (obs-calc) error of about 0.1 cm^{-1} for the set of Dyad, Pentade and Octad band origins [15]. This represents less than 0.01% in the relative errors. Even if the coupling parameters would be ten or hundred times less accurate, their predicted CT terms from the ab initio based PES can provide physically meaningful initial values for the further empirical EH optimisation. This was the second step of the procedure, which fully confirmed the above mentioned assumption.

An illustration for this two-steps procedure is given in Table 12, which displays the coupling parameters corresponding to strong interaction among upper vibrational states of the methane molecule. The first column of the "V-off diagonal coupling parameters" gives the CT values directly computed from the PES for orders o1, o2 and for some most important o3 terms.

Table 12. Low order interaction parametes for rovibrational polyads of 12CH4

					V-off diagonal coupling parameters (*)			relative
O	Rotational	Vibrational	Off-diagonal		Direct CT	Test 1 : 9 fitted par.	Test 2: 23 fitted par	variations
	ITO	ITO (**)	V	V'	from PES [ ]	to obs	to obs	dP/P
1	R 0(0, 0A1)	V+(23)	0010	0002	-88.06956	-88.3651	-87.95851	0.001
2	R 0(0, 0A1)	V+(35)	0101	0002	4.343237	4.02212	4.241919	0.023
1	R 0(0, 0A1)	V+(49)	0101	0010	77.30136	77.3324	77.10038	0.003
2	R 0(0, 0A1)	V+(80)	0200	0002	4.027476	3.81974	3.853933	0.043
2	R 0(0, 0A1)	V+(71)	0200	0002	-8.290924	-9.07810	-9.086398	-0.096
1	R 0(0, 0A1)	V+(94)	1000	0002	80.37199	79.3977	79.1547	0.008
1	R 0(0, 0A1)	V+(99)	1000	0200	1.652336	1.68502	1.682508	-0.018
1	R 1(1, 0F1)	V-(6)	0100	0001	-9.512905	-9.51987	-9.535905	-0.002
2	R 1(1, 0F1)	V-(25)	0010	0002	-0.196815	f	-0.194823	0.010
2	R 1(1, 0F1)	V-(28)	0010	0002	1.664667	f	1.660343	0.003
3	R 1(1, 0F1)	V-(40)	0101	0002	-0.086659	f	-0.777428	0.103
3	R 1(1, 0F1)	V-(42)	0101	0002	0.172254	f	0.168382	0.022
3	R 1(1, 0F1)	V-(38)	0101	0002	0.039201	f	0.041942	-0.070
3	R 1(1, 0F1)	V-(44)	0101	0002	0.127221	f	0.131208	-0.031
3	R 1(1, 0F1)	V-(46)	0101	0002	-0.062202	f	-0.064296	-0.034
2	R 1(1, 0F1)	V-(52)	0101	0010	-0.640969	f	-0.638820	0.003
2	R 1(1, 0F1)	V-(54)	0101	0010	1.251205	f	1.239689	0.009
3	R 1(1, 0F1)	V-(77)	0200	0002	0.240556	f	0.249630	-0.038
2	R 1(1, 0F1)	V-(83)	0200	0010	-0.483229	f	-0.471709	0.024
3	R 1(1, 0F1)	V-(87)	0200	0101	0.058273	f	0.065045	-0.116

3	R 1(1, 0F1)	V-(86)	0200	0101	-0.080631	f	-0.075643	0.062
3	R 1(1, 0F1)	V-(74)	0200	0101	0.028480	f	0.036405	-0.278
2	R 1(1, 0F1)	V-(97)	1000	0101	-0.114951	f	-0.121388	-0.056
	…	…	…	…	…	f(**)	f(**)	
N fitted v-off-diagonal parameters						**9**	**23**	
N fitted v-diagonal parameters						**272**	**273**	
Total Weighted fit St.Deviation (J_{max}=20)						**0.99**	**0.79**	

O : the order of the term in EH;
(*) with this notations we consider only interaction parameters among different upper vibrational states, whereas the couplings between various sublevels are included in the set of "v-diagonal parameters".
(**) Numerotation of vibrational tensors (111) corresponding to the MIRS scheme of order 6.
f: fixed to CT values ; f(#) : all higher order terms fixed to CT values. dP/P for the for parameters = (CT-fitted)/CT.
N fitted transitions =14652 (Jmax =20).

The rovibrational levels directly computed by CT from the PES for the Octad dataset are depicted in Figure 12. Note that the main feature of the ITO model (111) is that the so called Dyad-specific and Pentad-specific terms give a significant contribution also to the Octad and to higher polyads that essentially determines the resonance mixing of the corresponding wavefunctions shown by different colors in the right-hand side of the Figure. The (calc.-obs.) deviations for CT-predicted rovibrational energies can be seen in Figure 10. In general, the quality is very similar to the variational calculations [***] using the same PES. This means that the (calc.-obs.) deviations in this energy range are essentially limited by the uncertainty of the underlying ab initio PESs and not by the CT method. Many works aimed at improving (calc.-obs.) deviations by a least-square empirical fit of the PES parameters (see for example [WC] and references therein). This is computationally quite demanding procedure that usually results in the (calc.-obs.) deviations, which remain by two or three orders of magnitude larger that the experimental high-resolution accuracy 10^{-3} cm^{-1} for polyatomic molecules like methane, even for the band origins.

Instead of doing this, one can empirically optimise just a small part of parameters in the EH computed by CT. This is much faster, as the polyads are decoupled, and gives much better accuracy for a large set of experimental vibration-rotation transitions.

The second and third columns of the "V-off diagonal coupling parameters" part of Table 12 correspond to the simultaneous fine tuning of a restricted samples of H^{eff}(CT) parameters to presisely match experimental transitions in the Dyad, Pentade and Octad spectra up to Jmax=20. The total set of fitted parameters (< 300) was about 5 times smaller than in the work [Albert] . In this test calculations we have optimized only 9 interaction parameters (fit test 1) or 23 interaction parameters (fit test 2) whereas over 95% of the high-order off-diagonal coupling terms were held fixed to ab initio values predicted by CT. For 14652 observed transitions this gave calculations within the experimental accuracy for line positions with the weighted standard deviations of 0.99 and 0.79.

In the "test 2" , this corresponded to the RMS (calc.-obs.) deviations of 0.0002, 0.0007 and 0.0017 cm^{-1} for the Dyad, Pentade and Octad transitions correspondingly. We are not aware of an empirical optimized PES which could approach such an accuracy for five-atomic molecules.

The last colum of Table 12 shows that the fitted values of interaction parameters remain very close to the original values predicted by CT. This is also valid for principal low order diagonal parameters as was shown in Tables 3 and 6 of [15].

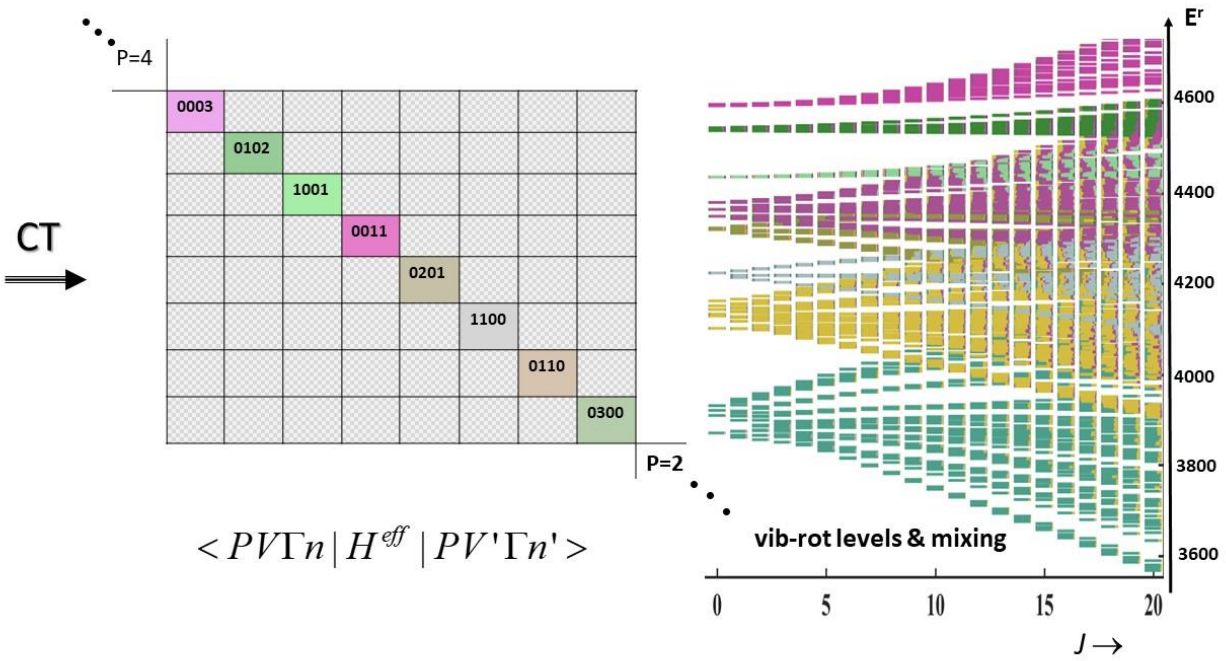

Figure 12. The scheme of CT for the Octad system (P=3) of CH_4 and the rovibrational levels with the basis state mixing coefficients indicated by the corresponding colors. $E^r = E_{vib\text{-}rot} - B_0J(J+1)$ is the standard representation for the reduced energies in cm^{-1}.

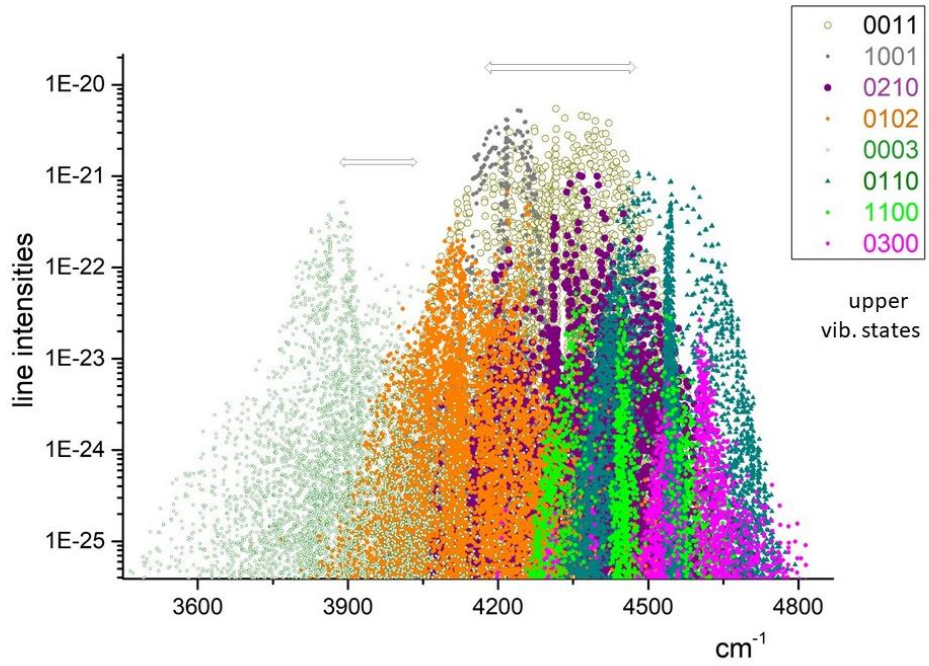

Figure 13 : Example of calculated intensities of the Octade system. The color codes of the bands correspond to the color code of the vibrational upper states . Horisontal arrows at the top of the figure sybolise the exchange of intensities due to the resonance coupling terms corresponding to the mixing of rovibrational wavefunctions depicted in Figure 12.

Another related issue is the modelling of line intensities. The rovibrational wavefunctions produced by the H^{eff} ("Fit test 2") of Table 12, were applied for a test fit of experimental line intensities using effective dipole transition moment (112). Earlier work [Daumont] using purely

empirical H^{eff} reported the RMS intensity deviation for the measured octade bands d_{RMS} = 10.4% and d_{RMS} = 11.3%. The wavefunctions of Heff (Fit test 2) permitted to obtain d_{RMS} = 7.5% with a similar set of data.

In Figure 13 the computed line intensities for the Octad system are shown with the color codes for the bands roughly corresponding to the color code of the upper ro-vibrational states of Figure 12. The exchange of intensities between stronger and weaker lines is determined by the mixing of rovibrational basis functions shown in Figure 12. These latter ones are in turn determined by ab initio coupling terms evaluated with the help of CT. One can conclude that *better wavefunctions produce better intensity fit.*

More elaborate EH models based on CT calculations have been used in the subsequent works [ ] devoted for analyses of experimental CH4 spectra of the Octad band system. It was shown that by fixing of high-order EH parameters to predicted CT values one obtains better extrapolations to weaker lines that permitted to increase assignments and improve the quality of line lists.

15. CT for molecules with large amplitude vibrations: discussion and prospective

The expansions of Section 5.2 are only appropriate if the amplitude of the vibrations is small compared to the internuclear distances. There is a large number of methods and models devoted to large amplitude vibrations [190, 191, 194, 211, 213, 215, 330-342] (and references therein). This list is of course not exhaustive, a more detailed references can be found in recent papers by Viglaska et al [215] and Egorov et al [341]. Here we briefly consider two versions for CT implementations based on the Hougen-Bunker-Johns (HBJ) approach [238] for the choice of the internal coordinates.

Let us designate ρ a large amplitude vibration coordinate as for example the inversion coordinate, similarly to notations of many previous works [215, 238, 342-347]. The following partition is often employed: : $H_0^{\rho} = H_0^{\rho}(\rho, \partial/\partial\rho)$ is the one-dimensional Hamiltonian of the large amplitude vibration and $H_0^{small} = \sum_k \omega_k (a_k^+ a_k + 1/2)$ is the zero-order Hamiltonian of other small amplitude vibrations. The full molecular Hamiltonian can be developed in usual power series of small vibrations q_k but not in a large amplitude coordinate ρ:

$$H_n = \left\{ \sum C_{i\ldots jl\ldots m}(\rho, \partial/\partial\rho; J_\alpha)\ a_i^+ \ldots a_j^+ a_l \ldots a_m \right\} + \{\ldots\}^+ = \frac{1}{2} \sum_{\mathbf{ub}} F_{\mathbf{ub}}(\rho, \partial/\partial\rho; J_\alpha)\ \{W_{\mathbf{ub}} \pm W_{\mathbf{bu}}\} \quad (112)$$

The first part of Eq.(87) is written in the representation of independently running indices and the second part in the representation of fixed mode indices. All the notations are similar to those of Section 5.3. Contrary to Sections 5.2-5.5 the expansion coefficients $C_{i\ldots jl\ldots m}$ and $F_{\mathbf{ub}}$ are no more constants but operators acting on the large amplitude coordinate ρ and on Euler angles.

In the literature two approaches for a partial separation of variables in the HBJ type Hamiltonian were applied leading to different formulation of effective models for non-rigid molecules.

(i) In the first one, the large amplitude vibration $(\rho, \partial/\partial\rho)$ is treated together with the rotation (J_α), both of them being separated out from small vibrations (q_k). This approach has been introduced by Hougen-Bunker-Johns [238] and Hoy, Bunker, Jensen et al [343-347] for their semirigid and nonrigid bending-rotational model. The works on structure and dynamics of quasi-linear molecules has been reviewed by Winnewisser [348]. A similar idea has been also applied by Papousek et al [349] and Spirko et al [350,351] for the inversion-rotation Hamiltonian of NH_3. A 4D bending-roational model of Coudert [352,353] applied for accurate data reduction for the lower vibration states of the water spectra was based on a similar concept but with different choice of the

coordinates. Schematically, if one neglects the resonances, this corresponds to the use of an effective large-amplitude-vibration-rotation Hamiltonian $^{[V]}\mathcal{H}^{eff} = {}^{[V]}\mathcal{H}^{eff}(\rho, \partial/\partial\rho; J_\alpha)$ in a non-degenerate state (V) of small vibrations. Such a model can be systematically derived by the general algorithm of CT with an appropriate choice of the modelling operator $\mathcal{A}$ (Section 2.2). The procedure of the separation of variables described in Section 3 is directly applicable in this case with the modelling operator analogous to (81): $\mathcal{A} = \sum_{s.a.v} \Omega_m a_m^+ a_m$. Here "s.a.v" means a summation over small amplitude vibrations which correspond to {X} variables of Section 3.1. $\mathcal{A}$ acts as unity operator on the large amplitude coordinate ρ which is considered as {y} coordinate. Rotational operators (J_α) are also considered as {Y} variables. Technically, the CT calculations are simplified if the $H_0^\rho = H_0^\rho(\rho, \partial/\partial\rho)$ term can be considered together with the perturbation. This is the case of a floppy large amplitude vibration with the characteristic frequencies << $\omega_k^{s.a.v.}$. The procedure of the separation of fast and slow variables of Section 3.1 can then be applied. The simplification is due to the properties (46) which in the concise notations for large-amplitude-vibration and rotation operators $F \equiv F_{\mathbf{ub}}(\rho, \partial/\partial\rho; J_\alpha)$ read

$$< F\ W_{\mathbf{ub}} > = F < W_{\mathbf{ub}} >, \qquad \frac{1}{\mathfrak{D}}(F\, W_{\mathbf{ub}}) = F \frac{1}{\mathfrak{D}}(W_{\mathbf{ub}}) \tag{113}$$

The action of CT operations on small vibration terms $< W_{\mathbf{ub}} >$, $\frac{1}{\mathfrak{D}}(W_{\mathbf{ub}})$ is exactly the same as in Eqs. (64,69,82). The transformed Hamiltonian takes the form

$$\tilde{H} = f(N_i, n_\varphi, h^{res(j)}; \rho, \partial/\partial\rho; J_\alpha, ...) + f^+(...) \tag{114}$$

For a pure vibrational problem a classical analogous of this procedure has been developed by Joyeux and Sugny [85,144] based on Birkhoff formulation [159] of the perturbation theory. Commutators is the CT recurrent scheme of Section 5 were replaced with the Poisson brackets.

(i) In the second approach suggested by Starikov and Tyuterev [107, 112, 342], the large amplitude coordinate ρ is treated together with small vibrations q_k . The aim is to separate all vibrations from the rotation as full as possible. The operator $H_0 = H_0^\rho + H_0^{small}$ is considered as a zero-order approximation. In the notations of Section 3.1 here {ρ , q_k } are {x} coordinates and {J_α } are {Y} variables. Let us take as an example a NH_3 type molecule [107,342] with the stationary Schrödinger equation for the 1D inversion cut $H_0^\rho \,|t^\pm> = \mathcal{E}_{t^\pm}\,|t^\pm>$. Here $\mathcal{E}_{t^\pm}$ are the zero order energies for symmetric and anti-symmetric inversion states. A suitable choice of the modelling operator is the following

$$\mathcal{A} = (1/2)\sum_t (E_{t^+} + E_{t^-})\mathbf{P}_t + \sum_{s.a.v} \Omega_m a_m^+ a_m \tag{115}$$

Here $\mathbf{P}_t = |t^+><t^+| + |t^-><t^-|$ are the projectors onto the zero order wave functions corresponding to inversion doublets. The action of CT operations on elementary Hamiltonian expansion terms takes the form

$$< F\ W_{\mathbf{ub}} > = \Phi\, W_{\mathbf{ub}}, \qquad \Phi = \sum_{ts} \Delta(\mathbf{P}_t F \mathbf{P}_s) \tag{116}$$

$$\frac{1}{\mathfrak{D}}(F\ W_{\mathbf{ub}}) = T\, W_{\mathbf{ub}} \quad , \qquad T = \sum_{ts} (1-\Delta)(\mathbf{P}_t F \mathbf{P}_s)/\{(\mathcal{E}_t + \boldsymbol{\omega}\cdot\mathbf{u}) - (\mathcal{E}_s + \boldsymbol{\omega}\cdot\mathbf{b})\} \tag{117}$$

Here $\mathcal{E}_t = (\mathcal{E}_{t^+} + \mathcal{E}_{t^-})/2$, and Δ is the extended Kronecker symbol

$$\Delta \equiv \Delta_{ts,\mathbf{ub}} = \begin{cases} 0, & if\ (\mathcal{E}_t + \boldsymbol{\omega}\cdot\mathbf{u}) - (\mathcal{E}_s + \boldsymbol{\omega}\cdot\mathbf{b}) > \eta \\ 1, & if\ (\mathcal{E}_t + \boldsymbol{\omega}\cdot\mathbf{u}) - (\mathcal{E}_s + \boldsymbol{\omega}\cdot\mathbf{b}) \le \eta \end{cases}$$

The parameter η is used as a resonance threshold for the denominator in Eq.(91b). In the absence of resonances and of degenerate vibrations $\Delta = \delta_{ts}\delta_{\mathbf{u},\mathbf{b}}$. According to Eq.(50) in this latter case a full separation of all vibrations is achieved and CTs result in effective rotational Hamiltonian for individual vibration state. This type of transformation modifies considerably the vibrational dependence of the rotation and centrifugal distortion constants [107,112, 342, 354-357]. The resulting expressions for effective Hamiltonians and dipole moments related to this approach were reported in [342] .

Recently Viglaska et al [215] have shown that the HBJ approach, which had been originally introduced for triatomics, was validated for more general case of polyatomic molecules and could lead to new computational scheme for numerically exact transformations of the nuclear motion Hamiltonian.

16. Conclusions

Variational methods versus effective models

Theoretical calculations of the positions and intensities of vibration-rotation lines are carried out using two complementary approaches: global variational methods for the nuclear motion calculations, or effective models localized at a particular spectral ranges covered by available experimental spectra. A comparison of two scheme of calculations if illustrated in Figure 15.1.

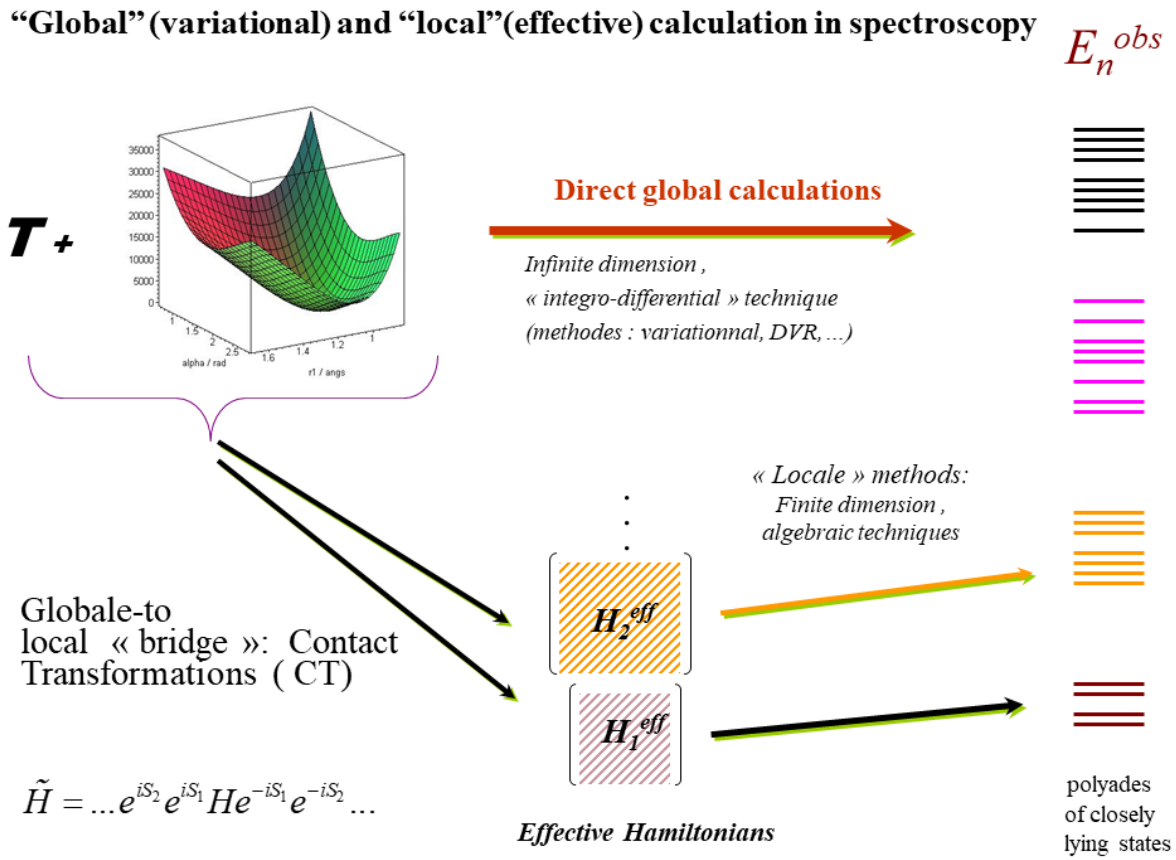

*Fig 16.1. => **Figure 14.** A scheme of two main theoretical approached for computing energy spectrum of a molecule from a potential energy surface. KEO is denoted by T. Effective*

Hamiltonians serve as intermediate models for describing polyads of closely lying states. They can by efficiently used for experimental data reduction in a particular energy range for a fine tuning of parameters initially computed from ab initio PESs

Variational methods for calculating molecular spectra are actively developed in many laboratories around the world (a large list of the relevent references was already given in the beginning of Section 5, Section 8, Section 12.1, and Section 14). Their major advantage is a completeness of calculation of the entire spectra including all hot bands. If the ab initio PES is sufficiently reliable, this can provide theoretical spectra up to the dissociation threshold [246, 358, 359] and sometimes metastable states above it [360,361]. This is particularly important for high-temperature or non-LTE conditions [362,363], in which very excited rovibrational states are pupolated. Several high-temperature databases like HITEMP [292, 364], ExoMol [365], NASA-AMES [366] and TheoReTS [297,367] for astrophysical and combustion applications have been recently created as reviewed in [291, 292, 368].

The accuracy of ab initio calculations based on line positions even for medium size molecules is still far from the experimental accuracy (0.001-0.0001 cm-1) of high-resolution spectra required for metrological applications, but they can provide extremely valuable information on low resolution spectra and band intensities. The variational method could be also used to empirically optimize potential energy surfaces, the parameters of which were adjusted to experimental energy levels. In some cases, this made it possible to approach spectroscopic accuracy for low-energy levels localized near the bottom of the potential well for relatively small light molecules of up to three or five atoms. Recently, the medium resolution predictions of spectra have been extended for six-atomic and seven-atomic molecules like C_2H_4 [369, 370] and SF_6 [232, 371] permitting to elucidate complex patterns of hot bands. However, for molecules with a large number of atoms, aiming at high-resolution accuracy in line positions, the “brute force” approach with exact KEO is extremely time-consuming because of the technical difficulties associated both with the accuracy of underlying ab initio PESs and DMSs and with large basis set dimension for the nuclear degrees of freedom. The corresponding matrices of a full nuclear motion Hamiltonain are in principle infinite dimensional, consequently variational and DVR method face basis set convergence problems involving specific truncation, compression,” pruning” issues etc [204, 372].

Methods of effective Hamiltonians and dipole moment operators accounting for strong coupling of various types of nuclear motion in molecules among closely lying levels offer a tool to study molecular problems, which is complementary to variational methods. The method of effective operators has historically been and still is the main tool for modeling spectra in a given spectral range with an experimental level of accuracy on line positions in certain energy ranges. The major advantage of the effective models is that this approach allows one to reduce an extent of calculations by focusing on a certain group of vibrational states “localized” within a limited energy interval. The latter is supposed to be of interest for an interpretation of a concrete experimental spectrum within a given wave number range. Thus, the dimension of matrices is dramatically reduced and computational realization becomes much simpler, that makes a metrological accuracy of calculations feasible provided that all resonance coupling interaction are correctly included in the model. For this reason, most of data included in spectroscopic databases for atmospheric applications like HITRAN [58], GEISA [59] , JPL [373], CDMS [374], S&MPO[251], STDS [302], MeCaSDa [375], CDSD [376], NOCD[377], ASD [378], and many other compilations - particularly for line positions - are essentially based on empirical effective models. Effective models and related computational codes ((RAM, ERAM, BELGI, XIAM, . . .) for large amplitude/ Internal rotation were reported in [401-406] (and refrerences therein)

Historically, the model parameters were adjusted using the least squares method to the experimental data. In a number of cases, the empirical model makes it possible to describe the vibration-rotation spectrum of this group with a high-resolution accuracy. However, it is well-

known that an EH cannot be unambiguously determined from a fit to experimental energies, particularly for quasi-degenerate polyads of coupled states [172-179] . A rapidly increasing number of poorly determinable EH parameters in the fit, lacking information for "dark" states and strong correlations among fitted parameters ("collinearity issue" [10]) make it mathematically ill-defined problem. In many cases, unreliable values of arbitrarily fitted resonance coupling parameters could then result to false extrapolations for the intensity transfer between weak and strong bands.

Mixed "ab initio/effective" approach

Using the CT or equivalent methods, it is possible, in principle, to obtain relationships between the full Hamiltonian of nuclear motion and effective spectroscopic models in a certain energy range. An inclusion of a priori information from ab initio calculations into the H^{eff}(CT) permits introducing physically meaningful values for the vibrational dependence of rotational constants and for the resonance coupling parameters. This allows for better ro-vibrational assignments and understanding resonance perturbations in spectra.

In Ref [15] , we have developed a hybrid "ab initio => CT / effective" approach for building a robust polyad ro-vibrational model using information from ab initio PES of the methane molecule. At the initial step, a full set of ro-vibrational terms, including higher-order ones in EH were derived from the PES using the MOL_CT program with the accuracy comparable to variational methods. At the second step, one can proceed by an empirical "fine tuning" for some of parameters [15,47, 233, 310, 316] . Only limited number of them well determined in the least squares fit where adjusted. This approach was recently systematically applied for analyses of spectra of $^{13}CH_4$ [315,379] , CF_4 [275] , NF_3[379] and ozone isotopologues [212,380,381].

The scheme of this mixed approach for an optimization of effective spectroscopic models using ab initio information is illustrated in Figure 15.1.

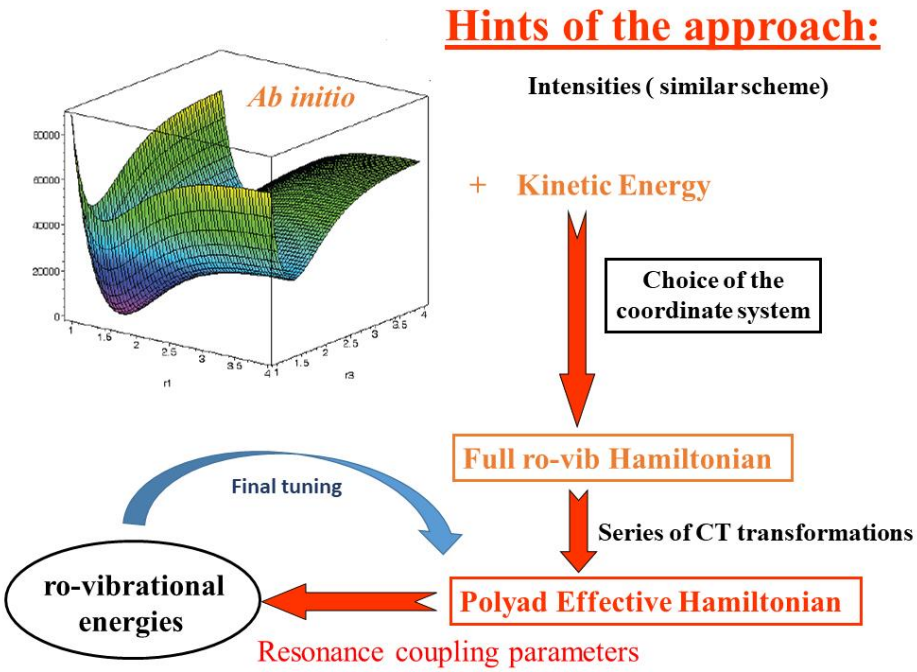

Fig 16.2. => **Figure 15.** Scheme the mixed approach for an optimization of effective spectroscopic models using ab initio information

Such approach significantly reduces the number of the fitted parameters when analysing and modeling experimental spectra. In addition, a better stability for the procedure of experimental data reduction is obtained with faster convergence of iterations [15]. In a certain sense, this permits a regularization of this "inverse spectroscopic problems" with improved extrapolation and convergence of the least squares fit method. A further prospective can be related to a development of EH using non-perturbative numerical method [165].

Another motivation for the ab initio derived spectroscopic model Hamiltonians is a possibility to explore the relation between classic and quantum dynamics of nuclear motion in molecules in polyad subspaces with a particular focus of strongly coupled states and qualitative changes induced by resonance interactions and bifurcations of periodic orbits.

Acknowledgements
The support from ANR-RNF TEMMEX project (grants ANR-21-30CE-0053-01 and RNF 22-42-090) is acknowledged. The GSMA laboratory of Reims University, France, acknowledges a support from SAMIA collaborative program.

APPENDIX I. COMMUTATOR EQUATIONS

A1. Basis definitions

In the context of the CT method for the stationary Schrödinger equation we consider the Hilbert space $\mathcal{E}$ spanned by wave-functions and the $\mathbb{L}$ algebra of operators (defined in Section 2.2) , which act in $\mathcal{E}$. By choosing the modeling operator $\mathcal{A}$ of CT we divide the algebra $\mathbb{L} = \mathbb{L}^{(\mathcal{A})} \oplus \mathbb{L}^{(\perp)}$ as discussed in Section 2.2). A manifold of operators acting in $\mathcal{E}$ has itself properties of space, where one can define certain basis set likes that defined in Sections 2.4, 5.3 as well as linear operation acting on operators, which are often called "transformators " or "super-operators" in the mathematical literatures since earlier works of Crawford [166], Finkelstein [384] and [383,385,386, 29,98].

A simple super-operator involved in CT is the operation of the extraction of the $\mathbb{L}^{(\mathcal{A})}$-contribution from any operator of CT :

$$< X >=< X >_{\mathcal{A}} = X^{(\mathcal{A})} \qquad \text{, where} \quad X^{(\mathcal{A})} \in \mathbb{L}^{(\mathcal{A})}$$

The most relevant for the CT method is the superoperator $\mathfrak{D}_B \equiv \underrightarrow{B} - \underleftarrow{B} = ad_B$ of a commutator with a certain operator B , where notations $\underrightarrow{B}$ and $\underleftarrow{B}$ stand for trivial operations of a multiplications from the right-hand side and from the left hand side $\underrightarrow{B}X \equiv BX$ and $\underleftarrow{B}X \equiv XB$, as defined for example in [383] . In other words, the action of $\mathfrak{D}_B(...)$ is a transformation within the algebra $\mathbb{L}$ converting an operator X to its commutator with B

$$\mathfrak{D}_B(X) \equiv (\underrightarrow{B} - \underleftarrow{B})X = [B, X] \text{ , where both } B \in \mathbb{L} \text{ and } X \in \mathbb{L} \qquad \text{(A1)}$$

Definitions of elementary functions of $\mathfrak{D}_B$ in the $\mathbb{L}$ algebra are straightforward in a usual way both for the *n*-th power

$$\mathfrak{D}_S^n(X) = \mathfrak{D}_S(...\mathfrak{D}_S(X)...) = [\underbrace{S,[S,...[S}_{n}, H]...]] \qquad \text{(A2)}$$

and for the exponential, accounting for the obvious property $[\underrightarrow{S}, \underleftarrow{S}] = 0$:

$$\{e^{\mathfrak{D}_S}\}X = \{e^{(\underrightarrow{S}-\underleftarrow{S})}\}X = \{\underrightarrow{e}^{S}\underleftarrow{e}^{-S}\}X = e^{S}Xe^{-S} \qquad \text{(A3)}$$

The Taylor series expansion for the exponent combined with (A2-A3) immediately results in the Backer-Hausdorff expansion

$$\{e^{\mathfrak{D}_S}\}X = \left\{\sum_{n=0}^{\infty}\frac{1}{n!}\mathfrak{D}_S^n\right\}X = X + [S,X] + ... + \frac{1}{n!}[\underbrace{S,[S,...[S}_{n},H]...]] + ... \quad , \qquad \text{(A4)}$$

which plays the central role in the CT method. Another way to define functions $F(\mathfrak{D})$ is using an integral transforms $F(x) = \int_a^b f(t)K(x,t)dt$ with a separable kernel $K(x_1 - x_2, t) = K(x_1,t)K(-x_2,t)$ like those of Fourier, Laplace or Mellin. Then

$$F(\mathfrak{D}_B)X = F(\underrightarrow{B} - \underleftarrow{B})X = \int_a^b f(t)K(B,t)XK(-B,t)dt \qquad \text{(A5)}$$

if these integral is well defined.

In view of Eq (A4), the CT can be considered as super operator acting on the Hamiltonian to convert it to an effective one $H \xrightarrow{CT} \tilde{H}$. The major point is how to define the generators of the transformations to achieve a desired simplification? Various partitions of the transformations and different conditions on the generators result in different but equivalent versions of the degenerate perturbation theory as discussed in [6,33,36].

A2. Solving commutator equations

As follows from Sections 2.2, 2.3 one needs to solve commutator equations (15-17) of the type

$$[H_0, X] = \Phi \qquad \text{that is} \quad \mathfrak{D}_{H_0}(X) = \Phi \qquad \text{(A6)}$$

where H_0 and Φ are known operator both belonging to the algebra $\mathbb{L}$, *whereas X is an unknown solution*. As in the context of CT we always need a commutator with H_0, this low case index will thus be omitted in what follows. That is, by definition $\mathfrak{D} \equiv \mathfrak{D}_{H_0}$. To solve the equation (A6) one needs an inverse operation $\mathfrak{D}^{-1} = (\mathfrak{D}_{H_0})^{-1} = (\underrightarrow{H}_0 - \underleftarrow{H}_0)^{-1}$ so that

$\mathfrak{D}^{-1}\mathfrak{D} = 1$ with the formal solution $X = \mathfrak{D}^{-1}(\Phi)$

The point is that the operation $\mathfrak{D}^{-1}$ is not well defined on the entire algebra $\mathbb{L}$ if a decomposition $\Phi = \Phi^{(H_0)} + \Phi^{(\perp_0)}$ would possess a contribution $\Phi^{(H_0)}$ commuting with H_0.

Let us begin with a particular simple choice of the CT modeling operator $\mathscr{A}$ equal to the zero-order Hamiltonian without quasi-degenerate levels (no accidental resonances !)

$$\mathscr{A} = H_0 = \sum_L E_L^{(0)} P_L, \qquad \text{where } P_L = \sum_{ij} |L,i><L,j| \qquad \text{(A7)}$$

Here P_L are the projectors on degenerate eigen-spaces spanned by the zero-order basis functions, consequently $<\Phi> = <\Phi>_{H_0} = \sum_L P_L \Phi P_L \in \mathbb{L}^{(H_0)}$ commute with H_0.

There are three possible cases:

(α) If $\Phi \in \mathbb{L}^{(H_0)}$, that is $<\Phi>_{H_0} \neq 0$, then the equation (A6) does not have a solution. This follows from $<[H_0, X]>_{H_0} = 0$ that can be symbolically written as $\mathfrak{D}(\mathbb{L}) \Rightarrow \mathbb{L}^{(\perp_0)}$

(β) If $\Phi \in \mathbb{L}^{(\perp_0)}$, that is $<\Phi>_{H_0} = 0$, then the equation (A6) has an unique solution at the sub-space $\mathbb{L}^{(\perp_0)}$:

$$X^{(\perp_0)} = \mathfrak{D}^{-1}(\Phi) = \sum_{LM}(E_L^{(0)} - E_M^{(0)})^{-1} P_L \Phi P_M, \qquad \text{where} \quad X^{(\perp_0)} \in \mathbb{L}^{(\perp_0)} \quad \text{(A8)}$$

(γ) If $\Phi \in \mathbb{L}^{(\perp_0)}$, that is $<\Phi>_{H_0} = 0$, then a general solution of eq.(A6) at the entire CT algebra $\mathbb{L}$ can be written as a sum of the particular solution (A8) plus an arbitrary term $<z>$ belonging to $\mathbb{L}^{(\perp_0)}$:

$$X = \mathfrak{D}^{-1}(\Phi) + <z>_{H_0}, \qquad \text{(A9)}$$

In the standard version of CT, the constraint $<X>_{H_0} = 0$ is commonly applied. By a appropriate choice of arbitrary terms $<z>$, we can obtain most of other published versions of degenerate perturbation theory as a particular cases of the generalized CT method as discussed in detail in [6,33,36].

A3. Quasi-degenerate case: account for the resonance couplings

To include quasi-degenerate states in the effective Hamiltonian we extend the definition of the CT modeling operator $\mathcal{A}$ as discussed in [6,36] and in Section 2.2 with a more flexible target requirement $[\tilde{H}, \mathcal{A}] = 0$. One of the possible ways is to define $\mathcal{A}$ by eqs (34-35) with the condition that the algebra of the CT transformed Hamiltonian would be enlarged $\mathbb{L}^{(\mathcal{A})} \supset \mathbb{L}^{(H_0)}$ by including polyads of nearby states . This approach also works for the case of overlapping polyads. Another possibility is to include in $<\tilde{H}>_{\mathcal{A}}$ all coupling terms which are necessary to describe strong interactions in considered experimental spectra. Other choices are possible in relation with the problem of separation of fast and slow variables.
In order to obtain a general solution of the commutator equations in this sense, which are valid on the entire CT algebra $\mathbb{L}$, the following definition is used through this work

$$\frac{1}{\mathfrak{D}}(\Phi) = \mathfrak{D}^{-1}\left(\Phi - <\Phi>_{\mathcal{A}}\right) \qquad \text{(A10)}$$

In general, the action of the inverse commutator operations can be written via integrals (A5) using Fourier transformation

$$\frac{1}{\mathfrak{D}}(\Phi) = i \lim_{\beta \to +0} \int_0^{\infty} \exp(-\beta t) \exp(-iH_0 t)\{\Phi - <\Phi>_{\mathcal{A}}\} \exp(iH_0 t) dt \qquad \text{(A11)}$$

or alternative transformations of Lapalce of Mellin [6]. In the particular case of $\mathcal{A}=H_0$, this coincides with the original definitions introduced by Primas [29,98] .
For practical calculations for the bound states, it is always possible to find an eigen-representation in the CT algebra L where the actions of superoperators $\frac{1}{\mathfrak{D}}(...)$ and of $<...>$ reduce to simple multiplication by appropriate constant factors. An example is given by ket-bra operators $P_{LM} = \sum_{ij} |L,i><_0\ _0 M,j|$ of the zero-order basis set . For the normal mode vibrational operators (60-63, 68) the solution is particularly compact as follows from (64-66,69,79).

APPENDIX II. VIBRATIONAL COMMUTATORS AND ANTICOMMUTATORS

Consider (anti)-commutator of two operators V_1 and V_2

$$[V_1^{\theta_1,\Gamma_1}, V_2^{\theta_2,\Gamma_2}]_{\pm} \equiv [\frac{1}{2}(N_1^{\Gamma_1} + (-1)^{\theta_1}(N_1^{\Gamma_1})^{+}), \frac{1}{2}(N_2^{\Gamma_2} + (-1)^{\theta_2}(N_2^{\Gamma_2})^{+})]_{\pm} =$$

$$\frac{1}{4}\{([N_1^{\Gamma_1}, N_2^{\Gamma_2}]_{\pm} + (-1)^{c+\theta_1+\theta_2}[N_1^{\Gamma_1}, N_2^{\Gamma_2}]_{\pm}^{+}) + +(-1)^{\theta_2}([N_1^{\Gamma_1}, (N_2^{\Gamma_2})^{+}]_{\pm} + (-1)^{c+\theta_1+\theta_2}[N_1^{\Gamma_1}, (N_2^{\Gamma_2})^{+}]_{\pm}^{+})\}$$

where c=1 for a commutator and c=0 for an anticommutator. It is seen that in order to calculate this it is necessary to calculate two (anti)-commutators $[N_1, N_2]_\pm$ and $[N_1, N_2^\pm]_\pm$. These commutators can be expressed as linear combinations of N-type operators with numerical coefficients A and B

$$[N_1^{\Gamma_1}, N_2^{\Gamma_2}]_\pm = \sum_i A_i N_i^{\Gamma} \text{ and } [N_1^{\Gamma_1}, (N_2^{\Gamma_2})^+]_\pm = \sum_j B_j N_j^{\Gamma},$$

where $\Gamma = \Gamma_1 \times \Gamma_2$. This yields

$$[V_1^{\theta_1,\Gamma_1}, V_2^{\theta_2,\Gamma_2}]_\pm = \frac{1}{2}\{\sum_i A_i V_{\vec{p}_i\vec{q}_i}^{c+\theta_1+\theta_2,\Gamma} + (-1)^{h_2}\sum_j B_j V_{\vec{r}_j\vec{s}_j}^{c+\theta_1+\theta_2,\Gamma}\}$$

Calculation of the product N_1N_2 is based on usage of the following expression for the one-dimensional elementary vibrational commutator (Appendix IX of Ref. 6)

$$[a^m, (a^+)^n]_- = \sum_{k=1}^{\min(m,n)} \frac{n!m!}{(n-k)!(m-k)!k!}(a^+)^{n-k}a^{m-k}$$

We have

$$N_1N_2 = N_{\vec{p}\vec{q}}N_{\vec{r}\vec{s}} = \sum_{k_1=0}^{\min(r_1,q_1)} \frac{r_1!q_1!}{(r_1-k_1)!(q_1-k_1)!k_1!}\sum_{k_2=0}^{\min(r_2,q_2)} \frac{r_2!q_2!}{(r_2-k_2)!(q_2-k_2)!k_2!}\sum_{k_3=0}^{\min(r_3,q_3)} \frac{r_3!q_3!}{(r_3-k_3)!(q_3-k_3)!k_3!}N_{\vec{x}\vec{y}}$$

where $\vec{x} = \vec{p} + \vec{r} - \vec{k}$, $\vec{y} = \vec{q} + \vec{s} - \vec{k}$, $\vec{k} = (k_1, k_2, k_3)$. To get N_2N_1 from N_1N_2 it is necessary to swap indices $p \leftrightarrow r$ and $q \leftrightarrow s$. Systematical use of the latter equation is sufficient to calculate coefficients A_i and B_j and then the commutator itself.

APPENDIX III. ROTATIONAL COMMUTATORS AND ANTICOMMUTATORS

By definition

$$\left[R_{m_1,n_1,2l_1}^{\theta_1,\Gamma_1}, R_{m_2,n_2,2l_2}^{\theta_2,\Gamma_2}\right]_\pm \equiv R_{m_1,n_1,2l_1}^{\theta_1,\Gamma_1}R_{m_2,n_2,2l_2}^{\theta_2,\Gamma_2} \pm R_{m_2,n_2,2l_2}^{\theta_2,\Gamma_2}R_{m_1,n_1,2l_1}^{\theta_1,\Gamma_1}$$

Substitution the shift and other algebraic properties of the angular momentums components [6] into this equation yields

$$\left[R_{m_1,n_1,2l_1}^{\theta_1,\Gamma_1}, R_{m_2,n_2,2l_2}^{\theta_2,\Gamma_2}\right]_\pm = \frac{1}{2}\{\sum_i A_i R_{m_i,n_i,2(l_1+l_2)}^{\theta_1+\theta_2+c,\Gamma} + (-1)^{\theta_2}\sum_{j,\alpha} B_{j,\alpha} R_{m_j,n_j,2(l_1+l_2+\alpha)}^{\theta_1+\theta_2+c,\Gamma}\},$$

where c=1 for a commutator and c=0 for an anti-commutator. $\Gamma = \Gamma_1 \times \Gamma_2$. Numerical coefficients A_i and B_j are defined according to equations

$$\left[Z_{+m_1n_1}, Z_{+m_2n_2}\right]_\pm = \sum_i A_i Z_{+m_in_i}, \left[Z_{+m_1n_1}, Z_{-m_2n_2}\right]_\pm = \sum_{j,\alpha} B_{j,\alpha} Z_{+m_jn_j} J^{2\alpha},$$

Taking into account commutational relations of J_x, J_y, J_z, J^2 and definitions of Section 6, after tedious but straightforward algebraic manipulations we get [39] for the case $m_1 \geq m_2$

$$\left[R_{m_1,n_1,2l_1}^{\theta_1,\Gamma_1}, R_{m_2,n_2,2l_2}^{\theta_2,\Gamma_2}\right]_\pm = \frac{1}{2}\{\sum_{i=0}^{n_1}\sum_{j=0}^{n_2} A_{ij} R_{(m_1+m_2),(n_1+n_2-i-j),2(l_1+l_2)}^{\theta_1+\theta_2+c,\Gamma_1\times\Gamma_2} +$$

$$(-1)^{h_2}\sum_{\alpha=0}^{m_2}\sum_{\beta=0}^{2m_2}\sum_{i=0}^{n_1}\sum_{j=0}^{n_2}\sum_{k=0}^{\beta} B_{\alpha\beta ijk} R_{(m_1-m_2),(n_1+n_2-i-j-k),2(l_1+l_2+\alpha)}^{\theta_1+\theta_2+c,\Gamma_1\times\Gamma_2}\},$$

where $A_{ij} = \frac{n_1!}{i!(n_1-i)!}\frac{n_2!}{j!(n_2-j)!}\left(\frac{m_1}{2}\right)^j\left(\frac{m_2}{2}\right)^i[(-1)^j \pm (-1)^i]$

and $B_{\alpha\beta ijk} = C_{\alpha\beta}^{m_2}\frac{n_1!}{i!(n_1-i)!}\frac{n_2!}{j!(n_2-j)!}\frac{\beta!}{k!(\beta-k)!}\left(\frac{m_1}{2}\right)^j\left(\frac{m_2}{2}\right)^i\left(\frac{m_1-m_2}{2}\right)^k[(-1)^{i+j+k} \pm (-1)^\beta]$

Numerical coefficients $C_{\alpha\beta}^m$ are connected with Loevdin polynomials $((a,b))^{[k]}$ see e.g. Ref. 6.

$$((a^2,b))^{[k]} = \prod_{i=0}^{k-1}[a^2-(b-i)(b-i-1)] = \sum_{\alpha=0}^{k}\sum_{\beta=0}^{2k} C_{\alpha\beta}^{k} a^{2\alpha} b^{\beta}, \quad ((a^2,b))^{[0]} = 1$$

For the case $m_1 < m_2$ it is necessary to swap (m_1,n_1) and (m_2,n_2) in the equation for $B_{\alpha\beta ijk}$.

References (Revision: v2)

Before N156 → unchanged !

Color code: blue = newly added
After adding or removal; the numbering is changed
Left number = new < right hand number = old

1. J. H. Van Vleck, On sigma-type doubling and electron spin in the spectra of diatomic molecules, Phys. Rev. **33,** 467 (1929).
2. G. Amat and H.H. Nielsen, J. Chem. Phys **36**, 1159 (1962).
3. G. Amat, H.H. Nielsen, G. Tarrago, *Rotation - vibration of polyatomic molecules* (Dekker, New York, 1971).
4. T. Oka, J. Chem. Phys. **47**, 5410 (1967).
5. I. M. Mills, in *Molecular Spectroscopy: Modern Research*, edited by K. Narahari Rao and C. W. Mathews, (Acadmic Press, New York, 1972), pp. 115-140.
6. Yu. S. Makushkin, Vl. G. Tyuterev, *Perturbation Methods and Effective Hamiltonians in Molecular Spectroscopy*, (Nauka, Novosibirsk, 1984) [in Russian].
7. M. R. Aliev and J. K. G. Watson, in *Molecular Spectroscopy: Modern Research* edited by K. Narahari Rao (Acadmic Press, Orlando, FL, 1985) pp. 1-67.
8. C. Camy-Peyret and J. M. Flaud, in *Molecular Spectroscopy: Modern Research*, edited by K. Narahari Rao (Acadmic Press, Orlando, FL, 1985).
9. E.L. Sibert, J. Chem. Phys. **88,** 4378 (1988).
10. K. Sarka, and J. Demaison, *Perturbation Theory, Effective Hamiltonians and Force Constants*. In *Computational Molecular Spectroscopy*; edited by P. Jensen, and P.R. Bunker (John Wiley & Sons Ltd. New York, 2000).
11. J.P. Champion, G. Pierre, M. Loete, in *Spectroscopy of the Earth's Atmosphere and Interstellar Medium,* edited by K. Narahari Rao (Academic Press, New York,1992), pp.339-442.
12. P.R. Bunker and R.E. Moss, *Mol. Phys.* **33**, 417 (1977).
13. D.W. Schwenke, J. Phys. Chem. **A105**, 2352 (2001).
14. A.V. Nikitin, M. Rey, J.P. Champion, Vl.G. Tyuterev, J. Quant. Spectrosc. Radiat. Transfer, 113 1034, (2012).
15. V. Tyuterev, S. Tashkun, M. Rey, R. Kochanov, A. Nikitin, T. Delahaye, J. Phys. Chem. **A117**, 13779 (2013).

16. L.S. Rothman and S.A. Clough, J. Chem. Phys. **55**, 504 (1971).
17. M. Herman and D.S. Perry, Phys. Chem. Chem. Phys. **15**, 9970 (2013).
18. H. Rabitz in *Effective Hamiltonians in Molecular Collisions, Modern Theoretical Chemistry III,* edited by W.H. Miller (Plenum, New York, 1976).
19. J.P. Malrieu, P. Durand, J.P. Daudey, J. Phys. A: 18, 809 (1985).
20. S. Huzinaga, J. Mol. Struct. 234, 51 (1991).
21. F. Mila and K.P. Schmidt in *Introduction to Frustrated Magnetism. Springer Series in Solid-State Sciences*, edited by C. Lacroix, P. Mendels, F. Mila. (Springer, Berlin, Heidelberg, 2011).
22. J. Wachsmuth and S. Teufel, American Mathematical Soc. 2014.
23. W. Shao, C. Wu, X.L. Feng, Phys. Rev. A95, 032124 (2017).
24. F. Neese, L. Lang, V.G. Chilkuri, in *Topology, Entanglement, and Strong Correlations Modeling and Simulation* edited by E. Pavarini and E. Koch (Forschungszentrum, Julich, 2020).
25. P. Gartner and V. Moldoveanu, Phys. Rev. A105, 023704 (2022).
26. N.N Bogolyubov, S.V. Tiablikov, ZETF **19**, 251 (1949).
27. C. Bloch, Nuclear Phys. **6**, 329 (1958).
28. J. Des Cloizeaux, Nuclear Phys. **20**, 321 (1960).
29. H. Primas, Rev. Mod. Phys. **35**, 710 (1963).
30. C. Soliverez, J. Phys. **C2**, 2161 (1969).
31. D.Klein, J. Chem. Phys. **61**, 786 (1974).
32. A. Chedin and Z. Cihla, J.Mol.Spectrosc. **49**, 289 (1974)
33. Vl.G. Tyuterev, in *Effective Hamiltonians in Intramolecular interactions and Infra-red spectra of Atmospheric gases*, p3-46, (1975).
34. F. Jorgensen, Mol. Phys. **29** 1137 (1975).
35. Yu.S. Makushkin and Vl.G. Tyuterev, Soviet Phys. J., **20** 898 (1977).
36. Vl.G. Tyuterev and V.I. Perevalov, Chem. Phys. Lett. **74**, 494 (1980).
37. E.L. Sibert, III. J.T. Hynes, W.P. Reinhardt, J. Chem. Phys. **77**, 3595 (1982).
38. P. Jensen and P.R. Bunker, J. Mol. Spectrosc. **118**, 18 (1986).
39. Vl.G. Tyuterev, S.A. Tashkun, H. Seghir, Proceedings of SPIE, **5311**, 164 (2004).
40. G.L. Manni, F. Aquilante, L. Gagliardi, J. Chem. Phys. **134**, 034114 (2011).
41. J.M. Flaud and C. Camy-Peyret, J. Mol. Spectrosc. **51**, 142 (1974).
42. S.A. Tashkun, V.I. Perevalov, J.L. Teffo, L.S. Rothman, Vl.G. Tyuterev, (1998) J. Quant. Spectrosc. Radiat. Transfer, **60**, 785 (1998).
43. L. Daumont, A.V. Nikitin, X. Thomas, L. Regalia, P. Von der Heyden, V. Tyuterev, M. Rey, V. Boudon, C. Wenger, M. Loëte, L.R. Brown, J. Quant. Spectrosc. Radiat. Transfer **116**, 101 (2013).
44. V. Boudon, L. Manceron, F. Kwabia Tchana, M. Loëte, L. Lago, P. Roy, Phys. Chem. Chem. Phys. **16**, 1415 (2014).
45. O.M. Lyulin, V.I. Perevalov, J. Quant. Spectrosc. Radiat. Transfer 177, 59 (2016).
46. A. Perrin, J.M. Flaud,, F. Kwabia-Tchana, L. Manceron, P. Groner Mol. Phys. 323 (2018).
47. A.V. Nikitin, A.A. Rodina, X. Thomas, L. Manceron, L. Daumont, M. Rey, K. Sung, A.E. Protasevich, S.A. Tashkun, I.S. Chizhmakova, V.G. Tyuterev, J. Quant. Spectrosc. Radiat. Transfer, **253**, 107061 (2020).
48. A. Barbe, S. Mikhailenko, E. Starikova, V. Tyuterev, J. Quant. Spectrosc. Radiat. Transfer, **276**, 107936 (2021).
49. J.M. Flaud, C. Camy-Peyret, K. Narahari Rao, D.W. Chen, Y.S. Hoh, J.P. Maillard, J. Mol. Spectrosc. **75,** 339 (1979).
50. J.M. Flaud, A. Barbe C. Camy-Peyret, J.J. Plateaux. J. Mol. Spectrosc. **177**, 34 (1996).
51. J.M. Flaud, T.A. Blake, W.J. Lafferty, Mol. Phys. **115**, 44 (2017).

52. J.M. Flaud, W.J. Lafferty, V. Malathy Devi, R.L. Sams,D. Chris Benner, J. Mol. Spectrosc. **267**, 3 (2011).
53. J.M. Flaud, W.J. Lafferty, F. Kwabia Tchana, A. Perrin, X. Landsheere, J. Mol. Spectrosc. **271**, 38 (2012)..
54. J.M. Flaud, F.K. Tchana, W.J. Lafferty, C.A. Nixon, Mol. Phys. **108**, 699 (2010).
55. J.M. Flaud, A. Anantharajah, F.K. Tchana, L. Manceron, J. Orphal, G. Wagner, M. Birk, J. Quant. Spectrosc. Radiat. Transfer, **224**, 217 (2019).
56. J.M. Flaud, F. Kwabia Tchana, W.J. Lafferty, A. Perrin, L. Manceron, M. Ndao, Mol. Phys., **116**, 3463 (2018).
57. J.M. Flaud, C. Camy-Peyret, C.P. Rinsland, M.A.H. Smith, V. Malathy Devi, *Atlas of ozone spectral parameters from microwave to medium infrared*. (Academic press, Boston; 1990).
58. I.E. Gordon, L.S. Rothman, R.J. Hargreaves, R. Hashemi, E.V. Karlovets, F.M. Skinner, E.K. Conway, C. Hill, R.V. Kochanov, Y. Tan, *et al.* (85 authors). J. Quant. Spectrosc. Radiat. Transfer **277**, 107949 (2022).
59. T. Delahaye, R. Armante, N.A. Scott, N. Jacquinet-Husson, A. Chedin, L. Crepeau, J. Mol. Spectrosc. **380**, 111510 (2021).
60. G.J. Cartwright and I.M. Mills, J. Mol. Spectrosc. **34**, 415, Journal of Molecular Spectroscopy (1970)
61.A.V. Nikitin, M. Rey, V.G. Tyuterev, J. Quant. Spectrosc. Radiat. Transfer, 200, 90 (2017).
62. E. Starikova, A. Barbe, M.-R. De Backer, V.G. Tyuterev, . Quant. Spectrosc. Radiat. Transfer 257, art. no. 107364 (2020)
63. A. Perrin, L. Manceron, R. Armante, F. Kwabia-Tchana, P. Roy D. Doizi, Mol.Phys. Published online: 13 Oct 2021 https://doi.org/10.1080/00268976.2021.1987543
64. R.T. Lawton and M.S. Child, Mol. Phys. **44**, 709 (1981).
65. L. Halonen, M.S. Child, S. Carter, Mol. Phys. **47**, 1097 (1982).
66. W.G. Harter, C.W. Patterson, J. Chem. Phys. **80**, 4241 (1984).
67. B.I. Zhilinskií, I.M. Pavlichenkov, Sov. Phys. JETP **65**, 221 (1987).
68. D.A. Sadovskií, B.I. Zhilinskií, J.P. Champion, G. Pierre, J. Chem. Phys. **92**, 1523 (1990).
69. L. Xiao and M.E. Kellman, J. Chem. Phys. **93**, 5805 (1990).
70. M.E. Kellman, J. Chem. Phys. **83**, 3843 (1985).
71. D.A. Sadovskii and B.I. Zhilinskii. Phys. Rev. **47*A***, 2653 (1993).
72. M.E. Kellman, Annu. Rev. Phys. Chem **46**, 395 (1995).
73. G. Jolicard, Annual Rev. Phys. Chem. **46**, 83 (1995).
74. T. Sako and K. Yamanouchi, Chem. Phys. Lett. **264**, 403 (1996).
75. T. Weston and M.S. Child, Chem. Phys. Lett. **262**, 751 (1996).
76. Z. M. Lu and M.E. Kellman, J. Chem. Phys., **107**, 1 (1997).
77. S.C. Farantos, R. Schinke, H. Guo, M. Joyeux, Chem. Rev. **109**, 4248 (2009).
78. L. Halonen, in *Computational Molecular Spectroscopy*, edited by P. Jensen, P.R. Bunker, (John Wiley & Sons, 2000).
79. B. Zhilinskii, Phys. Rep. **341**, 85 (2001).
80. T. Sako, K. Yamanouchi, F. Iachello, J. Chem. Phys. **117**, 1641 (2002).
81. M.S. Child in in *Computational Molecular Spectroscopy*, edited by P. Jensen, P.R. Bunker, (John Wiley & Sons, 2000).
82. C. Jung, H.S. Taylor, E. Atilgan, J. Phys. Chem. **A106**, 3092 (2002).
83. H. Waalkens, C. Jung, H.S. Taylor, J. Phys. Chem. **A106**, 911 (2002).
84. M. Joyeux, S.C. Farantos, R. Schinke, (2002) J. Phys. Chem. **A106**, 5407 (2002).
85. M. Joyeux and D. Sugny, Can. J. Phys., **80**, 1459 (2002).
86. I.N. Kozin, D.A. Sadovskii, B.I. Zhilinskii, Spectrochim. Acta, **A61,** 2867 (2004).
87. I.M. Pavlichenkov and B.I. Zhilinskii, Ann. Phys. **184**, 1 (1988).
88. M.E. Kellman and V. Tyng Acc. Chem. Res. **40**, 243 (2007).

89. D.A. Sadovskii and B.I. Zhilinskii, Phys. Lett. **A383**, 452 (2019).
90. R. Prosmiti, S.C. Farantos, H. Guo, Chem. Phys. Lett. **311**, 241 (1999).
91. Multidimensional Quantum Dynamics: MCTDH Theory and Applications; edited by H.D. Meyer, F. Gatti, G.A. Worth, (Wiley-VCH, Weinheim, 2009).
92. F. Mauguiere, M. Rey, V. Tyuterev, J. Suarez, S.C. Farantos, J.Phys. Chemi. **A114**, 9836 (2010).
93. F. Mauguiere, V. Tyuterev, S.C. Farantos, Chem. Phys. Lett., **494**, 163 (2010).
94. F.A. Mauguiere, P. Collins, Z.C. Kramer, B.K. Carpenter, G.S. Ezra, S.C. Farantos, S. Wiggins, J. Chem. Phys. **144**, 054107 (2016).
95. M. Micciarelli, R. Conte, J. Suarez, M. Ceotto J. Chem. Phys. **149**, 064115 (2018).
96. O.V. Egorov, F. Mauguiere, V.G. Tyuterev, Russian Physics Journal, **62**, 1917 (2020).
97. H.H. Nielsen, Rev. Mod. Phys. **23**, 90 (1951).
98. H. Primas, Helv. Phys. Acta **34**, 331 (1961)
99. M.R. Aliev, V.T. Alexanyan, Opt. Spektrosk. **24**, 695 (1968) (in Russian).
100. Yu.S. Makushkin, V.G. Tyuterev, Opt. Spektrosk. **35**, 439 (1973) (in Russian).
101. A. Chedin, Z. Cihla, J. Mol. Spectrosc. **45**, 475 (1973).
102. Yu.S. Makushkin, Vl.G. Tyuterev, Phys. Lett. **A47**, pp. 128 (1974).
103. Vl.G. Tyuterev in *High Resolution Molecular Spectroscopy*, (Nauka, Novosibirsk, 1976), pp.93-115. (in Russian).
104. M.R. Aliev, J.K.G. Watson, J. Mol. Spectrosc. **61**, 29 (1976).
105. Yu.S. Makushkin, V.G. Tyuterev, Soviet Phys. J., **20**, 904 (1977).
106. M.R. Aliev, J.K.G. Watson, J. Mol. Spectrosc. **75**, 150 (1979).
107. V.I. Starikov, Vl.G. Tyuterev, Opt. Spectrosk., **51**, 268 (1981).
108. V.I. Perevalov, Vl.G. Tyuterev, B.I. Zhilinskii, J. Physique Paris, **43**, 723 (1982).
109. V.I. Zakharov, Vl.G. Tyuterev, Soviet Phys. J. **25**, 749 (1982).
110. D. Papousek, M.R. Aliev *Molecular vibration-rotation spectra* (Elsevier, Academia, 1982).
111. V.I. Starikov, Vl.G. Tyuterev, Soviet Phys. J. **25**, 921 (1982).
112. V.I. Starikov, B.I. Makhanchejev, Vl.G. Tyuterev, J. Physique Lett. **45**, 11 (1984).
113. VI.G. Tyuterev, T.I. Velichko, Chem. Phys. Lett. **104** 596 (1984).
114. V.I. Zakharov, V.G. Tyuterev, JOSA **B2**, 387 (1985).
115. T.I. Velichko, V.Ya.; Galin, Yu.S. Makushkin, V.G. Tyuterev, *Analytical Calculations Using Computers in Molecular Spectroscopy*, (Novosibirsk, Nauka, 1986) (in Russian).
116. B. Zhilinskii, V. Perevalov, V.G. Tyuterev, *Method of irreducible tensorial operators in the theory of molecular spectra*. (Nauka, Novosibirsk, 1987). (in Russian).
117. E.L. Sibert III, Comput. Phys. Commun. **51**, 149 (1988).
118. E.L. Sibert III, J. Chem. Phys. **90**, 2672 (1989)
119. E. L. Sibert III, Int. Rev. Phys. Chem. **9**, 1 (1990).
120. A.B. McCoy, D.C. Burleigh, E.L. Sibert III, J. Chem. Phys. **95**, 7449 (1991).
121. A.B. McCoy and E.L. Sibert III, J. Chem. Phys. **95**, 3476 (1991).
122. A.B. McCoy and E.L. Sibert III, in: *Advances in Molecular Vibrations and Collision Dynamics*. edited by J.M. Bowman, and M.A. Ratner, (Greenwich: JAI Press Inc., 1991).
123. A.B. McCoy and E.L. Sibert III, Mol. Phys. **77**, 697 (1992).
124. D.C. Burleigh, A.B. McCoy and E.L. Sibert III, J. Chem. Phys. **104**, 480 (1996).
125. Y. Pak, E.L. Sibert III, R.C. Woods, J. Chem. Phys. **107,** 1717 (1997).
126 T.J. Lukka and E. Kauppi, J. Chem. Phys. 103, 6586 (1995).
127. V.I. Starikov and Vl.G. Tyuterev in *The spectroscopy of non-rigid molecules*, (Novosibirsk, Nauka, 1997) (in russian)
127. Vl.G. Tyuterev, in *Symmetry and Perturbation Theory*, edited by G. Gaeta (New Jersey, World Scientic Publishing, 2002)
128. X.G. Wang and E.L. Sibert III, J. Chem. Phys. **113**, 5384 (2000).

129. X. G. Wang, E. L. Sibert III and J. M. L. Martin, J. Chem.Phys., 2000, 112, 1353–1366
130. J. Zúñiga, A. Bastida, A. Requena, E.L. Sibert III, J. Chem. Phys. **116**, 7495 (2002).
131. S.G. Ramesh and E.L. Sibert III, J. Chem. Phys. **120**, 11011 (2004).
132. S.G. Ramesh and E.L. Sibert III, Mol. Phys. **103**, 149 (2005).
133. J. Zúñiga, J.A.G. Picon, A. Bastida, A. Requena, J. Chem. Phys. **126**, 244305 (2007).
134. P. Cassam-Chenai, Y. Bouret, M. Rey, S.A. Tashkun, A.V. Nikitin, Vl.G. Tyuterev, Int. J. Quantum Chem., **112**, 2201 (2012).
135. S.V. Krasnoshchekov, E.V. Isayeva, N.F. Stepanov, J. Phys. Chem. **A116**, 3691 (2012).
136. S.V. Krasnoshchekov and N.F. Stepanov, J. Chem. Phys. **139,** 184101(2013).
137. S.V. Krasnoshchekov, N.C. Craig, N.F. Stepanov, J. Phys. Chem. **A117,** 3041 (2013).
138. S.V. Krasnoshchekov, E.V. Isayeva, N.F. Stepanov, J. Chem. Phys. **141**, 234114 (2014).
139. S.V. Krasnoshchekov, N.Vogt, N.F. Stepanov, J. Phys. Chem. **A119,** 6723 (2015).
140. S.V. Krasnoshchekov and N.F. Stepanov, J. Phys. Chem. **A119**, 1616 (2015).
141. S. Krasnoshchekov, X. Chang, V. Pupyshev, D. Millionshchikov, Phys. Letters **A384,** (2020).
142. M. Joyeux, J. Chem. Phys. **109**, 2111 (1998).
143. M. Joyeux and S.Buyukdagli Chem. Phys. Letters, **412**, 200 (2005).
144. M. Joyeux and D. Sugny, J. Chem. Phys. **112**, 31 (2000).
145. F. Legay, Cahiers de Physique. **12**, 416 (1958).
146. Watson, J.K.G. J.Mol. Spectrosc., **40**, 536 (1971).
147. Yu.S. Makushkin and Vl.G. Tyuterev, Opt. Spektrosk. **1**, 59 (1974).
148. J.M. Flaud and C. Camy-Peyret, J. Mol. Spectrosc. **55**, 278 (1975).
149. M.R. Aliev, Soviet Physics - Uspekhi, **19**, 627 (1976).
150. J.K.G. Watson, M, Takami, T.Oka, J. Chem. Phys. **70**, 5376 (1979).
151. M.R. Aliev, V.M. Mikhailov, J.K.G. Watson, J. Mol. Spectrosc. **118**, 544 (1986).
152. M. Loete, Can. J. Phys. **66**, 17 (1988).
153. O.N. Sulakshina, Yu.G. Borkov, Vl.G. Tyuterev, A. Barbe, J. Chem. Phys. **113**, 10572 (2000).
154. J. Lamouroux, S.A. Tashkun, Vl.G. Tyuterev, Chem. Phys. Lett. **452**, 225 (2008).
155. P. Cassam-Chenaï and J. Liévin, J. Chem. Phys. **136**, 174309 (2012).
156. A. Barbe, M.R. De Backer, E. Starikova, S.A. Tashkun, X. Thomas, V. Tyuterev, J. Quant. Spectrosc. Radiat. Transfer, **113**, 829 (2012).

---------- newly added ----------

157. Christiansen, O. Møller–Plesset Perturbation Theory for Vibrational Wave Functions. J. Chem. Phys. 2003, 119 (12), 5773

158. Bowman, J. M. The Self-Consistent-Field Approach to Polyatomic Vibrations. Acc. Chem. Res. 1986, 19 (7), 202–208.

159. Gerber, R. B.; Ratner, M. A. Self-Consistent-Field Methods for Vibrational Excitations in Polyatomic Systems. Adv. Chem. Phys. 1988, 70, 97–132.

160. Hansen, M. B.; Sparta, M.; Seidler, P.; Toffoli, D.; Christiansen, O. New Formulation and Implementation of Vibrational Self-Consistent Field Theory. J. Chem. Theory Comput. 2010, 6 (1), 235–248.

161. G. Rauhut, J. Chem. Phys. **127**, 184109 (2007).

162. Y. Scribano D. Lauvergnat and D. M. Benoit

Fast vibrational configuration interaction using generalized curvilinearcoordinates and self-consistent basis
THE JOURNAL OF CHEMICAL PHYSICS 133, 094103 _2010_

163. R. Garnier, M. Odunlami, V. Le Bris, D. Bégué, I.e Baraille, and O. Coulaud
Adaptive vibrational configuration interaction (A-VCI): A posteriori error estimation to efficiently compute anharmonic IR spectra
The Journal of Chemical Physics 144, 204123 (2016);

164. T. Mathea , and G. Rauhut
Assignment of vibrational states within configuration interaction calculations
J. Chem. Phys. 152, 194112 (2020);

165. Tina Mathea, Taras Petrenko, and Guntram Rauhut
VCI Calculations Based on Canonical and Localized Normal
Coordinates for Non-Abelian Molecules: Accurate Assignment of the Vibrational Overtones of Allene
Phys. Chem. A 2021, 125, 990−998

167. O. Christiansen, Vibrational Coupled Cluster Theory. J. Chem. Phys. 2004, 120 (5), 2149–2159

168 . 1034Z. Bacic, J.C. Light, Annu. Rev. Phys. Chem. **40,** 469 (1989).

169 M. Mladenović, **Discrete variable approaches to tetratomic molecules**: Part I: DVR(6) and DVR(3)+DGB methods
Spectrochimica Acta Part A: Molecular and Biomolecular Spectroscopy
Volume 58, Issue 4, 1 March 2002, Pages 795-807

170. X-G. Wang and T. Carrington, J. Chem. Phys. 130, 094101
(2009). doi:10.1063/1.3077130

171. A.Baiardi, J.Bloino, and V.Barone
Simulation of Vibronic Spectra of Flexible Systems: Hybrid DVR-Harmonic Approaches
J. Chem. Theory Comput. 2017, 13, 2804−2822

172. Tucker Carrington Jr, Using collocation to study the vibrational dynamics of molecules Spectrochimica Acta Part A: Molecular and Biomolecular Spectroscopy
Volume 248, 5 March 2021, 119158

173. D. W. Schwenke, J. Phys. Chem. **100**, 2867 (1996); **100**, 18884 (1996)

174. <=[200] Nikitin, A.V., Rey, M., Tyuterev, V.G.
An efficient method for energy levels calculation using full symmetry and exact kinetic energy operator: Tetrahedral molecules (2015) Journal of Chemical Physics, 142 (9), art. no. 094118,

175. Yurchenko, S. N.; Thiel, W.; Jensen, P. Theoretical ROVibra-tional Energies (TROVE): A robust numerical approach to the calculation of rovibrational energies for polyatomic molecules. J. Mol. Spectrosc. 2007, 245, 126−140

176 M. Rey, A.V. Nikitin, V.G. Tyuterev, Phys. Chem. Chem. Phys. **15**, 10049 (2013).

---------- After that N=> N+20 (except for the new blue refs !)----------
Left number = new < right hand number = old

New< Old
177< 157. D. Papousek, J.M.R. Stone, V. Spirko, J. Mol. Spectrosc. **48**, 17 (1973).

178< 158. D. Papousek J. Mol. Struct. **C100,** 179 (1983).
179< 159. G.D. Birkhoff, in *Dynamical Systems* AMS Colloquium, New York, **9**, (1966).
180< 160. F.G. Gustavson, Astron. J. **71**, 670 (1966).
181< 161. V.I. Zakharov, V.G. Tyuterev, Laser and Particle Beams, **5**, 27 (1987).
182< 162. H.R. Jauslin, S. Guerin, A. Deroussiaux, in *Chaos - The Interplay Between Stochastic and Deterministic Behaviour* edited by P. Garbaczewski, A. Weron, M. Wolf,(Lecture Notes In Physics, Springer Verlag, 1995).
183< 163. H.R. Jauslin, S. Guérin, S. Thomas, Physica **A279**, 432 (2000).
184< 164. S. Guerin and H.R. Jauslin, Adv. Chem. Phys. **125**, 1 (2003).
185< 165. M. Rey (private communication)
186< 166. A. Crawford, Nuovo Cimento **10**, 698 (1958)
187< 167. F. Jorgensen and T. Pedersen, Mol. Phys. **27**, 33 (1974).
188< 168. F. Jorgensen and T. Pedersen, Mol. Phys. **27**, 959 (1974).
189< 169. V. Kvasmleka and A. Holubec, Chem. Phys. Letters **32**, 489 (1975).
190< 170. P. Cassam-Chenaï, J. Math. Chem. **49**, 821 (2011).
191< 171. J.K.G. Watson, Mol. Phys. **103**, 3283 (2005).
192< 172. V.I. Perevalov and Vl.G. Tyuterev, J. Mol. Spectrosc., **96**, 56 (1982).
193< 173. V.I. Perevalov, Vl.G. Tyuterev, B.I. Zhilinskii, Chem. Phys. Lett., **104**, 455 (1984).
194< 174. J.K.G. Watson, J. Chem. Phys. **46**, 1935 (1967).
195< 175. E.I. Lobodenko, O.N. Sulakshina, V.I. Perevalov, Vl.G. Tyuterev, J. Mol. Spectrosc. **126**, 159 (1987).
196< 176. V.I. Perevalov, Vl.G. Tyuterev, B.I. Zhilinskii, J. Mol. Spectrosc. **103**, 147 (1984).
197< 177. V.I. Perevalov, Vl.G. Tyuterev, B.I. Zhilinskii, J. Mol. Spectrosc. **111**, 1 (1985).
198< 178. Vl.G. Tyuterev, J.P. Champion, G. Pierre, V.I. Perevalov, J. Mol. Spectrosc. **105**, 113 (1984).
199< 179. G. Tyuterev, J.P. Champion, G. Pierre, V.I. Perevalov, J. Mol. Spectrosc. **120**, 49 (1986).
200< 180. X. Huang, D.W. Schwenke, T.J. Lee, J. Chem. Phys. **134**, 044320 (2011).
201< 181. F. Holka, P.G. Szalay, J. Fremont, M. Rey, K.A. Peterson, V.G. Tyuterev, J. Chem. Phys. **134**, 094306 (2011).
202< 182. F.J. Dyson, Phys. Rev. **75**, 486 (1949).
203< 183. W. Magnus, Commun. Pure and Appl. Math. **7**, 649 (1954).
204< 184. S. Carter and N. Handy, Comput. Phys. Rep. **5**, 117 (1986).
205< 185. S. Carter and N. C. Handy, Mol. Phys. **52**, 1367 (1984).
206< 186. P. Jensen, J. Mol. Spectrosc. **128**, 478 (1988).
207< 187. D.W. Schwenke, J. Chem. Phys. **118**, 10431 (2003).
208< 188. X. Huang, D.W. Schwenke, T.J. Lee, J. Chem. Phys. **129,** 214304 (2008).
209< 189. K.L.R. Brown, X. Huang, D.W. Schwenke, T.J. Lee, S.L. Coy, K.K. Lehmann, J. Quant. Spectrosc. Radiat. Transfer **113**, 1066 (2012).
210< 190. E. Matyus, J. Simunek, A. Csaszar, J. Chem. Phys. **131**, 074106 (2009).
211< 191. C. Fabri, E. Matyus, and A.G. Csaszar, Spectrochim. Acta, **A119**, 84 (2014).
212< 192. D. Lauvergnat and A. Nauts, Phys. Chem. Chem. Phys. **12**, 8405 (2010).
213< 193. D. Lauvergnat, J. Luis, B. Kirtman, H. Reis, and A. Nauts, J. Chem. Phys. **144**, 084116 (2016).
214< 194. A. Nauts and D. Lauvergnat, Mol. Phys. **116**, 3701 (2018).
215< 195. T. Carrington and X.G. Wang, Wiley Interdiscip. Rev.: Comput. Mol. Sci. **1**, 952 (2011).
~~196. X.G. Wang and T. Carrington, Jr., Mol. Phys. **110**, 825 (2012). Excluded !~~
216< 196. X.G. Wang and T. Carrington, Jr. Chem. Phys. **144**, 204304 (2016).

217< 197. S.N. Yurchenko, R.J. Barber, A. Yachmenev, W. Thiel, P. Jensen, J. Tennyson, J. Phys. Chem. **A113**, 11845 (2009).
218< 198. S.N. Yurchenko, R.J. Barber, J. Tennyson, W. Thiel, P. Jensen, J. Mol. Spectrosc. **268**, 123 (2011).
219< 199. S.N. Yurchenko, A. Yachmenev, R. Ovsyannikov, J. Chem. Theory Comput. **13**, 4368 (2017).
~~200. A.V. Nikitin, M. Rey, V.G. Tyuterev, J. Chem. Phys. **142**, 094118 (2015).~~

220. Nikitin, A.V., Protasevich, A.E., Rodina, A.A., Rey, M., Tajti, A., Tyuterev, V.G.
Vibrational levels of formaldehyde: Calculations from new high precision potential energy surfaces and comparison with experimental band origins
(2021) Journal of Quantitative Spectroscopy and Radiative Transfer, 260, art. no. 107478,

221< 201. A.V. Nikitin, A.E. Protasevich, M. Rey, V.G. Tyuterev, J. Chem. Phys. **149** 124305, (2018).
222< 202. M. Rey, A.V. Nikitin, V.G. Tyuterev, Mol. Phys. **108**, 2121 (2010).

203. ~~M. Rey, A.V. Nikitin, V.G. Tyuterev, Phys. Chem. Chem. Phys. **15**, 10049 (2013).Excluded~~

223.Rey, M., Nikitin, A.V., Campargue, A., Kassi, S., Mondelain, D., Tyuterev, V.G.
Ab initio variational predictions for understanding highly congested spectra: Rovibrational assignment of 108 new methane sub-bands in the icosad range (6280-7800 cm-1)
(2016) Physical Chemistry Chemical Physics, 18 (1), pp. 176-189.

224< 204. M. Rey, A.V. Nikitin, V.G. Tyuterev, J. Quant. Spectrosc. Radiat. Transfer **164**, 207 (2015).
~~205. Z. Bacic, J.C. Light, Annu. Rev. Phys. Chem. **40,** 469 (1989).~~

---------- After that N=> N+19 (except for the new blue refs !)----------

225< 206 . B.T. Sutcliffe and J. Tennyson, Internat. J. Quantum Chem. **39**, 183 (1991).

226. M.Jacon L.Daumont J.-L.Teffo Application of the DVR method to the vibration-rotation spectrum of N_2O: derivation of the dipole moment derivatives in Radau coordinates Journal of Quantitative Spectroscopy and Radiative Transfer Volume 83, Issues 3–4, 1 February 2004, Pages 435-444

---------- After that N=> N+20 (except for the new blue refs !)----------

227< 207. J. Tennyson, M. Kostin, P. Barletta, G. Harris, O. Polyansky, J. Ramanlal, N. Zobov, Comp. Phys. Commun. **163**, 85 (2004).
228< 208. G. Li and H. Guo, J. Mol. Spectrosc. **210**, 90 (2001).
229< 209. V. Szalay, J.Chem.Phys. **105**, 6940 (1996)
230< 210. J.C. Light, and T. Carrington Jr., Adv. Chem. Phys. **114**, 263 (2000).
231< 211.V.A. Mandelshtam and H.S. Taylor, J. Chem. Phys. **102**, 7390 (1995).
232< 212. T.P. Grozdanov, V.A. Mandelshtam, H.S. Taylor, J. Chem. Phys.**103**, 7990 (1995)
233< 213. K. Sadri, D. Lauvergnat, F. Gatti, and H.D. Meyer, J. Chem. Phys. **141**, 114101 (2014).
234< 214. K. Sadri, D. Lauvergnat, F. Gatti, and H.D. Meyer, J. Chem. Phys. **136**, 234112 (2012).

235< 215. D. Viglaska, M. Rey, A.V. Nikitin, V.G. Tyuterev, J. Chem. Phys. **153**, 084102 (2020).
236< 216 I.M. Mills, J. Mol. Spectrosc. **5,** 334 (1961).
237< 217. A.V. Sergeev and D.Z. Goodson , Mol. Phys. **93**, 477 (2010).
238< 218. P. Cassam-Chenaï and J. Liévin, Int. J. Quantum Chem. **93**, 245 (2003).
239< 219. Z.J. Gong, D.A. Matthews, P.B. Changala, J.F. Stanton J. Chem. Phys. **149**, 114102 (2018).
240< 220. P.R. Franke, J.F. Stanton, G.E. Douberly, *J. Phys. Chem.* ***A*****125**, 1301 (2021).
241< 221. Q. Yang, M. Mendolicchio, V. Barone, J. Bloino Front. Astron. Space Sci., (2021).
242< 222. J.M. Bowman, T. Carrington, H.D. Meyer, Mol. Phys. **106,** 2145 (2008).
243< 223. S. Carter, A.R. Sharma, J.M. Bowman, P. Rosmus, R. Tarroni, J. Chem. Phys. **131**, 224106 (2009).
244< 224. S. Carter, J.M. Bowman, N.C. Handy, Mol. Phys., **110,** 775 (2012).
245< 225. J.K.G. Watson, Mol. Phys. **15,** 479 (1968).
246< 226. J.K.G. Watson, Mol. Phys. **79,** 943 (1993).
247< 227. E.B. Wilson Jr. and J.B. Howard, J. Chem. Phys. **4**, 260 (1936).
248< 228. B.T. Darling, D.M. Dennison, Phys. Rev. **57**, 128, (1940).
249< 229. A.R. Hoy, I.M. Mills, G. Strey, Mol. Phys. **24**, 1265 (1972).
250< 230. V. Boudon, J.P. Champion, T. Gabard, M. Loete, F. Michelot, G. Pierre, M. Rotger, Ch.Wenger, M. Rey, J. Mol. Spectrosc. **228**, 620 (2004).
251< 231. A.V. Nikitin, J.P. Champion, Vl. G. Tyuterev, J. Mol. Spectrosc. **182**, 72 (1997).
252< 232. M. Rey, I.S. Chizhmakova, A.V. Nikitin, V.G. Tyuterev, Phys. Chem. Chem. Phys., **23**, 12115 (2021).
253< 233. A.V. Nikitin, I.S. Chizhmakova, M. Rey, S.A. Tashkun, S. Kassi, D. Mondelain, A. Campargue, V.G. Tyuterev, J. Quant. Spectrosc. Radiat. Transfer, **203**, 341 (2017).
254< 234. S.A.Tashkun, J. Quant. Spectrosc. Radiat. Transfer **231**, 88 (2019).

⇨ 255. Watson J K G. Determination of centrifugal distortion coefficients of asymmetric-top molecules. J. Chem Phys 1967;46:4189–96.

256< 235 S. Flügge, *Problems in quantum mechanics*, (Vl Springer-Verlag, Berlin-Heidelberg-New York, 1971)

257< 236. H Partridge, D.W. Schwenke J. Chem. Phys. **106**, 4618 (1997).

---------- After that N=> N+20 (except for the new blue refs !)----------

258< 238. T. Hougen, P. R. Bunker, and J. W. C. Johns, J. Mol. Spectrosc. **34**, 136, (1970).
…
258< 239. V.I. Starikov, S.A. Tashkun, Vl.G. Tyuterev, J. Mol. Spectrosc. **151**, 130 (1992).
259< 240. S.N. Mikhailenko, Vl.G. Tyuterev, V.I. Starikov, K.K. Albert, B.P. Winnewisser, M. Winnewisser G. Mellau, C. Camy-Peyret, R. Lanquetin, J.M. Flaud, J.W. Brault. J. Mol. Spectrosc. **213**, 91 (2002).
260< 241. O. Polyansky, A. Kyuberis, N. Zobov, J. Tennyson, S. Yurchenko, L. Lodi, Mon. Not. R. Astron. Soc. **480,** 2597 (2018)
261< 242. M.S. Child, T. Lawton Chem. Phys. Lett. **87**, 217 (1982).
262< 243. K.K. Lehmann, J. Chem. Phys. **79**, 1098 (1983).
263< 244. C. Camy-Peyret, J.M. Flaud, J.P. Maillard, G. Guelachvili, Mol. Phys., **33**, 1641 (1977).

264< 245. J.Y. Mandin, J.P. Chevillard, C. Camy-Peyret, J.M. Flaud, J.W. Brault, J. Mol. Spectrosc. **116**, 167 (1986).
265< 246. A.G. Csaszar, E. Matyus, T. Szidarovszky, L. Lodi, N.F. Zobov, S.V. Shirin, O.L. Polyansky, J. Tennyson, J. Quant. Spectr. Radiat. Transfer **111**, 1043 (2010).
266< 247. J. M. L. Martin, J. Chem. Phys., **108**, 2791 (1998).
267< 248. J. Zuniga, A. Bastida, A. Requena, J. Chem. Phys. **115**, 139 (2001).
267< 249. X. Huang , D.W. Schwenke, T.J. Lee, J. Chem. Phys. **140**, 114311 (2014).
268< 250. Vl.G. Tyuterev, S.A. Tashkun, D.W. Schwenke, A. Barbe, SPIE Proceedings **5311**, 176 (2004).
269< 251. Yu.L. Babikov, S.N. Mikhailenko, A. Barbe, Vl.G. Tyuterev, J. Quant. Spectrosc. Radiat Transfer, **145**, 169 (2014). Updated at http://smpo.univ-reims.fr and http://smpo.iao.ru.

---------- newly added ----------
270. H.M.Pickett, E.A.Cohen,L.R.Brown, C.P.Rinsland, M.A.H.Smith, V.Malathy Devi, A.Goldman, A.Barbe, B.Carli, M.Carlotti
The vibrational and rotational spectra of ozone for the (0, 1, 0) and (0, 2, 0) states
Journal of Molecular Spectroscopy,Volume 128, Issue 1, March 1988, Pages 151-171
271 . J.-M. Colmont , B. Bakri, J. Demaison , H. Ma¨der, F. Willaert ,
Vl.G. Tyuterev, A. Barbe., Journal of Molecular Spectroscopy 233 (2005) 293–296

---------- After that N=> N+21 (except for the new blue refs !)----------

273< 252. Vl.G. Tyuterev, J. Mol. Spectrosc. **151**, 97 (1992).
274< 253. J.M. Flaud, C. Camy-Peyret, Mol.Phys. **32**, 523 (1976).
275< 254. S.A. Clough and F.X. Kneizys J. Chem. Phys. **44**:1855 (1965).
276< 255. J.M. Flaud, C. Camy-Peyret, V. Malathy Devi, C.P. Rinsland, M.A.H. Smith. J. Mol. Spectrosc. **124**, 209 (1987).
277< 256. J.M. Flaud and R. Bacis, Spectrochim. Acta, **A54,** 3 (1998).

278< 257. A. Barbe, M.R. De Backer-Barilly, E. Starikova, S.A. Tashkun, X. Thomas, Vl.G. Tyuterev, J. Quant. Spectrosc. Radiat. Transfer **113**, 829 (2012).
279< 258. L.N. Fletcher G.S. Orton, N.A. Teanby, P.G.J. Irwin, Icarus **202**, 543 (2009).
280< 259. O. Ulenikov, E. Bekhtereva, V. Kozinskaia, J. Zhen, S. He, S. Hu, Q. Zhu, C. Leroy, L. Pluchart, J. Quant. Spectrosc. Radiat. Transfer **83**, 599 (2004).
281< 260. A.V. Nikitin, J.P. Champion, R.A.H. Butler, L.R. Brown, I. Kleiner J. Mol. Spectrosc. **256**: 4 (2009).
282< 261. V. Malathy Devi, I. Kleiner, R.L. Sams, L.R. Brown, D.C. Benner, L.N. Fletcher, J. Mol. Spectrosc. **298**, 11 (2014).
283< 262. R. Ovsyannikov, S.N. Yurchenko, M. Carvajal, W. Thiel, P. Jensen, J. Chem. Phys. **129**, 044309 (2008).
284< 263. A.V. Nikitin, F. Holka, Vl.G. Tyuterev, J. Fremont, J. Chem. Phys. **131**, 244312 (2009).
285< 264. A. V. Nikitin, J.P. Champion, Vl.G.Tyuterev, L.R. Brown, G. Mellau, J. Mol. Structure, **517**, 1 (2000)
286< 265. M. Rey, A.V. Nikitin, V.G. Tyuterev, J. Chem. Phys. **141**, 044316 (2014).
287< 266. M. Rey, A.V. Nikitin, V.G. Tyuterev, J. Phys. Chem. **A119**, 4763 (2015).
288< 267. X.G. Wang and T. Carrington Jr. J. Chem. Phys. **141**, 154106 (2014).
289< 268 D.W. Schwenke and H. Partridge, Spectrochim. Acta **A57**, 887 (2001).
290< 269. A.V. Nikitin, M. Rey, V.G. Tyuterev, Chem. Phys. Lett. **501,** 179 (2011).
291< 270. O. Ulenikov, E. Bekhtereva, S. Albert, S. Bauerecker, H. Hollenstein, M. Quack, J. Phys. Chem. **113**, 2218 (2009).

292< 271. C. Scheutz, P. Kjeldsen, E. Gentil, Waste Manage. Res., **27**, 716 (2009).
293< 272. V. Boudon, D. Bermejo, R.Z. Martınez, J. Raman Spectrosc., , **44**, 731 (2013).
294< 273 M. Carlos, O. Gruson, C. Richard, V. Boudon, M. Rotger, X. Thomas, C. Maul, C. Sydow, A. Domanskaya, R. Georges, P. Soulard, O. Pirali, M. Goubet, P. Asselin, T.R. Huet, J. Quant. Spectrosc. Radiat. Transfer, **201**, 75 (2017).
295< 274. M. Rey, I.S. Chizhmakova, A.V. Nikitin, V.G. Tyuterev, Phys. Chem. Chem. Phys. **20**, 21008 (2018).
296< 275. M. Mattoussi, M. Rey, M. Rotger, A.V. Nikitin, I. Chizhmakova, X. Thomas, H. Aroui, S. Tashkun, V.G. Tyuterev, J. Quant. Spectrosc. Radiat. Transfer **226**, 92 (2019).
297< 276. P.F. Bernath, Phil. Trans. R Soc. **A372**, 20130087 (2014).
298< 277. G. Tinetti, T. Encrenaz, A. Coustenis, Astron. Astrophys. Rev. **21**, 63 (2013).
299< 278. G.C. Rhoderick and W.D. Dorko, Environ. Sci. Technol. **38**, 2685 (2004).
300< 279. T.J. Lee, J.M.L. Martin, P.R. Taylor, J. Chem. Phys. **102**, 254 (1995).
301< 280. R. Marquardt and M. Quack, J. Phys. Chem. **108**, 3166 (2004).
302< 281. R. Marquardt and M. Quack, J. Chem. Phys. **109**, 10628 (1998).
303< 282 D.W. Schwenke, Spectrochimica Acta Part **A58**, 849 (2002).
304< 283. A.V. Nikitin, M. Rey, V.G. Tyuterev, J. Chem. Phys. **145**, 114309 (2016).
305< 284. S.N. Yurchenko, J. Tennyson, R.J. Barber, W. Thiel, J. Mol. Spectrosc. **291**, 69 (2013).
306< 285. S.N. Yurchenko and J. Tennyson, Mon. Not. R. Astron. Soc. **440**, 1649 (2014).
307< 286. M Majumder, S.E. Hegger, R. Dawes, S. Manzhos, X.G. Wang, T. Carrington Jr., J. Lid, H. Guo, *Mol. Phys.* **113**, 1823 (2015).
308< 287. A. Owens, S.N. Yurchenko, A. Yachmenev, J. Tennyson, W. Thiel, J. Chem. Phys. **145**, 104305 (2016).
309< 288. X.G. Wang and T. Carrington Jr., J. Chem. Phys. **119,** 101 (2003).
310< 289. X.G. Wang and T. Carrington Jr., J. Chem. Phys. **121,** 2937 (2004).
311< 290. M. Ghysels, S. Vasilchenko, D. Mondelain, S. Béguier, S. Kassi, A. Campargue, J. Quant. Spectrosc. Radiat. Transfer **215**, 59 (2018).
312< 291. A. Wong, P.F. Bernath, M. Rey, A.V. Nikitin, V.G., Tyuterev, Astrophys. J. Suppl. Series **240**, 4, (2019).
313< 292. R.J. Hargreaves, I.E. Gordon, M. Rey, A.V. Nikitin, V.G. Tyuterev, R.V Kochanov, L.S. Rothman, Astrophys. J. Suppl. Series, **247**, 55 (2020).
314< 293. A. Foltynowicz, L. Rutkowski, I. Silander, A.C. Johansson, V. Silva de Oliveira, O. Axner, G. Soboń, T. Martynkien, P. Mergo, K.K. Lehmann, Phys. Rev. Lett. 126, 063001 (2021).
315< 294. A. Foltynowicz, L. Rutkowski, I. Silander, A.C. Johansson, V. Silva de Oliveira, O. Axner, G. Soboń, T. Martynkien, P. Mergo, . K. Lehmann, Phys. Rev. A103, 022810 (2021).
316< 295. M. Rey, A.V. Nikitin, B. Bezard, P. Rannou, A. Coustenis, V.G. Tyuterev, Icarus **303**, 114 (2018)
317< 296. M. Rey, A.V. Nikitin, V.G. Tyuterev, Astrophys. J. **847** (2), aa8909 (2017).
318< 297. M. Rey, A.V. Nikitin, Y. Babikov, Vl.G. Tyuterev, J. Mol. Spectrosc. **327**, 138 (2016).
319< 298. A.V. Nikitin, A.E. Protasevich, M. Rey, V.G. Tyuterev, J. Chem. Phys. **149**, 124305 (2018).
320< 299. D.N.Kozlov, D.A. Sadovskii, P.P. Radi, J. Mol. Spectrosc. **291**, 23 (2013).
321< 300. L.R. Brown, K. Sung, D.C. Benner, V.M. Devi, V. Boudon, T. Gabard, C. Wenger, A. Campargue, O. Leshchishina, S. Kassi, D. Mondelain, L. Wang, L. Daumont, L. Regalia, M. Rey, X. Thomas, V.G. Tyuterev, O. M. Lyulin, A.V. Nikitin, H.M. Niederer, S. Albert, S. Bauerecker, M. Quack, J.J. O'Brien, I.E. Gordon, L.S. Rothman, H. Sasada, A. Coustenis,

M.A.H. Smith, T. Carrington Jr., X.G. Wang, A.W. Mantz, P.T. Spickler, J. Quant. Spectrosc. Radiat. Transfer, **130**, 201 (2013).
322< . Vl.G. Tyuterev, Yu.L. Babikov, S.A. Tashkun, V.I. Perevalov, A. Nikitin, J.P. Champion, J.C. Hilico, M. Loete, C.L. Pierre, G. Pierre, Ch. Wenger, J. Quant. Spectrosc. Radiat. Transfer **52**, 459 (1994).
323< 302. Ch. Wenger and J.P. Champion, J. Quant. Spectrosc. Radiat. Transfer **59**, 471 (1998).
324< 303. S. Albert, S. Bauerecker, V. Boudon, L.R. Brown, J.P. Champion, M. Loëte, A. Nikitin, M. Quack, Chem. Phys. **356**, 131 (2009).
325< 304. H.M. Niederer, X.G. Wang, T. Carrington, Jr., S. Albert, S. Bauerecker, V. Boudon, M. Quack, J. Mol. Spectrosc. **291**, 33 (2013).
326< 305. O. Ulenikov, E. Bekhtereva, S. Albert, S. Bauerecker, H.Niederer, M. Quack, J. Chem. Phys. **141**, 234302 (2014).
327< 306. B. Amyay, M. Louviot, O. Pirali, R. Georges, J. Vander Auwera, V. Boudon, J. Chem. Phys. **144**, 24312 (2016).
328< 307. B. Amyay, A. Gardez, R. Georges, L. Biennier, J. Vander Auwera, C. Richard, V. Boudon, J. Chem. Phys. **148**, 134306 (2018).
329< 308. Y.A. Ba, C. Wenger, R. Surleau, V. Boudon, M.Rotger, L. Daumont. et al, J. Quant. Spectrosc. Radiat. Transfer **130**, 62 (2013).
330< 309. V. Boudon, J.P. Champion, T. Gabard, M. Loëte, M. Rotger, C. Wenger, in: *Handbook of High-Resolution Spectroscopy, Fundamentals and Theory, Vol 3: Special Techniques and Applications* edited by M. Quack and F. Merkt, (John Wiley & Sons, Ltd; 2011). pp. 1437–60 .
331< 310. A.V. Nikitin, A.A. Rodina, X. Thomas, L. Manceron, L. Daumont, M. Rey, K. Sung, A.E. Protasevich, S.A. Tashkun, I.S. Chizhmakova, V.G. Tyuterev, J. Quant. Spectrosc. Radiat. Transfer **253**, 107061 (2020).
332< 311 A.J. Dorney and J.K.G. Watson, J. Mol. Spectrosc. **42**, 1 (1972).
333< 312. W.G. Harter and C.W. Patterson, J. Chem. Phys. **80**, 4241 (1984).
334< 313. D.A. Sadovskii and B.I. Zhilinskii, Mol. Phys. **65**, 109 (1988).
335< 314. X.G. Wang and E.L. Sibert, J. Chem. Phys. 1999, **111**, 4510−4522.
336< 315. E. Starikova, A.V. Nikitin, M. Rey, S.A. Tashkun, D. Mondelain, S. Kassi, A. Campargue, V.G. Tyuterev, J. Quant. Spectrosc. Radiat. Transfer **177**, 170 (2016).
337< 316 A.A. Rodina, A.V. Nikitin, L. Manceron, X. Thomas, L. Daumont, M. Rey, K. Sung, A.E. Protasevich, S.A. Tashkun, Vl. G. Tyuterev, J. Quant. Spectrosc. Radiat. Transfer. **279**, 108021 (2022).
338< 317. A.V. Nikitin, B.M. Krishna, M. Rey, S.A. Tashkun, Vl.G Tyuterev, J. Quant. Spectrosc. Radiat. Transfer **167**, 53 (2015).
339< 318. R.R. Gamache, B. Vispoel, M. Rey, A. Nikitin, V. Tyuterev, O. Egorov, I.E. Gordon, V. Boudon, J. Quant. Spectrosc. Radiat. Transfer **271**, 107713 (2021).
340< 319. M.R. Aliev, D. Papousek, A. Urban, J. Mol. Spectrosc. **124**, 285 (1987).
341< 320. M.R. Aliev and V.M. Mikhailov, Acta Physica Hungarica, **55**, 293 (1984).
342< 321. V.I. Perevalov, O.M. Lyulin, Vl.G. Tyuterev, M. Loete, J. Mol. Spectrosc. **149**, 15 (1991).
343< 322. V.I.Perevalov, E.I. Lobodenko, O.M. Lyulin, J.L. Teffo, J. Mol. Spectrosc. **171**, 435, (1995).
344< 323. E.V. Karlovets and V.I. Perevalov, Opt. Spectrosc. **119**, 16 (2015).
345< 324. J. Lamouroux , THÈSE de Docteur de l'Université de Reims Champagne-Ardenne, 2007
346< 325. T. Delahaye, THÈSE de Docteur de l'Université de Reims Champagne-Ardenne, 2014
347< 326. T. Delahaye , M. Rey, S. Tashkun, V. Tyuterev, HRMS Colloquium, Bologna, Italy 2014

348< 327. R.A. Toth, J. Opt. Soc. Am. **B10**, 1526 (1993).
349< 328. A. Nikitin, J.P. Champion, V.G. Tyuterev, J. Quant. Spectrosc. Radiat. Transfer **82**, 239 (2003).
350< 329. D. Sadovskii and B. Zhilinskii, J. Quant. Spectrosc. Radiat. Transf. **42**, 575 (1989).

---------- newly added ----------

351. Rodina, A.A., Nikitin, A.V., Thomas, X., Manceron, L., Daumont, L., Rey, M., Sung, K., Tashkun, S.A., Tyuterev, V.G. Improved line list of 12 CH 4 in the 3760-4100 cm -1 region
(2019) Journal of Quantitative Spectroscopy and Radiative Transfer, 225, pp. 351-362

---------- After that N=> N+22 (except for the new blue refs !)----------

352< 330. J. Laane, M. Dakkouri, B. Van der Veken, H. Oberhammer, in *Structures and Conformations of Non-Rigid Molecules*, NATO ASI Series, Series C: Mathematical and Physical Sciences (Springer Science+Business Media, B.V., 1993).
353< 331. Y.E. Smeyers, *Structure and Dynamics of Non-Rigid Molecular Systems*, (Springer-Science + Business Media, B.V., 2012).
354< 332.A. Perrin, J. Orphal, J.-M. Flaud, S. Klee, G. Mellau, H. Mader, D. Walbrodt, and M. Winnewisser, J. Mol. Spectrosc. **228**, 375 (2004).
355< 333. S. Yurchenko, W. Thiel, M. Carvajal, H. Lin, P. Jensen, Adv. Quantum Chem. **48**, 209 (2005).
356< 334. J.M. Bowman, X. Huang, N.C. Handy, S. Carter, J. Phys. Chem. **A111**, 7317 (2007).
357< 335. F. Gatti and C. Iung, Phys. Rep. **484**, 1 (2009).
358< 336. C. Fabri, E. Matyus, and A. Csaszar, J. Chem. Phys. **134**, 074105 (2011).
359< 337. S. Carter, A.R. Sharma, J.M. Bowman, J. Chem. Phys. **135**, 014308 (2011).
360< 338. K. Sung, L.R. Brown, X. Huang, D.W. Schwenke, T.J. Lee, S.L. Coy, K.K. Lehmann, J. Quant. Spectrosc. Radiat. Transfer **113**, 1066 (2012).
361< 339. I. Kleiner and J.T. Hougen, J. Mol. Spectrosc. **368**, 111255 (2020).
362< 340. T. Nguyen, W. Stahl, H.V.L. Nguyen, I. Kleiner, J. Chem. Phys. **154**, 49418 (2021).
363< 341. O. Egorov, M. Rey, A. V. Nikitin, D. Viglaska, J. Phys. Chem. **A125**, 10568 (2021).
364< 342.V.I. Starikov and Vl.G. Tyuterev, *Intramolecular Ro-Vibrational Interactions and Theoretical Methods in the Spectroscopy of Non-Rigid Molecules* (Nauka, Novosibirsk, 1997),pp. 1–203 (in Russian).
365< 343. A.R. Hoy, and P.R. Bunker, J. Mol. Spectrosc. **52**, 439 (1974).
366< 344 A.R. Hoy, and P.R. Bunker, J. Mol. Spectrosc. **74**, 1, (1979).
367< 345. P.R. Bunker, B.M. Landsberg, B.P. Winnewisser, J. Mol. Spectrosc. **74**, 9, (1979).
368< 346. P. Jensen, P.R. Bunker, J. Mol. Spectrosc. **99**, 348 (1983).
269< 347. P. Jensen, P.R. Bunker, J. Mol. Spectrosc. **118**, 18 (1986).
370< 348. B.P. Winnewisser, in *Molecular Spectroscopy: Modern Research*, edited by K.N. Rao (Academic Press, Orlando (1985)) pp. 321-420
371< 349. D. Papousek, J.M.R. Stone, V. Spirko, J. Mol. Spectrosc. **48**, 17 (1973).
372< 350. V. Spirko, J.M.R. Stone, D. Papousek, J. Mol. Spectrosc. **60**, 159 (1976).
373< 351. V. Špirko and W.P. Kraemer, J. Mol. Spectrosc. **133**, 331 (1989).
374< 352. L.H. Coudert, J. Mol. Spectrosc. **165**, 406 (1994).
375< 353. L.H. Coudert, G. Wagner, M. Birk, Yu.I. Baranov, W.J. Lafferty, J.M. Flaud, J. Mol. Spectrosc. **251**, 339 (2008).
376< 354. V.I. Starikov, B.H. Makhanchejev, Vl.G. Tyuterev, Opt. Spectrosk., **55**, 467 (1983).
377< 355. V.I. Starikov, A.A. Pozdniakov, Vl.G. Tyuterev, Opt. Spectrosk., **68**, 302 (1990).
378< 356. V.I. Starikov, Vl.G. Tyuterev, Soviet Phys. J. **25**, 762 (1982).
379< 357. V.I. Starikov, B.N. Makhancheev, Vl.G. Tyuterev, Soviet Phys. J. **27**, 780 (1984).

380< 358. M. Grechko, O. Boyarkin, T. Rizzo, P. Maksyutenko, N. Zobov, S. Shirin, L.Lodi, J.Tennyson, A. Császár, O. Polyansky J. Chem. Phys. **131**, 221105 (2009)
381< 359 V. Kokoouline, D. Lapierre, A. Alijah, V. Tyuterev, Phys. Chem. Chem. Phys., **22** , 15885 (2020)
382< 360.T. Szidarovszky, A. Csaszar , Mol. Phys., **111**, 2131 (2013)
383< 361. D. Lapierre, A. Alijah, R. Kochanov, V. Kokoouline, V. Tyuterev, Phys. Rev. A, **94** (4),042514 (2016)
384< 362. Lopez-Puertas, M.; Taylor, F.W. Non LTE Radiative Transfer in the atmosphere. *Series on Atmospheric, Oceanic and Planetary Physics.* World scientific, Singapore, Vol. 3. (2001)
385< 363. R. Gamache, B. Vispoel , M. Rey, V. Tyuterev, A. Barbe, A. Nikitin, O. Polyansky, J.Tennyson, S. Yurchenko, A. Csaszar, T. Furtenbacher, V. Perevalov, S. Tashkun, Icarus, **378,** 114947(2022)
386< 364. L. Rothman, I. Gordon, R. Barber, H. Dothe, R. Gamache, A. Goldman, V. Perevalov, S. Tashkun, J. Tennyson, J. Quant. Spectrosc. Radiat. Transfer, **111** , 2139 (2010)
387< 365. J. Tennyson, and S. Yurchenko , *Astronomy & Geophysics*, **62**, 6.16 (2021)
388< 366. X. Huang, D. Schwenke, T. Lee, J. Mol. Struct. **1217**, 128260 (2020)
389< 367. M. Rey, A. Nikitin, V. Tyuterev, Astrophysical Journal, **847** (2), aa8909, (2017)
390< 368. J. Tennyson, S. Yurchenko, Mol. Astrophys. **8**, 1 (2017)
391< 369. M. Rey, T. Delahaye, A. Nikitin, V. Tyuterev, (2016) Astronomy and Astrophysics, **594,** A47, (2016)
392< 370. B. Mant, A. Yachmenev, J. Tennyson, S. Yurchenko, *Monthly Notices of the Royal Astronomical Society*, **478**, 3220 (2018)
~~371. M. Rey, I. Chizhmakova, A. Nikitin, V. Tyuterev, Phys. Chem. Chem. Phys., **23** , 12115 (2021) repeated ! N232~~

393 Nikitin, A.V., Rey, M., Chizhmakova, I.S., Tyuterev, V.G.
First Full-Dimensional Potential Energy and Dipole Moment Surfaces of SF6
(2020) Journal of Physical Chemistry A, 124 (35), pp. 7014-7023.

394< 372. G. Avila, T.Carrington , J. Chem. Phys. **137**, 174108 (2012)
395< 373. H. Pickett, R. Poynter, E. Cohen, M. Delitsky, J. Pearson, H. Müller,J. Quant. Spectrosc. Radiat. Transf. **60**, 883 (1998)
396< 374. C. Endres, S. Schlemmer, P. Schilke, J. Stutzki, H. Mueller, J. Mol. Spect. **327,** 95 (2016)
397< 375. Y. Ba, C. Wenger, R. Surleau, V. Boudon, M. Rotger, L. Daumont, et al., J. Quant. Spectrosc. Radiat. Transf. **130,** 62 (2013)
398< 376. S. Tashkun, V. Perevalov, R. Gamache, J. Lamouroux, J. Quant. Spectrosc. Radiat. Transfer, **228**, 124 (2019)
399< 377. S. Tashkun, V. Perevalov, N. Lavrentieva, J. Quant. Spectrosc. Radiat. Transfer, **177**, 43 (2016)
400< 378. O. Lyulin, and V. Perevalov, J. Quant. Spectrosc. Radiat. Transfer, **201**, 94 (2017)

---------- newly added ----------

401. H.Hartwig and H.Dreizler, *Z. Naturforsch* **51a**, 923-932 (1996).

402. S.Herbers and V.L.Nguyen, *J.Mol.Spectrosc.* **370**, 111289 (2020)

403. P. Groner, *J. Chem. Phys.* **107**, 4483-4498 (1997).

404. V.V. Ilyushin, Z. Kisiel, L. Pszczółkowski, H. Mäder, J.T. Hougen, "A New Torsion-Rotation Fitting Program for Molecules with a Six-Fold Barrier: Application to the Microwave Spectrum of Toluene", *Journal of Molecular Spectroscopy* 259, 26-38 (2010).

405. V. Ilyushin, "Millimeter wave spectrum of nitromethane", *Journal of Molecular Spectroscopy* 345, 64-69 (2018).

406. BELGI: Kleiner and J. T. Hougen, J. Chem. Phys. 119, 5505 (2003)

---------- After that N=> N+28 ----------

407< 379. E. Starikova, K. Sung, A. Nikitin, M. Rey, J. Quant. Spectrosc. Radiat. Transfer, **235**, 278 (2019)
408< 380. O. Egorov, A. Nikitin, M. Rey, A. Rodina, S. Tashkun, V. Tyuterev, J. Quant. Spectrosc. Radiat. Transfer, **239**, 106668, (2019)
409< 381. A. Barbe, E. Starikova, M.R. De Backer, V. Tyuterev, J. Quant. Spectrosc. Radiat. Transfer, **218**, 231 (2018)
410< 382. A. Barbe, S. Mikhailenko, E. Starikova, V. Tyuterev, Molecules, **27** (3), 911 (2022)
411< 383. S. Tani, Progr. Theor.Phys.,**11**,190 (1954)
412< 384. D. Finkelstein, Commun. Pure *Appl. Math. **8**, 245* (*1955*)
413< 385. M. Rosenblum, Duje Math.T., **23**, 263 (1957)
414< 386. F. J. Murray , J. Math. Phys. **3**, 451 (1962);